INVESTIGATION OF IRIS RECOGNITION IN THE VISIBLE SPECTRUM

A THESIS SUBMITTED TO

THE UNIVERSITY OF KENT

IN THE SUBJECT OF ELECTRONIC ENGINEERING

FOR THE DEGREE

OF DOCTOR OF PHILOSOPHY (PHD)

By

Petru Radu

March 2013

To my wife Claudia, who supported me each step of the way and to my two sons,

Ioan and Ştefan

Acknowledgements

Above all, I would like to thank God and Virgin Mary for their mercy and help that they gave me to complete this doctoral thesis. With their support I had the opportunity to step in the marvellous world of science and the motivation to carry on my work in front of the difficulties.

In this wonderful experience I also have been supported and supervised by many people to whom I would like to express my deepest gratitude.

This thesis would not have been possible without the help and patience of my supervisors, Dr. Konstantinos Sirlantzis and Dr Gareth Howells. Possessing excellent recruiting skills, they observed and believed in my abilities and offered me the occasion to start pursuing the Ph.D. degree. Not only their unsurpassed knowledge in pattern recognition and image processing, but also their good advice, friendship and support have been invaluable on both academic and personal level. They made the time working on my Ph.D. an unforgettable experience. I admire my supervisors' ability in helping me balance research interests and personal pursuits, which I appreciate from my heart.

In addition, I have been very privileged to get to know and collaborate with Dr. Farzin Deravi and Dr. Sanaul Hoque. From them I learned various options on how to tackle research problems, how to enhance the publications resulted from my work and how to develop high research standards. They always inspired me to work hard and to be positive at all time.

A very special thanks to my wife Claudia for her personal support and great patience at all times. She is the one who made most sacrifices by creating a working environment at home for me, when it was necessary. Her kindness, friendship and love motivated me the most to work hard and to publish papers. Our two sons that were born during my Ph.D., Ioan and Ştefan, are the most wonderful gift ever.

Furthermore, I will be always grateful to my mother (Ana Radu) and my father (Gheorghe Radu) who always encouraged me to study and gave me their full support in all my academic and personal decisions. Their life has been an example of perseverance, seriousness, humbleness and promptitude to me. They are the parents that every person

could ever dream of.

I will forever be grateful to Dr. Valentina Balas for offering me her support to study at University of Kent in a very important moment of my life. Her generosity, encouragement and advice have been extremely valuable to me during the last 9 years of my life. Her academic career has always inspired and motivated me.

I am also thankful to Priest Nikolaos Kokliotis, who was always there for me and my family and gave us the right advice at the right time. He inspired me the enthusiasm and balance needed to work hard and to distinguish the things that are really important in life.

Many thanks to Prof. Mike Fairhurst for offering me the opportunity to step towards an academic career. To Dr Richard Guest and Winston Waller, who made my experience at School of Engineering and Digital Arts an interesting and fruitful one.

I must not forget to thank George McConnon, my previous colleague, who gave me significant support when I started the Ph.D. I am also very thankful to all my colleagues from the Image and Information Engineering Research Lab, who made my day-to-day life more enjoyable. A special thanks to Bogdan Gherman, Shivam Gunes, Paul Oprea and Ali Asad. Also, I would like to thank my neighbour, Polixeni Koureas, for all her support that she gave to my family while I was working and to Priest Ştefan Negrean, for encouraging me to step strong and smooth in the research environment.

And finally, I am very grateful to the financial support given by the European Union NOmadic Biometric Authentication (NOBA) project, which was funded by ERDF under the Interreg IV A program (Ref. No. 4051).

Abstract

Among the biometric systems that have been developed so far, iris recognition systems have emerged as being one of the most reliable. In iris recognition, most of the research was conducted on operation under near infrared illumination. For unconstrained scenarios of iris recognition systems, the iris images are captured under visible light spectrum and therefore incorporate various types of imperfections. In this thesis the merits of fusing information from various sources for improving the state of the art accuracies of colour iris recognition systems is evaluated. An investigation of how fundamentally different fusion strategies can increase the degree of choice available in achieving certain performance criteria is conducted. Initially, simple fusion mechanisms are employed to increase the accuracy of an iris recognition system and then more complex fusion architectures are elaborated to further enhance the biometric system's accuracy. In particular, the design process of the iris recognition system with reduced constraints is carried out using three different fusion approaches: multi-algorithmic, texture and colour fusion and multiple classifier systems. In the first approach, one novel iris feature extraction methodology is proposed and a multi-algorithmic iris recognition system using score fusion, composed of 3 individual systems, is benchmarked. In the texture and colour fusion approach, the advantages of fusing information from the iris texture with data extracted from the eye colour are illustrated. Finally, the multiple classifier systems approach investigates how the robustness and practicability of an iris recognition system operating on visible spectrum images can be enhanced by training individual classifiers on different iris features. Besides the various fusion techniques explored, an iris segmentation algorithm is proposed and a methodology for finding which colour channels from a colour space reveal the most discriminant information from the iris texture is introduced. The contributions presented in this thesis indicate that iris recognition systems that operate on visible spectrum images can be designed to operate with an accuracy required by a particular application scenario. Also, the iris recognition systems developed in the present study are suitable for mobile and embedded implementations.

Table of Contents

List of tables

List of figures

List of publications

Journal papers:

1. P. Radu, K. Sirlantzis, G. Howells, S. Hoque, F. Deravi, "Information Fusion for Unconstrained Iris Recognition", *International Journal of Hybrid Information Technology*, vol. 4, pp. 1-12, 2011.
2. P. Radu, K. Sirlantzis, G. Howells, S. Hoque, F. Deravi, "A Review of Information Fusion Techniques Employed in Iris Recognition Systems", *International Journal of Advanced Intelligent Paradigms*, vol. 4 (3/4), pp. 211-240, 2012.
3. P. Radu, K. Sirlantzis, G. Howells, S. Hoque, F. Deravi, "A Colour Iris Recognition System Employing Multiple Classifier Techniques", *Electronic Letters on Computer Vision and Image Analysis*, vol. 12 (2), pp. 54-65, 2013.
4. P. Radu, K. Sirlantzis, G. Howells, S. Hoque, F. Deravi, "A Multi-algorithmic Colour Iris Recognition System", selected for publication in an extended version in *Intelligent Decision Technologies: an International Journal*, 2013.

Conference papers:

1. P. Radu, K. Sirlantzis, G. Howells, S. Hoque, F. Deravi, "A Versatile Iris Segmentation Algorithm", *Proceedings of the Special Interest Group on Biometrics and Electronic Signatures (BIOSIG)*, Darmstadt, Germany, 2011, pp. 137-150.
2. P. Radu, K. Sirlantzis, G. Howells, S. Hoque, F. Deravi, "A Visible Light Iris Recognition System Using Colour Information", *Proceedings of the 9th International Conference on Signal Processing, Pattern Recognition and Applications*, Crete, Greece, 2012, pp. 106-113.
3. P. Radu, K. Sirlantzis, G. Howells, S. Hoque, F. Deravi, "A Multi-algorithmic Colour Iris Recognition System", *5th International Workshop on Soft Computing Applications"*, Szeged, Hungary, 2012 – **best student paper award**.
4. P. Radu, K. Sirlantzis, G. Howells, S. Hoque, F. Deravi, "Image Enhancement vs Feature Fusion in Colour Iris Recognition", *Proceedings of the 3rd IEEE International Conference on Emerging Security Technologies,* Lisbon, Portugal, 2012, pp. 53-57.
5. P. Radu, K. Sirlantzis, G. Howells, S. Hoque, F. Deravi, "Optimizing 2D Gabor Filters for Iris Recognition", *4th IEEE International Conference on Emerging Security Technologies*, Cambridge, U.K., 2013.

List of abbreviations

ANN – Artificial Neural Networks

DI – Decidability Index

DWT – Discrete Wavelet Transform

EER – Equal Error Rate

FAR – False Acceptance Rate

FRR – False Rejection Rate

GAR – Genuine Acceptance Rate

HD – Hamming distance

MCS – Multiple Classifier Systems

PCA – Principal Component Analysis

ROC – Receiver Operating Curve

SVM – Support Vector Machines

Chapter 1
Introduction

This chapter will present the generic fundamentals of iris recognition systems, analysing both their advantages and limitations. The problem description and motivation will also be discussed and finally, the research objectives will be highlighted.

1.1 Background

Security of any type of networks and resources has a vital role in our day by day life. Robust authentication methods have to be developed to confirm or deny that the person that tries to be authenticated has the permission to access a system. The three main types of authentication are passwords, tokens and biometrics. While the password may be cracked and tokens may be stolen, the biometric-based authentication is more difficult to be forged than the other two. The physical or behavioural characteristic of a person that may be acquired by a sensor and stored in a database for recognition is called a *biometric trait* or *modality*. A computer system that employs pattern recognition algorithms to process features extracted from biometric modalities is a *biometric system*.

The randomness and richness of iris texture were suggested as potential biometric identification means back in 1980s by Drs Flom and Safir. The first implementation of an iris recognition system capable of an automatized authentication was done by Prof John Daugman in 1994, at Cambridge University (Daugman 1993). Since then, researchers' interest in iris recognition has grown substantially and many other high performing iris authentication algorithms have been published (Boles and Boashash 1998; Ma, Wang et al. 2002; Ma, Tan et al. 2004). However, Daugman's pioneering approach is deployed in most of the commercial and military iris recognition devices currently available.

There are four main reasons why iris modality has become a strong biometric (Daugman 1993; Jain, Flynn et al. 2007):

1) the randomness inherent in its morphogenesis;

2) the claimed stability over time, which reduces the influence of ageing on recognition accuracy;

3) the accessibility of the iris, which eliminates the need of a direct contact between the user and the acquisition device;

4) the protection of which the iris benefits, being part of an internal organ.

The pioneering iris recognition system proposed in (Daugman 1993) uses phase binary features generated by taking the sign of the real and complex value of the pixels of the iris image after the image is filtered with 2D Gabor filters. This phase-based coding applied on near infrared images is the basis of the majority of the iris recognition systems

deployed all over the world in highly secure areas, such as airports or military camps.

Besides the phase-based coding approach, in the available literature there are 3 other important categories of iris recognition methodologies. Together with the most representative works from each category, these are:

a) zero-crossing-based representations, where the wavelet transform's zero-crossings form the features (Boles and Boashash 1998);

b) texture analysis, where multichannel Gabor filters in (Ma, Wang et al. 2002), circular symmetric filters in (Ma, Tan et al. 2003), or Laplacian of Gaussian filters structured in a Laplacian pyramid in (Wildes 1997) are used to extract the features;

c) local intensity variations, where the appearing or vanishing of texture details in iris structure is used to form the feature vector (Ma, Tan et al. 2004).

After the iris image is acquired, a typical iris recognition system operates in four main phases: segmentation, normalization, feature extraction and classification or matching. These stages are illustrated in Figure 1.1, where x_s, y_s and x_p, y_p are the coordinates of the pixels lying on the pupil boundary and iris to sclera boundary respectively.

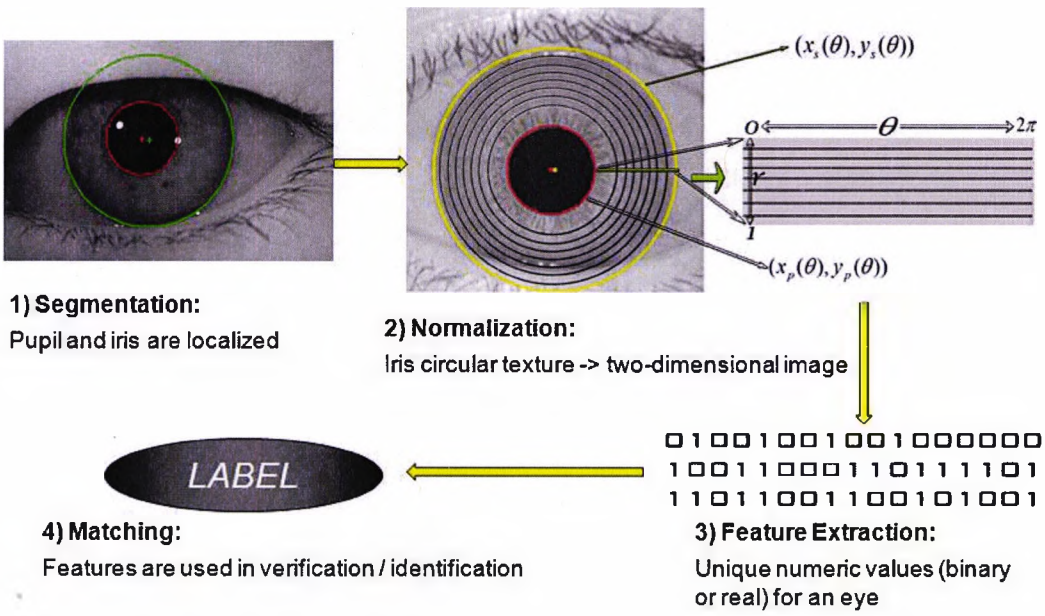

Figure 1.1: Iris Recognition stages

The robustness of the Daugman's approach (Daugman 1993) for iris recognition rely on the properties of the Hamming distance authentic and impostor distributions. One of the most desirable properties of a biometric system, especially if it is used for border control, is to have a False Acceptance Rate (FAR) as small as possible. When matching 2 binary features generated by the 2D Gabor filter, each bit has equal probability p=0.5 of being a 0 or a 1. Making the analogy with fair coin tosses, the theoretical distribution of Hamming distances is given by the binomial (Bernoulli) distribution. When features extracted from different users are matched, the Hamming distance will be approximately 0.5, due to the properties of the Bernoulli distribution, while the same users' features will have a Hamming distance close to 0. A threshold between 0 and 0.5 has to be set in order to take an accept/reject decision. A typical value of the threshold is in the range of [0.27; 0.33], as recommended in (Daugman 2004) for various levels of false matches. The impostors' distribution will terminate very fast, and this fact allows the iris recognition system to operate having a FAR approximately 0. Throughout this thesis we will refer to the iris recognition systems based on binary features and Hamming distances as being a classical iris recognition system.

1.2 Discussion

Although the operation of a classical iris recognition approach has a FAR approximately equal to 0 if the threshold of the Hamming distances is correspondingly set, the False Rejection Rate (FRR) of the system is not close to 0. This is due to the fact that when comparing two iris images belonging to the same user, the dissimilarity measure (i.e. Hamming distance) will increase significantly if one of the iris images is not of an acceptable quality (Tabassi, Grother et al. 2011).

The major disadvantage of a classical iris recognition approach is that it only operates efficiently on near infrared iris images. The melanin pigment, which gives the colour of the eye (Hosseini, Araabi et al. 2010), is not visible in near infrared spectrum. As the reflections from the environmental light sources are captured by the melanin pigment, in near infrared spectrum there are no occlusions caused by the reflections.

In order for the near infrared illumination to be effective, usually the user is asked to

come very close to the acquisition device, to align his eyes with the device and to stand still for a few moments. These constraints are not a significant problem in the enrolling phase, where an individual supervises the process, but in the testing phase, these constraints significantly decrease the practicability of an iris recognition system. To support the prior affirmation, we bring a concrete example: we mention that in 2012, the United Kingdom Border Agency's iris biometric scanning system was removed from service from a number of UK airports, due mainly to the very high rate of false rejection (Daily Mail 2012). According to the press releases, the FRR was too large in some airports, transforming a 9 million British pounds investment in a failure (Daily Mail 2012). What actually caused this high FRR was the poor quality of the iris images acquired in the operational phase. People tired from long journeys were supposed to obey a number of constraints inside the iris scanner which led to poor quality near infrared iris images. This fact reveals that the classical iris recognition technology might not be as robust as it is claimed to be in the literature.

The removal of iris gates from the UK's airports shows the need of an iris recognition methodology which is able to cope with noisy images acquired in the operational stage of the biometric system. The term "noise" is used to refer to various artefacts that affect the iris image quality, as mentioned in (McConnon, Deravi et al 2011). The constraints imposed by the necessary near infrared illumination could be eliminated if the iris images are acquired in the visible spectrum. Although a high accuracy can be obtained using iris biometric, it has not been widely implemented yet on common devices, such as laptops or cell phones mainly because of the constraints implied by the necessity of near infrared illumination. Therefore, a desirable property of an iris recognition system is to be able to operate on colour iris images, whilst maintaining a high accuracy.

Colour iris recognition may be a controversial topic. On one hand the majority of currently deployed iris recognition systems use near infrared illumination. This fact led to the formation of large iris databases which contain images acquired under near infrared illumination and in (Bowyer, Hollingsworth et al. 2012) colour iris recognition is considered to "counter to the approach used by all commercial systems ... and also counter to the majority of academic research". On the other hand, as the mobile phones and tablets become more computationally capable and the need of biometric authentication on this type of devices is apparent, it is necessary that colour iris recognition algorithms be deployed on

such common devices. Mobile phone applications, like BioWallet (Mobbeel 2009) claim to be capable of iris recognition "with a mobile device using only its camera". The advantages and disadvantages of near infrared iris recognition and colour iris recognition are presented in Table 1.1.

	Advantages	Disadvantages
Near infrared	- Almost perfect accuracy claimed on images acquired during enrolment stage, with supervision; - 0 false acceptance rate, due to the rapid termination of impostors' distribution; - Low template size; - Computationally efficient;	- Not designed to cope with noisy iris images; - Requires a high degree of cooperation from the user due to the near infrared illumination; - Images are acquired using expensive acquisition cameras; - Decreased practicability;
Colour	- May be implemented on common hardware, as laptops or mobile phones; - Cheap acquisition cameras; - Increased practicability; - May use eye colour as soft biometric;	- Lower performance compared to near infrared iris recognition systems; - Strong noise present in the images due to melanin pigment;

Table 1.1. Advantages and disadvantages of near infrared and colour iris recognition

1.3 Motivation and research objectives

One of the pioneers of iris recognition in the visible spectrum is Hugo Proenca, who organized an iris recognition competition for colour images called Noisy Iris Challenge Evaluation (NICE) (Lab 2009). It took place in 2 parts: part1 assessed only the segmentation of a subset of UBIRISv2 dataset (Proenca, Filipe et al. 2010) and in part 2 the classification algorithms were assessed on the same images. The winning algorithm of part 1 is described in (Tan, He et al. 2010) and the best algorithm from part 2 is presented in (Tan, Zhang et al. 2012). Proenca et al analyzed the results of the second part of NICE competition in (Proenca and Alexandre 2012), and they reported that by employing a multi-algorithmic approach between the top 5 ranked algorithms, the accuracy of the system increased significantly. However, the accuracies of the tested iris recognition systems are not comparable to the accuracies reported by near infrared recognition systems. The above mentioned competition had numerous participants from all over the world, which indicates that researchers are focusing more and more on colour iris recognition.

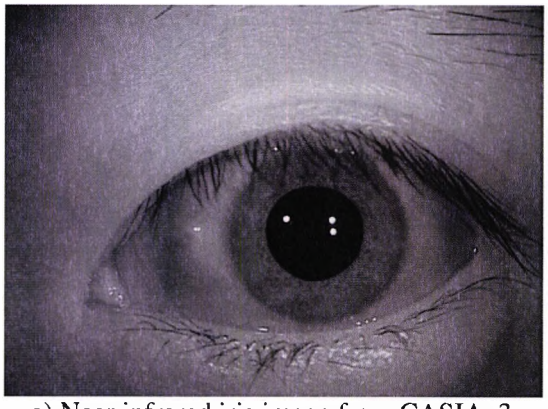

a) Near infrared iris image from CASIAv3 database

b) Colour iris image from UBIRISv1 database

Figure 1.2: Iris images acquired under visible and near infrared illumination

The noise present in colour iris images captured in unconstrained environments makes the classical iris recognition approach to perform poor on this type of images, as shown in (Radu, Sirlantzis et al. 2011). The difference between an iris image acquired under near infrared illumination and one acquired in the visible spectrum may be observed in Figure 1.2.

This work is mainly motivated by the apparent need of a high performing colour iris recognition system, with performances similar to those reported for near infrared iris recognition systems. By developing such a biometric system, in the same time, issues such as the following will be implicitly addressed:

- "unlocking" iris recognition technology on common devices, such as mobile phones, tablets and embedded devices using standard cameras;
- making iris recognition an affordable biometric authentication technique for organizations and institutions by eliminating the need of expensive near infrared acquisition cameras;
- allowing the usage of soft biometrics from an eye image, such as the eye colour, skin texture and the region around the eye (Park, Jillela et al. 2011);
- increasing the distance between the user and acquisition device;
- outdoor iris recognition;

- eliminating the exposure of the eye to near infrared illumination;
- considerably increasing the range of scenarios and applications where iris recognition may be deployed.

As the results from the second part of the above mentioned NICE competition showed that the accuracy of a colour iris recognition system may be increased by employing various fusion techniques (Proenca and Alexandre 2012), it appears that appropriate algorithms which fuse various information from the colour eye images are the way to be followed for colour iris recognition.

The United States National Institute of Standards and Technology (NIST) conducted a series of iris recognition competitions (Grother, Tabassi et al. 2009), where the submitted algorithms were tested on large scale databases containing near infrared iris images. These competitions allowed the creation of an ISO standard for near infrared iris images (Lu and Lu 2005), which will promote the interoperability between various iris recognition acquisition devices and authentication algorithms. Generally the near infrared iris image data standard specifies the thresholds for different iris image quality measures, which from a practical point of view are translated into how large the constraints on the user have to be.

For iris images acquired in the visible spectrum there hasn't been created a standard yet, but over the past several years advances have been made in colour iris recognition. The investigation made in thesis represents a basis for future work towards the standardization of colour iris images for iris recognition with reduced constraints.

The main aim of the work to be presented here is the investigation of different types of fusion techniques which could be successfully employed in colour iris recognition. By developing information fusion algorithms, we aim to find the best balance among accuracy, computational resources, security and flexibility in a colour iris recognition system. In this way, the obtained colour iris recognition systems are suitable to be deployed both in mobile and static scenarios. The information fusion techniques developed throughout this work have a gradually increasing complexity. More specifically, the investigation reported will analyse and evaluate three main types of information fusion approaches which may be employed in colour iris recognition:

1) multi-algorithmic approach (Ross, Nandakumar et al. 2006), reported by the organizers of NICE competition (Proenca and Alexandre 2012);

2) texture and colour fusion approach (Park, Jillela et al. 2011), where the eye colour is treated similar to soft biometric information;

3) Multiple Classifier Systems (MCS) approach (Kuncheva 2004), a powerful tool of Pattern Recognition, which hasn't been widely employed in iris recognition.

1.4 Contribution and thesis organization

The generic contribution of this thesis is the investigation of how the three information fusion techniques mentioned previously in Section 1.3 are beneficial to be employed in colour iris recognition systems. The contributions corresponding to the iris recognition algorithms which employ one of the three individual fusion approaches may be listed as follows:

1) Iris recognition employing multi-algorithmic approach:

   a. A versatile iris segmentation methodology is introduced;

   b. An informational theoretic analysis of iris texture for different colour channels is introduced;

   c. An iris feature extraction method based on a 3-bit encoder of the 8-neighborhood is proposed;

2) Iris recognition employing texture and colour fusion approach:

   a. A method to optimize the parameters of 2D Gabor filters for colour iris images is proposed;

   b. A binarization method of real-valued colour features based on wavelet transform is presented;

   c. A fuzzy logic score fusion technique between colour features and texture information is introduced;

3) Iris recognition employing MCS approach:

   a. Adaptation of standard iris features proposed in the literature for near infrared iris images to be useful in colour spectrum;

   b. A MCS architecture which enhances the iris recognition system's accuracy and robustness on colour iris images is proposed;

   c. A comparison of the accuracy of the iris recognition system employing MCS obtained on 50% and 100% of the available iris texture information.

The remainder of the thesis is organized as follows: Chapter 2 will introduce the literature of relevance to colour iris recognition systems, focusing on the biometric systems which employ information fusion techniques. Chapter 3 will analyse the multi-algorithmic approach for iris recognition, by fusing at score level 3 basic iris recognition algorithms. Chapter 4 will introduce a novel fusion approach between iris texture information and eye colour and Chapter 5 will investigate how MCS architectures may be developed for colour iris recognition. Finally, the conclusions, limitations and directions for future work are given in Chapter 6.

Chapter 2
Literature Review

This chapter will present the state of the art in iris recognition techniques operating on colour iris images. Initially the most representative standard near infrared iris recognition algorithms will be described and then the focus is moved towards the algorithms that use colour information for a less controlled environment operation. The benefits and drawbacks of the fusion mechanisms employed in the reviewed iris recognition systems are highlighted.

2.1 Introduction

Among the biometric systems that have been developed so far, iris recognition systems have emerged as being one of the most reliable (Wildes 1997). A review of iris recognition systems may be found in (Bowyer, Hollingsworth et al. 2008), having a generic content, covering the "historical development" and state of the art up to 2007 in "image understanding for iris biometrics". The review made in (Bowyer, Hollingsworth et al. 2008) discusses all the 4 phases of an iris recognition system together with existing iris images datasets, and is describing mainly near infrared iris recognition systems.

A significant increase in the number of papers published on iris recognition occurred after 2008. A work that reviews the papers published on iris recognition between 2008 and 2010 is found in (Bowyer, Hollingsworth et al. 2012). In this review paper, a number of colour iris recognition systems were included, which suggests that the researchers' interest in colour iris recognition is increasing. This second review also analyses the different aspects of iris recognition systems in general, from iris image acquisition, to datasets and multi-biometrics involving iris.

As more and more papers have been focusing on iris recognition systems with reduced constraints, the need of a survey of these papers was apparent. A review that strategically categorizes iris recognition systems which address operation under reduced constraints using various fusion techniques and different sources of information is made in (Radu, Sirlantzis et al. 2012). In contrast to the 2 previous reviews made by Bowyer et al, the review paper in (Radu, Sirlantzis et al. 2012) focuses mainly on the classification stage of recent iris recognition systems in which a fusion technique is employed.

This chapter will review the most significant colour iris recognition techniques which employ information fusion techniques and therefore do not fit the pattern of a classical iris recognition system. However, the foundations of the iris recognition systems which employ information fusion techniques are the classical approaches that were initially proposed in the literature. This chapter will not detail the segmentation, normalization and pre-processing of the iris image, it will focus on feature extraction and information fusion. A work that reviews the segmentation methodologies employed in iris recognition may be found in (Radman, Jumari et al. 2011).

Along this work the terms "multimodal system" and "multibiometric system" are

used to denote two different things. The issue of information fusion in multibiometric systems is discussed in (Ross and Jain 2003). One could consider the fusion in multibiometric systems as the combination of information belonging to different modalities. Arun Ross et al proposed a taxonomy of multibiometric systems in (Ross, Nandakumar et al. 2006; Jain, Flynn et al. 2007). They divide these systems into six categories, where one of them is the multimodal system. Four of the categories refer to biometric systems that use only one modality, by fusing information resulted from different feature extraction methods (multi-sensor systems and multi-algorithm systems in Ross's taxonomy), from more than one instance of the same modality, e.g. both irises (multi-instance systems) and from more than one sample of the same trait (multi-sample systems). The sixth category, i.e. hybrid systems, refers to those biometric systems that comprise combinations of the previous five categories.

In the taxonomy proposed by Ross et al, a multibiometric system has a "broader scope than layered biometrics", including not only systems where different biometric modalities are fused, but also systems which operate on a single modality, but use various sources of information. The term "multibiometric" is used according to this taxonomy along this work.

The remainder of this chapter is organized as follows: Section 2.2 will present the most popular iris recognition techniques to acquaint the reader with the main classical approaches developed along the years for iris recognition. Section 2.3 will review the colour iris recognition systems available in the literature and in Section 2.4 the iris recognition algorithms which use information extracted from more than one wavelengths spectrum are surveyed. The chapter conclusions are given in Section 2.5.

2.2 Popular iris recognition techniques

The iris recognition approaches surveyed in this section have a classical structure of an iris recognition system, in the sense that they employ a single feature extraction method and a distance based matching. Their performances were reported only on iris images acquired in near infrared spectrum.

The most common iris recognition technique is also the first one which was

proposed in the literature and is depicted in (Daugman 1993). The working principle of this method is depicted in section 1.1 (see Figure 1.1). It was designed to operate on near infrared images and when it is applied on noisy colour iris images, its error rates are more than double, as reported in (Radu, Sirlantzis et al. 2011). The Hamming distance (HD) used for matching gives the system simplicity and makes it very convenient for practical implementations. The pioneering iris recognition approach is also computationally efficient as it relies on the fact that the *iris codes* are expressed in binary format and not in floating point numbers.

In 1996, Wildes et al propose in (Wildes, Asmuth et al. 1996) another system for iris recognition. The system proposed by Wildes et al is compared with the Daugman's system in (Wildes 1997). For feature extraction, isotropic band pass decomposition is derived from application of Laplacian of Gaussian filters to the image. A Laplacian pyramid is built with 4 different levels corresponding to 4 resolutions of the original image. The rationale behind these multi-scale representations is that some features of the iris texture are distinctive at higher resolutions and others are more distinctive at lower resolutions. For matching, the correlation between 2 images is computed for different bands and further, a variance of the correlations is computed. This method was developed only for the verification scenario. The reported FAR and FRR were 0, but only for a small number of users.

Another approach for iris recognition was proposed by W. Boles and B. Boashash in 1998 (Boles and Boashash 1998). Grey level intensity values for virtual concentric circles, with the centre at the pupil's centre represent data sets called *iris signature*. The iris signatures are periodic functions of period N and the zero crossing representations of the dyadic wavelet transform form the actual feature. The matching phase consists of calculating a degree of dissimilarity between zero crossing representations of probe and gallery images. No numeric accuracies were reported for FAR or FRR.

A reference iris recognition algorithm was developed by Li Ma et al using multichannel Gabor filtering (Ma, Wang et al. 2002). The unwrapped image is vertically divided into eight smaller sub-images. 20 Gabor filters with different frequencies and directions are applied on each of the eight sub-images and a total of 160 output images are obtained. For each one of the 160 images, the mean absolute deviation is computed and the matching distance is the weighted average of the 160 values. For performance evaluation, 50 iris classes were used and with 5 training samples, the identification rate was 99.09%.

The FAR and FRR were not explicitly specified, only the ROC (receiving operating characteristic) curve has been provided.

Li Ma et al developed another iris recognition technique, using circular symmetric filters (Ma, Wang et al. 2002). The unwrapped image is enhanced with local histogram equalization and noise is removed with low pass Gaussian filter. In feature extraction phase, circular symmetric filters were used. The difference between circular symmetric filters and 2D Gabor filters is the sinusoidal function, which in this case is circular and symmetric. Also, circular symmetric filters do not have an imaginary part. In the filtered image, average absolute deviation is computed on 8 x 8 pixel blocks, resulting in a total of 384 feature values. The classification method used is a modified version of Nearest Feature Line (Li and Lu 1999). The algorithm was tested on 134 classes with a 99.85% correct identification rate.

The above mentioned algorithms are among the most popular iris recognition approaches available in the literature. Other classical iris recognition techniques have been developed along the years and their reported performances were comparable to the accuracies of the above mentioned algorithms. Table 2.1 summarizes the characteristics of the most representative classical iris recognition algorithms available in the literature.

References	**Feature Extraction**	**Performance**
(Daugman 1993), (Daugman 2007)	Complex-valued coefficients obtained with 2-D Gabor filters. Their real and imaginary part signs specify the coordinates of a phasor in a complex plane, resulting 2048 bits. (Iris Code)	Very fast matching process due to binary features type. EER ≈ 0.1 %
(Wildes, Asmuth et al. 1996)	Normalized correlations computed between 8x8 pixel blocks for 4 resolutions of the image which are building a Laplacian Pyramid of Gaussian filters.	Tested only in verification mode. FAR=0% and FRR=0% for 100 users.
(Boles and Boashash 1998)	Zero-crossing representations of wavelet transform at different resolution levels over concentric circles. (Iris Signature)	Not reported numerically, only graphically.
(Ma, Wang et al. 2002)	1-D Vector of 160 Average Absolute Deviations of 64x64 sub-images processed with 2-D Gabor Filters.	Identification rate = 99% on 50 users.
(Ma, Wang et al. 2002)	1-D Vector of 384 Average Absolute Deviations of 8x8 sub-images after applying Circular Symmetric Filters on unwrapped image.	Identification rate = 99.85% on 134 users.
(C. Tisse, L. Martin et al. 2002)	768 bits are obtained from the *analytic* image – Hilbert Transform of the initial image.	Computationally effective, tested on 30 classes with no numerical accuracies reported.
(Ma, Tan et al.	Position of local sharp variations of the unwrapped	Identification Rate=100%

References	Feature Extraction	Performance
2004)	image from which 1-D Intensity Signals are obtained. The positions are determined with 1D dyadic wavelet, resulting in a 1D vector of 660 integer components.	for 306 users.
(Lu and Lu 2005)	First a map of dark blob pixels is obtained by filtering the iris image with a Gaussian filter followed by a Laplacian differential operator. Then, by applying morphological operations, the most discriminant blobs are segmented.	EER=0.14 % for 108 users.
(Miyazawa, Ito et al. 2005)	A function of the 2D Discrete Fourier transform of iris image is computed for different 11 by 11 pixels sub-windows. The maximum of the functions for each sub-window forms the feature vector.	EER=0% for 108 users.
(Peng, Jun et al. 2006)	Modified log-Gabor filters are used to extract binary iris phase features, similar to Daugman's approach.	EER=0.28 % for 108 users.
(Monro, Rakshit et al. 2007)	Differences of discrete cosine transform coefficients are computed between overlapped angular regions from the unwrapped iris image.	Identification rate=100% and EER=0.05% for 306 users.
(Yu, Zhang et al. 2007)	Multi-channel 2D Gabor filters are applied and from the resulted sub-images 512 key points are extracted.	Identification rate=97.18% for 108 users.

Table 2.1. Classical iris recognition systems

In iris recognition, a measurement of performance of the biometric system is the Decidability Index (DI) *d'*. This statistical metric is often preferred to report the discriminative capability of an iris recognition system (Bouridane 2009). DI is a measure of separability of the authentic and impostor score distributions of a biometric system and is given by the following equation:

$$d' = \frac{|\mu_a - \mu_i|}{\sqrt{\frac{\sigma_a^2 + \sigma_i^2}{2}}} \tag{2.1}$$

where μ_a and μ_i are the means of authentic and impostors distributions and σ_a, σ_i are the standard deviations of the distances corresponding to the authentic and impostor distributions respectively. The distributions are obtained by computing the distances between all possible combinations of authentic and impostor images. The DI reported by the pioneering iris recognition approach of Daugman (Daugman 1993) has a value of approximately 7 for iris images acquired using different acquisition devices and 14 for iris images acquired by the same acquisition device. These values of the DI are considered the

best in the literature, but are obtained on images acquired mostly under the enrolment stage, where the constraints put on the user were high.

2.3 Colour iris recognition systems

After very high accuracies were reported for iris recognition systems operating on near infrared images, researchers started to develop colour iris recognition methodologies too. Around the year 2005 the first colour iris recognition works were published (Proença and Alexandre 2005), (Qiu, Sun et al. 2005). The number of works published along the years that are using colour iris images for biometric recognition is illustrated in Figure 2.1. We included in Figure 2.1 the papers published on IEEE Xplore, SpingerLink and Science Direct, as these appear to be the three major sources of publications in the field of colour iris recognition.

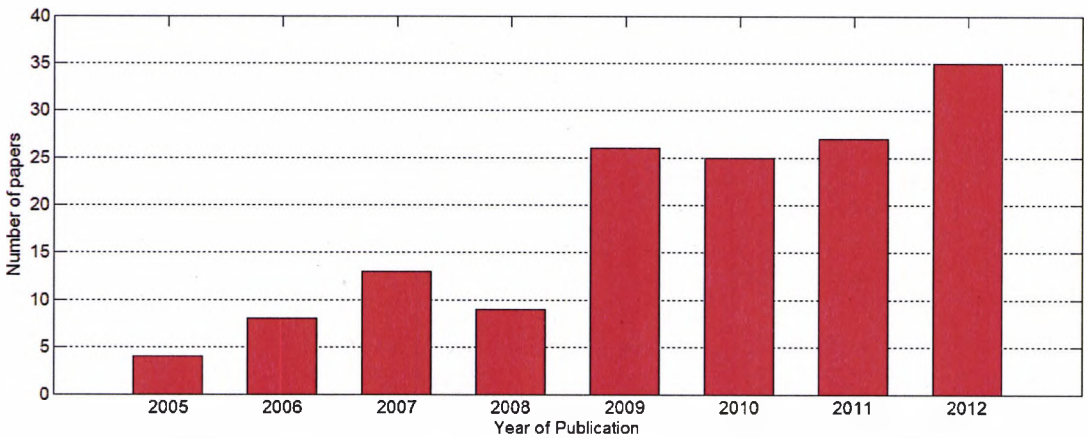

Figure 2.1. Colour iris recognition related papers published from 2005 to 2012

A similar figure to Figure 2.1, but for all iris recognition related papers from IEEE Xplore and SpringerLink may be found in the review of Bowyer et al (Bowyer, Hollingsworth et al. 2012). It may be observed in the figure from the Bowyer's et al review paper that the number of papers published on iris recognition in the first 8-9 years after 1994 has similar values to the colour iris recognition papers included in Figure 2.1. This

fact clearly shows that researchers' interest in colour iris recognition is increasing. The accuracies of the colour iris recognition systems published is not yet comparable to those of near infrared iris recognition systems, as it is observed in (Proenca and Alexandre 2012).

In this section we will review the colour iris recognition systems by grouping them according to their corresponding matching / classification approach. Subsection 2.3.1 will discuss the distance-based matching, subsection 2.3.2 will analyse the multi-algorithmic colour iris recognition systems and subsection 2.3.3 will analyse the colour iris recognition systems which employ statistical-based approaches for classification.

2.3.1 Colour iris images databases

At the moment of writing this thesis, there are only 3 publicly available colour iris images datasets. The first colour iris images dataset publicly available was UPOL (Dobeš and Machala 2004). This dataset was released in 2004 and contains colour RGB images acquired in a highly controlled environment using a professional camera. It has 64 users enrolled with 3 images for left and right eyes, totalling 384 iris images. The images are 768 by 576 pixels in raw format. The iris is already segmented in this database.

In the same year, UBIRISv1 database (Proença and Alexandre 2005) was released for public use. This database consists of 1877, colour RGB images with a size of 800x600 pixels. It was collected from 241 individuals in 2 sessions. The enrolment was made using only the right eye with 5 images for each user. In the first session the images are captured by minimizing noise factors. In the second session the environment is one with reduced constraints and noise factors are present in the images, such as poor focus, reflections and luminosity variations. In the first session, all 241 users have been enrolled, resulting in a total of 1205 images, while in the second session, only 132 users out of the 241 are enrolled. The diameter of the iris is approximately 350 pixels, larger than the recommended iris diameter of 200 pixels for near infrared iris images (Daugman 2004).

In 2009, the second version of the UBIRIS database was released (Proenca, Filipe et al. 2010). The setup for the image acquisition of UBIRISv2 database aimed for an acquisition of images in a significantly unconstrained environment. The images were captured at a distance of 4 to 8 meters, while the subjects were walking. The images were

acquired in two separate sessions from 261 subjects, with 15 images per session per subject. Approximately 60% of the users are present in both sessions. The iris images have a dimension of 800 by 600 pixels and the average iris diameter is 140 pixels, which is equal to the minimum recommended diameter for near infrared iris images (Daugman 2004). Figure 2.2 illustrates iris images from all the three datasets.

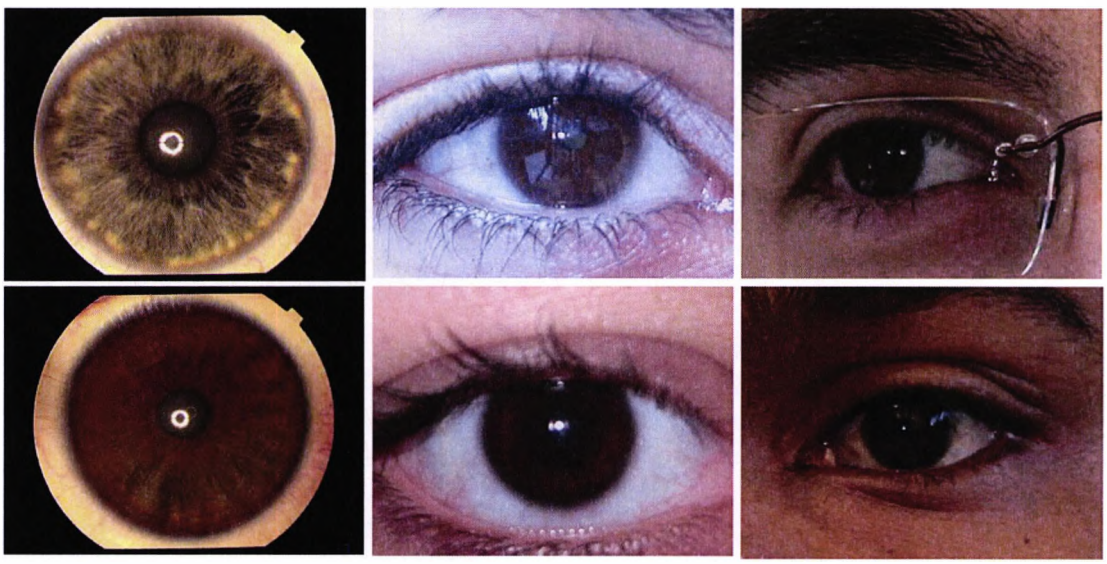

a) b) c)

Figure 2.2. Colour iris images from a) UPOL; b) UBIRISv1; c) UBIRISv2 databases

2.3.2 Colour iris recognition systems employing distance-based matching

As the need of a colour iris images database was apparent, Hugo Proenca et al collected a 241 users database called UBIRISv1 (Proença and Alexandre 2005), which is publicly available since 2005. Experimental results were reported on this database by the vast majority of colour iris recognition publications. This section will review the colour iris recognition systems which employ a traditional distance computation in the matching phase, similar to iris recognition systems operating under near infrared illumination.

In (Castañon, de Oca et al. 2006) the iris features were represented by a set of cumulative histograms computed for small rectangular sub-windows from the unwrapped iris image. In the matching phase Euclidean distance was computed between all possible combinations of images. The obtained EER of the system was approximately 9% when images from 173 users were used. The same Euclidean distance is used in (Proença and Alexandre 2007), where the features are real-valued vectors generated by the calculations of entropies from overlapped angular patches of unwrapped iris image. An EER of 8.9% was reported for 80 users from UBIRISv1 database.

The classical HD was employed in (Proenca and Alexandre 2007) to observe the benefits of a quality assessment method in matching the noisy colour iris images. The aim of the quality assessment was to select parts of the binary iris code which are maximizing an objective function. The objective function is a sum of quality values measured for bit strings extracted from different areas of the image. Only the selected parts of the total 2048 bits iris code are used to calculate the Hamming distance. By employing this quality assessment phase to reduce the feature size of the iris image, Proenca et al reported an EER of 6% for 40 subjects from UBIRISv1 database, while with the classical Daugman's approach the reported EER was 12%. HD was also employed in (Szewczyk 2007) to match the binary features extracted using bi-orthogonal wavelets. The coefficients of wavelet image decomposition were compared to their median value and one bit was stored as 0 if the corresponding wavelet coefficient was less than the median, otherwise the bit is set to 1. The bits corresponding to the fourth level of decomposition were reported to be more discriminative. A remarkable EER of only 0.6% was reported for a number of 241 users from UBIRISv1 database, Session 1. This result was obtained by not including 12 occluded iris images in the experimental setup. The obtained DI was 6.3, comparable to the DI reported in the pioneering iris recognition approach (Daugman 1993) for near infrared images. In (Hui, x et al. 2010), 1D and 2D log-Gabor filters are used for extracting phase bits from 200 iris images of UBIRISv1 dataset and the matching is done using the same HD. An EER of 2.83% is reported for the 200 colour iris images.

In (Bodade, Talbar et al. 2008) features were extracted using multi-directional complex wavelets by computing the energies and standard deviations of detailed sub-bands coefficients. A feature vector of 72 real values is created and the matching is done by employing a Canberra distance. The experimental setup is not the classical one, where all

the possible distances are computed. A number of 500 images were used from UBIRISv1 database for training and the rest for testing. The reported mean FRR for a value of the FAR=0 was 2.6%, but the severely occluded iris images were not included in the experiments. Complex wavelets were used also in (Hariprasath and Mohan 2008) to extract binary iris features of length 4096. The matching is performed using a Hamming distance, but the results are reported only for 30 users from UBIRISv1 database.

Wavelets were employed in (Jing, Xinge et al. 2008) to extract iris feature from colour images. The feature vector consists of the barycentre of the positive wavelets coefficients and the barycentre of the negative wavelets coefficients for a number of filtered sub-band coefficients. A feature size of 384 real values was obtained. The distance between two feature vectors was computed using a modified Euclidean distance. The experiments were run on all colour iris images from UPOL database (Dobeš and Machala 2004) and 1000 images from UBIRISv1 database. The results are only reported graphically, but they are comparable to the results obtained using Daugman's approach. The advantage of Jing et al method compared to Daugman's approach is that is very robust to the shifting of the unwrapped image, i.e. insensitive to eye rotation caused by head tilt. Jing et al extend the above described algorithm in (Jing, Xinge et al. 2008).

Grey level co-occurrence matrix (GLCM) is adapted in (Chen, Huang et al. 2009) for colour iris images by expanding the classical matrix in the third dimension corresponding to the colour channels of a colour space. The 3D GLCM is computed for four different directions of the neighbour pixels and for various sub-images of the original unwrapped iris image. The final feature vector is obtained by averaging statistical measures obtained from matrices corresponding to the 4 directions. In the matching phase, the Euclidean distance was employed. The experiments were conducted on 195 classes from UBIRISv1 dataset, Session 1 and the obtained EER was 1.13 %.

An iris recognition method which considers the edges of the iris texture is proposed in (Sudha, Puhan et al. 2009). The major advantage of this approach is that the edge maps of the texture are binary strings and they are appropriate for mobile or embedded implementations. A modified Hausdorff distance is employed in the matching stage. The method was benchmarked on UPOL (Dobeš and Machala 2004) dataset and the reported identification accuracy was 98.44 %. A higher identification accuracy is obtained in (Radu, Sirlantzis et al. 2011) on UPOL database, by using the classical 2D Gabor filters. In the

latter work, the identification accuracy reaches 100% using only the red channel of the iris images. The classical Daugman's approach, with modifications in the segmentation stage is also applied in (Ferreira, Lourenço et al. 2010) on UBIRISv1 dataset, with a reported identification rate of 87.2 %.

A shape-based iris feature extraction is proposed in (Hosseini, Araabi et al. 2010). After the colour iris images are enhanced, they are binarized to obtain the discriminative shapes from the iris texture. The extracted shape descriptors are three: the radius vectors from the centre of the shape to its border, for a given direction; the size of the shape of the iris texture for a given direction and the angle of the tangent at boundary points. The final feature size is 2400 integer-valued components, with a maximum value of 256. They are converted to gray (binary) codes and the matching is done using a product of sums of individual sub-feature HDs. In the experimental results, the reported GAR was 95.90% for UBIRISv1 Session 1 and 94.92% for Session 2, when the FAR was equal to 1%, but the noisiest 50 iris images were not included in the experiments. These accuracies were reported for 4 gallery and one probe iris image.

In (Lili, Wen-Shiung et al. 2010), embedded zerotree wavelets, which were introduced in (Shapiro 1993), are used to extract binary features from colour iris images. Initially, the iris image passes through discrete wavelet transform, and the obtained coefficients are binarized using a threshold generated by the zerotree method. The experiments were run on 975 images from UBIRISv1 dataset, Session 1 and the reported identification rate was 100%, while the reported EER is 0%. These accuracies were reported for 3 gallery and two probe iris images. The same experimental setup with 3 gallery images and 2 probe images was created in (Farouk 2011) to benchmark a colour iris recognition system. In the latter approach, the features are represented by labelled graphs nodes. A similarity function is introduced to compare two graphs. In the experiments, 1171 iris images from UBIRISv1 dataset, Session 1, are used. The reported identification rate is 97.17 %.

A colour iris recognition method based on weighted co-occurrence phase histograms is proposed in (Li, Liu et al. 2012). Using the gradients obtained after edge detection, the space between 0 and 2π is divided in bins and for a given pixel pair that are at a fixed distance, the bin corresponding to the angle between the two pixels is incremented. In the matching phase, the Bhattacharyya distance is employed. This method was tested on

UBIRISv2 dataset and it was ranked 5th in NICE II (Lab 2009) competition, with a DI of 1.47 and an EER of 0.22, for 1000 noisy iris images. The same Bhattacharyya distance is employed in the colour iris recognition algorithm from (Liu and Li 2012) which uses scale invariant features extracted from the iris texture. The algorithm extracts the features from non-overlapping sub-images of the unwrapped image. The reported EER is 7.66% for 1430 images from UBIRISv1 dataset and 24.66% for the 1000 images of UBIRISv2 dataset used for training in NICE II competition.

The 7th place in NICE II competition was obtained also by a distance-based algorithm, depicted in (Li and Ma 2012). In the latter work, the gallery image is divided into 16 by 16 pixels non-overlapping blocks and they are registered individually with their corresponding sub-images from the probe image. Classical 2D Gabor filters are employed for feature extraction and modified HD is used for matching. The reported DI on 1000 images from UBIRISv2 database is 1.18. The 8th place in NICE II competition was obtained by the method presented in (Szewczyk, Grabowski et al. 2012). An empirical approach is used to find the appropriate reverse bi-orthogonal dyadic wavelet transform, for which symmetry is possible. The wavelet coefficients were binarized by comparing them to their median value. The reported DI is equal to 1.09, when the method was tested on 1000 images from UBIRISv2 dataset. The experimental results of the NICE competition are analysed in (Proenca and Alexandre 2012).

A zero-crossing of the curvelet transform coefficients is employed in (Ahamed and Bhuiyan 2012) to extract real valued features from colour iris images, similar to the original method proposed in (Boles and Boashash 1998) for near infrared iris images (see Table 2.1). The zero crossings of the 4th level of decomposition coefficients are calculated, after an image background subtraction is applied to enhance the iris texture. For the matching phase, a correlation coefficient was computed. In the experimental setup, 4 images were used for training and one for testing. The reported EER for UBIRISv1 database is 2.49 % and the identification rate is 97.5 %.

Hyper-complex or quaternion representations of phase information from iris texture are employed in (Ghouti and Al-Qunaieer 2009) to extract iris features. Essentially, the quaternion numbers are extensions of the regular complex numbers to higher dimensions. The method is benchmarked on UBIRISv1 database, but the accuracies are only graphically reported. Quaternion numbers are also used in (Kumar and Tak-Shing 2012) to encode the

phase information from the iris texture. In the latter work, the algorithm is benchmarked on the 1000 iris images from UBIRISv2, which were used in NICE II competition, but the experimental results are only reported graphically.

From the papers surveyed in this subchapter we may conclude that the iris recognition approaches which employ a classical distance based matching and using only a single feature extraction method may have limitations in coping with noisy colour iris images. The majority of the colour iris recognition systems surveyed in this subchapter do not report a remarkable accuracy on noisy iris images. The only high accuracies are reported by the works where the noisy colour iris images were not included in the experimental setup. From colour iris images, features may be extracted using more than one approach and various fusion techniques are more beneficial to use over the traditional distance-based matchers. In the next section we will analyse the colour iris recognition algorithms which extract multiple types of features.

2.3.3 Multi-algorithmic colour iris recognition systems

Two of the main iris recognition approaches, one based on 2D Gabor filters (Daugman 1993) and the second based on zero crossing representation (Boles and Boashash 1998) which were initially proposed for near infrared iris images, are used in (Wang and Han 2006). A min-max score level fusion was employed to combine the scores generated by the two iris recognition approaches. The experiments were conducted using 780 good quality images from UBIRISv1 dataset and the obtained EER was equal to 0.27%. The work mentioned above is extended in (Wang, Han et al. 2007), where the same two classical iris recognition algorithms were employed, but the fusion was done using Support Vector Machines (SVM). The reported EER on the 780 good quality images from UBIRISv1 database is equal to 0.41%.

In (Sun, Melgani et al. 2008) the binary phase features are extracted by applying log-Gabor filters on the red, green and blue channels. A range of basic fusion techniques are employed to fuse at the score level the match scores yield by each colour channel. The best accuracy was reported for the weighted sum fusion rule, with an identification rate of 90.7% for all the images of UBIRISv1 dataset, Session 1, and 66.1% for all the images of

UBIRISv1 dataset, Session 2. Log-Gabor filters are also employed in (Fenghua and Jiuqiang 2009) together with Discrete Cosine Transform, to extract two feature types. The fusion methodology employed was SVM. The dataset used in the experiments was UBIRISv1, of which a number of good quality 1030 images were used. The reported EER is equal to 0.33%.

A work describing an iris recognition system processing colour iris images from UPOL database (Dobeš and Machala 2004) may be found in (Demirel and Anbarjafari 2008). RGB iris images were converted to Hue Saturation Intensity (HSI) colour space and the features used are the histograms of the HSI space. For each channel, a correlation coefficient was computed between the histograms of the testing and enrolled images. The fusion of the three results was done at the decision level by majority voting. The same authors used in (Demirel and Anbarjafari 2008) six histograms as features extracted from colour iris images: three obtained from RGB channels and three from YCbCr colour space. The similarity between histograms was computed with Kullback-Leibler Distance and the fusion of the 6 class labels was realised with the same fusion technique of majority voting. Besides the decision level fusion, a score-level fusion was also used. The 6 histograms were concatenated and the Kullback-Leibler Distance was computed for the extended feature vectors. With this fusion technique, the correct recognition rate was 98.44%, slightly better than the accuracy obtained with majority voting technique employed in the initial work.

A majority voting fusion mechanism is also employed in (Proenca and Alexandre 2007) to deal with non-cooperative iris recognition. After segmentation, the unwrapped iris image is divided into six regions and on those regions 2D Gabor wavelet feature extraction techniques are applied. Consequently six distinct biometric signatures are obtained. For each region, a dissimilarity threshold was set for features extracted from that region. When an input image is presented to the system, if most of the dissimilarity values are below the respective threshold of a region, the image is considered to be of an authentic user. The EER reported for 800 colour iris images from UBIRIS v1 database is 2.38%. 2D wavelet decomposition was employed also in (Tajbakhsh, Misaghian et al. 2009) to extract features from overlapped regions of the unwrapped iris texture. A region based approach for colour iris recognition is motivated by the potential noise reduction, by splitting the noisy regions into several blocks. Wavelet coefficients were selected for each block and they were binarized by comparing them to 0 and by finding the positions of the zero crossing of the

first derivative. The binary strings resulted from the 2 coding strategies were concatenated. The method was benchmarked on UBIRISv1 dataset, using the subjects enrolled in both sessions. Two out of ten images were used as gallery and the remaining eight for testing. The reported EER is 0.66%.

Three types of features are extracted in (Mukherjee and Chanda 2011) from colour iris images: GLCM based features, edge based features and Local Binary Pattern (LBP) based features. The fusion is made using a two-class SVM and the experimental setup employed a five-fold cross validation. The reported verification accuracy was 99.6 % on UBIRISv1 database.

An information theoretic analysis of which colour channel reveals better the iris texture is presented in (Radu, Sirlantzis et al. 2011). According to the results reported in (Radu, Sirlantzis et al. 2011), the red and green channels reveal better the iris texture from the RGB colour space and the intensity channel from HSI colour space. The classical phase features are extracted from the red, green and intensity channels and a score level fusion is employed. All the images from UBIRISv1 dataset were used in the experiments. When using 4 gallery images and 1 probe image for all the users, the reported rank 1 identification rate for all Session 1 images is 99.25% and 91.96% for the Session 2 images.

In (De Marsico, Nappi et al. 2011) features are extracted from colour iris images using LBP and the Laplacian operator proposed in (Lu and Lu 2005) for near infrared images. A score level fusion is applied by taking the average of the individual scores. The images were converted to grayscale before feature extraction. The method was benchmarked on UBIRISv1 database and UBIRISv2 database and was ranked the sixth in NICE II competition (Proenca and Alexandre 2012), with a DI of 1.25.

This subsection reviewed the iris recognition systems where more than one feature type is extracted from the iris texture and a score level fusion is employed. The works reviewed in this subsection indicate that a multi-algorithmic approach is beneficial for colour iris recognition. The accuracy of multi-algorithmic approaches employed in colour iris recognition systems are generally higher compared to the accuracies reported by the distance-based approaches. The down side of the multi-algorithmic iris recognition systems is the longer processing time needed for additional feature extraction and information fusion.

2.3.4 Colour iris recognition systems employing statistical-based matching

One of the first colour iris recognition algorithms that employed a statistical-based classification is depicted in (Qiu, Sun et al. 2005). In the feature extraction phase, the classical 2D Gabor filters were employed. Two real valued features were stored for 240 Gabor filters, resulting in a feature vector of 480 components. The two features are represented by the Gabor Energy and Gabor Energy Ratio. The method was benchmarked on a joint dataset composed of mixed colour images from UPOL (Dobeš and Machala 2004) and UBIRISv1 and near infrared images from CASIAv1 (Inst. of Automation 2004). An AdaBoost algorithm (Kuncheva 2004) was used to learn a classification function and the reported identification accuracy is 86.48 %.

A different approach to those generally used for texture analysis was employed in (Garza Castañón, de Oca et al. 2006) to extract iris features from colour images. The feature extraction method consisted in applying stochastic autoregressive models with exogenous input, which is usually used to model the behaviour of a dynamic system in discrete time. The experiments were conducted on 173 users from UBIRISv1 database, with a rank 1 identification accuracy of 86.31%.

The colour of the iris is used in (Krichen, Chenafa et al. 2007) to reduce the number of classes which possibly contain genuine images. The possible pixel colours are reduced to a smaller number and a modified Hausdorff Distance is computed between the hue channel pixel distributions for a number of images. From the hue channel distributions, a Gaussian Mixture Model is trained on two classes: light coloured irises and brown irises. When a new probe image is presented to the system, only the irises having a light/dark colour corresponding to the highest probabilities produced by the Gaussian Mixture Models are considered. The method was benchmarked on 1727 images from UBIRISv1 database and the reported EER is 1.2% for the first session and 8% for the second session. The reliability of eye colour to be used as a soft biometric is also analysed in (Dantcheva, Erdogmus et al. 2011), where an eye detection approach is proposed using the eye colour. In (Qin 2011) an iris database indexing technique based on colour information is proposed. The benefits of fusing colour features and texture information is also shown in (Proença and Santos 2012).

In (Lee, Huang et al. 2007) features are extracted from different regions of the

unwrapped image using local edge patterns techniques. 2D Linear Discriminant Analysis (LDA) is first employed to reduce the feature dimensionality and the nearest neighbour classifier is used for classification. In the experimental setup, 2 images for each class were used for training and the remaining for testing. A FRR of 0.055% was obtained for a FAR of 0.01%, when the images from UBIRISv1 database, Session 1, were used. The noisiest 34 images were not included in the experiments.

Inspired by the near infrared iris recognition system from (Ma, Tan et al. 2004) (see Table 2.1), Tajbakhsh et al adapted the initial method in (Tajbakhsh, Araabi et al. 2009) to cope with colour iris images. The algorithm aims to find the key local variations from the iris texture by considering the average of several lines of pixels as a signal. On this signal wavelets are applied to find the positions of the local minimums and maximums. The positions are converted to a binary string and the matching is done using the classical HD. The adaptation of the algorithm from (Ma, Tan et al. 2004) to be used on colour iris images consists in overlapping the patches of lines of pixels which were averaged and in using Support Vector Machines in the matching stage. The reported EER on UBIRISv1 database was 0.4% for Session 1 and 3% for Session 2, but the noisiest 7% of the iris images were not included in the experiments.

An iris image enhancement methodology by using image level fusion is described in (Vatsa, Singh et al. 2008). With the observation that an iris image needs different enhancement techniques, as different noise types are present in different regions, a set of 7 enhancement functions are applied to one image. On the resulting images, a SVM learning algorithm is used to select the high quality regions from each image. The obtained regions are combined to form a final good quality iris image. In feature extraction, similar to (Vatsa, Singh et al. 2006), 1-D log polar Gabor filters were used to retain global information and the Euler number was employed to extract topological features. The final decision is obtained by using a SVM with a matching score fusion. Testing databases were CASIA v3 (Inst. of Automation 2006), ICE (Technology 2006) and UBIRIS v1. Experimental results in verification and identification show the important role played by the proposed image quality enhancement technique. The robustness of the method was assessed by combining all the three databases into a larger one, with 2085 classes, obtaining a rank 1 identification accuracy of 97.21 %.

The authors of the work described in the previous paragraph use different channels

of colour iris images for a pixel level fusion in (Vatsa, Singh et al. 2010). Quality score measures of each red, green and blue channel are computed and two channels with lower quality are fused at the pixel level by Redundant Discrete Wavelet Transform. The red channel performs better in most of the cases, thus the green and blue channels are combined. Matching scores are computed separately for the high quality channel and for and for the fused image. Score level fusion is done with probabilistic SVM. The reported accuracies show the benefit of using multichannel information from RGB iris images.

In (Roy and Bhattacharya 2009) Daubechies wavelets are used to extract texture information and SVM is used for classification. The experiments results on UBIRISv1 dataset reported a Genuine Acceptance Rate (GAR) of 97.13% for a FAR equal to 0.001 %. The same authors made another step towards non-ideal iris recognition in (Roy, Bhattacharya et al. 2011), where features from four different regions of the unwrapped iris image are extracted using Daubechies wavelet transform. The main contribution of this work consists in a novel feature selection method for dimensionality reduction of the features. Four feature selection methods are applied, i.e. k-Nearest Neighbour, SVM, Entropy based algorithm and T-statistics and after that, Genetic Algorithms are employed to select the best features. The length of the feature vector was reduced from 140 to 105. For classification, Adaptive Asymmetrical SVMs are used. The system is benchmarked on ICE (Technology 2006), West Virginia University Database (Makthal and Ross 2005) and UBIRIS v1 dataset (Proenca and Alexandre 2004). The obtained performance was encouraging, with 97.41% Correct Recognition Rate and 0.47 EER on the combined dataset.

Daubechies wavelet decomposition is also employed in the colour iris recognition system from (Babu and Vaidehi 2011). The wavelet coefficients are fed as input to an Independent Component Analysis (ICA), which will calculate the independent components. 512 independent components for one unwrapped iris image represent the iris features. In the classification stage, a fuzzy logic technique is employed. The method is benchmarked on UBIRISv1 database, Session 1, using 4 iris images per user for training and one for testing. The reported rank 1 identification rate is 97%.

Using image matrix-based Linear Discriminant Analysis (2D-LDA) applied in horizontal and vertical direction, colour iris images from UBIRISv1 database, Session 1, (Proenca and Alexandre 2004) were classified in (Wen-Shiung, Chi-An et al. 2009). A

signal level fusion was used in this work, because the 2D-LDA implies the usage of the mean image of the training samples. Two dimensional Principal Component Analysis (2D-PCA) was also applied to classify the same training images. 3 training images per user were used from 220 users. The obtained EER was 0.95% for 2D-LDA and 0.78% for 2D-PCA. Combining these two approaches, an increase in the system's accuracy was obtained, with an EER of only 0.74%.

In (K. N. Pushpalatha, Aravind Kumar Gautham et al. 2012), features are extracted from the frequency spectrum. Magnitude and phase are used as iris features and SVM is employed in the classification stage. A rank 1 identification rate is reported for UPOL dataset (Dobeš and Machala 2004).

Binary features were extracted in (Wang, Zhang et al. 2012) using 2D Gabor filters with various parameters for different patches of the iris and a HD is computed for each patch. In the second stage, these distances are the inputs of an AdaBoost learning algorithm (Kuncheva 2004), which is used to select and combine the most discriminative distances. The dataset used was a subset of 1000 images from UBIRISv2 (Proenca, Filipe et al. 2010), but no numerical accuracies were reported. This algorithm was ranked the second best performing classification approach for the noisy iris images in NICE II (Lab 2009) competition.

Probabilistic Neural Networks are employed in (Sundaram and Dhara 2011) in the classification stage of a colour iris recognition system. The features are extracted using a GLCM approach. The method is benchmarked on UBIRISv1 dataset, using 190 classes. The images are split in 3 gallery images and 2 probe images per class are and the reported identification rate is 97.00 %.

A visible light iris recognition system which employs a standard MCS architecture is presented in (Radu, Sirlantzis et al. 2012). The MCS is composed of linear classifiers trained on different sets of real valued features extracted using circular symmetric filters (Ma, Wang et al. 2002) with different parameters. The posterior probabilities of the linear classifiers are fused with a mean combiner. The system from (Radu, Sirlantzis et al. 2012) distinguishes itself from the majority of the published iris recognition systems by being able to operate in identification scenario without accessing the database of enrolled individuals. Its performance on UBIRIS version 1 database is comparable to other system's performances reported in the literature.

In this subsection the colour iris recognition methodologies which use a statistical-based approach for the matching phase were surveyed. There are two main conclusions that emerged after reviewing the papers from this subsection:

- There is a small number of works that employ MCS in the matching stage of a colour iris recognition system, although MCS have been shown to be highly efficient fusion techniques;
- The colour of the iris has a significant potential in increasing the accuracy of a colour iris recognition system when an adequate fusion method between texture and colour is employed.

One major drawback of the colour iris recognition systems that employ statistical-based methods for the matching phase is that these methods usually require a training phase. A biometric system which needs to retrain its classification module after each enrolment is not suitable for scenarios where the enrolment of new users occurs frequently, e.g. border access control.

2.3.5 Colour iris recognition techniques using the periocular region

The term "periocular" refers to the region in the immediate vicinity of the eye (Unsang, Ross et al. 2009). In colour eye images, the periocular region is rich in information that could be used as soft biometrics for colour iris recognition systems. The key periocular region features are illustrated in Figure 2.3, using as an example an image from UBIRISv2 dataset. An overview of the periocular recognition, as a biometric modality on its own is made in (Padole and Proenca 2012).

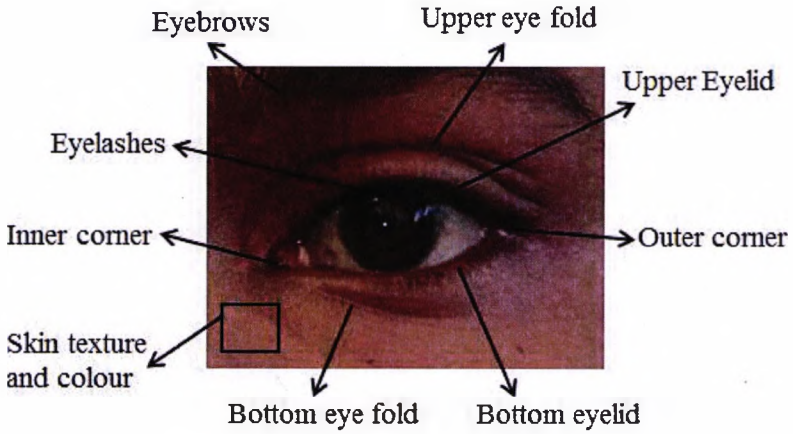

Figure 2.3. Key periocular region features

The main advantage of using the periocular information in a colour iris recognition system consists in helping the biometric system to reduce the errors made when the iris contains a significant amount of noise. In (Unsang, Ross et al. 2009) a feasibility study of periocular biometrics on colour iris images is made, without using the information from iris texture. 958 iris images from UBIRISv2 (Proenca, Filipe et al. 2010) database were used. The eye images which contain eyebrows were separated by those that do not contain eyebrows. Local and global features were extracted and the reported rank 1 identification accuracy was 77%. As the iris texture has not been used, this is an encouraging accuracy and shows that periocular data has a significant potential in increasing colour iris recognition systems' accuracy. A similar rank 1 identification accuracy is obtained on periocular data in (Bharadwaj, Bhatt et al. 2010), using all the images from UBIRISv2 database.

In (Tan, Zhang et al. 2012) the iris recognition system used in addition to iris texture information about the eye color and the eye together with the skin texture around the eye, i.e. the periocular data (Park, Jillela et al. 2011; Radu, Sirlantzis et al. 2012). From the iris texture, ordinal measures (Zhenan and Tieniu 2009) and histograms of different colour spaces have been used as features. From the periocular region and from the iris, features called textons (Zhu, Guo et al. 2005) were extracted. Semantic information, like left/right eye and density distribution of eyelashes was also used as a forth base feature type. The

weighted sum was used as a trainable combiner between the base classifiers and the weights are learned from the training dataset via exhaustive search. The above described approach obtained the first position in NICE II competition (Lab 2009), with a DI of 2.57.

5 iris feature types were extracted in (Santos and Hoyle 2012) from images acquired under visible light. These feature types are local binary patterns and scale invariant feature transform extracted from the periocular region and 1-D, 2-D wavelet zero-crossing representation and binary codes from 2D Gabor filters from the iris texture respectively. For the 2 features extracted from the periocular region, a distance-ratio based scheme and the Euclidean distance respectively are used as base classifiers. For the 1-D and 2-D wavelet zero crossing dissimilarity measures are computed and for the binary feature, the classical Hamming distance is employed. For the fusion of the 5 scores, a logistic regression based approach was used as a trainable combiner. The EER obtained for a subset of 1000 images from UBIRISv2 database is 18.48 % and this algorithm was ranked the third in NICE II (Lab 2009) competition.

The same 1000 colour iris images from NICE II (Lab 2009) competition were used in (Shin, Nam et al. 2012) to develop a sequential fusion which works in 3 phases: in the first phase it decides if the test image belongs to the right or left eye; in the second phase colour information from various colour spaces is used and in the 3rd phase binary features were extracted from red, green and gray image channels. For the binary features three HDs were obtained and a matching score fusion is performed using the weighted sum combiner. This approach obtained the fourth highest rank in NICE II competition with an EER of 16.94 % and a DI of 1.63.

An experiment in which volunteers were asked to compare pairs of periocular images from both visible and near infrared spectrums is conducted in (Hollingsworth, Darnell et al. 2012). The participants had to give a yes/no answer for each pair of eye images according to their perception if the images belong to the same person or not. The obtained human accuracy was 88% for the visible light periocular images and 79% for the near infrared images. The computer algorithms run on periocular images obtained similar accuracies. A high identification accuracy is claimed on periocular data in (Joshi, Gangwar et al. 2012). Features were extracted using LBP and Direct Linear Discriminant Analysis and the obtained identification accuracy on UBIRISv2 database is 94%.

Although there is a small number of papers that use periocular data to enhance iris

recognition accuracy in the visible spectrum, the reported improvements brought by fusing iris texture and periocular data are remarkable. The first places in NICE II competition (Lab 2009) were obtained by algorithms which used the periocular data in addition to information extracted from the iris. Moreover, the winning algorithms of NICE II competition employed colour features to boost even more the biometric system's accuracy. However, for an efficient usage of iris colour information and periocular data in an iris recognition system, a vital role is played by the fusion mechanism employed. As observed from the review made in this section, trivial score-level fusion might not be sufficient to maximize the biometric system's accuracy and there is still a significant amount of research to be done in finding the optimum fusion methods for iris recognition with reduced constraints.

2.4 Iris recognition algorithms employing multispectral fusion

Most of the commercial iris recognition systems use iris images acquired in the near infrared spectrum in the 700nm to 900nm range. The visible spectrum ranges from 400nm to 700 nm. It is interesting to see how information from images acquired in the 2 spectrums may be combined together for an enhanced accuracy. There are very few works published on iris recognition systems which use iris images acquired at wavelengths outside the range of 400nm – 900nm. In this subsection we will survey the works that employ a multispectral approach for iris recognition systems.

In (Park and Kang 2005) an anti-spoofing method for iris recognition systems is proposed, based on a multi-spectrum iris image acquisition. Iris images are acquired at two wavelengths: 780 nm and 900 nm. The images acquired in the two wavelengths were fused at the pixel level employing a gradient based fusion. The classical phase based iris recognition algorithm (Daugman 1993) was used in the experiments, but only images from 4 users were collected. The system was able to successfully reject counterfeit iris images, while accepting the images acquired by the biometric system's device.

A multispectral iris images database was collected by Boyce et al at West Virginia

University, United States, and the acquisition setup is described in (Boyce, Ross et al. 2006). The acquired images comprised spectral information as follows: red at 670nm; green at 540 nm; blue at 475 nm and near infrared at 800 nm. The images were collected from 24 users. The employed iris recognition algorithm was the classical Daugman's approach (Daugman 1993). The red channel yields higher accuracy than the green and blue channels. The possibility of matching iris images across different wavelengths was analysed. The ROC curves plotted for cross-spectral matching showed that the performance was decreasing with the increasing of the differences between the wavelengths. This indicates that at various wavelengths, different information is extracted from the iris texture. A score level fusion of the multispectral information was also applied and it was found that the fusion between the near infrared, red and green channel yields the best accuracy among the possible channel fusion. The study from (Boyce, Ross et al. 2006) is extended in (Ross, Pasula et al. 2009) for wavelengths beyond 900 nm. Iris images were acquired under illuminations at 8 wavelengths: 950, 1050, 1150, 1250, 1350, 1450, 1550 and 1650nm. The images were acquired from 25 subjects, enrolled with left and right eyes. The experimental results confirm the possibility of performing cross-spectral matching beyond 900 nm. Also, fusing at the score level the HDs obtained from matching at 5 wavelengths results in a good separation between genuine and impostor score distributions.

Another study of the possibility of matching near infrared images against visible spectrum images is made in (Jinyu, Nicolo et al. 2010). Images from West Virginia University multispectral database (Boyce, Ross et al. 2006) composed from red, a combination between green and blue and near infrared channels were used. A Feed Forward Neural Network is used to predict at pixel level the near infrared model of the image from the red channel and the channel with the combination between blue and green. Binary features were extracted using an enhanced version of the publicly available algorithm of Libor Masek (Masek 2003). The experimental results show that the predicted model of near infrared images is very useful, with an insignificant degradation of EER compared to the case when only near infrared images are used.

The acquisition of iris images at different wavelengths requires additional hardware resources and design efforts. In (Ngo, Ives et al. 2009) the design and implementation of a multispectral iris images acquisition system is detailed. An acquisition system that is able to capture both near infrared and colour iris images simultaneously is presented in (Chia-Te,

Sheng-Wen et al. 2010). Another acquisition system which acquires iris images at 700, 780 and 850 nm simultaneously is described in (Yazhuo, Zhang et al. 2012). Also, in the same work, a summary of the existing multi-spectral databases is made.

Multispectral iris recognition is relatively a new topic in biometrics research, with significantly less works published compared to colour iris recognition. Generally, multispectral iris recognition reveals its benefits when a fusion between the information extracted from the images acquired at different wavelengths is employed. If such a fusion is employed, the multibiometric system could be considered a multi-sample iris recognition system, according to the taxonomy introduced in (Ross, Nandakumar et al. 2006). The acquisition process in a multispectral iris recognition system is more complex than the near infrared spectrum acquisition and from this reason the enrolment phase will require a higher effort, decreasing the practicability of the iris recognition system.

2.5 Chapter conclusions

Iris recognition is one of the most accurate and reliable biometric authentication methods available. Although the reported accuracies of the iris recognition systems are among the highest in biometrics, the environment in which the user is enrolled and authenticated is a highly constrained one. The constraints are necessary so that the near infrared illumination is good enough for a good quality iris image to be captured. Therefore, one of the key desirable properties of an iris recognition system is to be able to cope with colour iris images, yet performing comparably to the near infrared iris recognition systems.

In this chapter the iris recognition systems that were benchmarked on colour iris images datasets were reviewed. The classical near infrared iris recognition approach, based on phase information of the iris texture is not effective when applied to noisy colour iris images, as reported in a number of publications. The colour iris recognition approaches which rely on a single type of features and employ a classical distance based matching (i.e. where training is no typically needed) are not very successful when coping with noisy colour iris images. The improvement in a colour iris recognition system's accuracy is brought by using multiple sources of information, employing either a multi-algorithmic approach or a statistical based approach.

The accuracies of the colour iris recognition systems have not yet reached the level of the accuracies reported for near infrared iris recognition systems. This fact is highlighted by the results reported in the NICE II competition. The organizers of NICE II competition fused at the score level the best performing algorithms submitted to the competition and their conclusion was that by finding a proper fusion methodology between various approaches the accuracy on colour iris images may be increased. A promising path in colour iris recognition systems is the fusion between the information extracted from the iris texture and additional information, such as eye colour and periocular data. Therefore, one of the key components of a colour iris recognition system is the employed fusion mechanism.

While the research efforts of the reviewed colour iris recognition approaches were concentrated mainly on the feature extraction stage, there is still a significant amount of research to be done on the information fusion techniques applied in these biometric systems. Along this thesis we aim to build robust information fusion techniques which applied to colour iris recognition systems will lead to a superior accuracy of these types of biometric systems compared to the current state of the art accuracies.

Chapter 3
Basic fusion of iris recognition algorithms with adaptations for visible spectrum

This chapter will present the development of a multi-algorithmic iris recognition system comprising three pattern recognition algorithms which will operate independently on colour iris images. The matching scores of the three algorithms are combined. Also, an information theoretical analysis methodology of iris texture from colour images is proposed.

3.1 Introduction

The previous chapter reviewed the iris recognition techniques that were developed to address the issue of dealing with noisy iris images acquired in the visible spectrum. From the surveyed works it was concluded that by applying various information fusion techniques the accuracy of the colour iris recognition system could be enhanced. The three main information fusion techniques employed in colour iris recognition systems are: multi-algorithmic approach, statistical-based approach and periocular and colour data integration approach.

According to the taxonomy proposed by (Ross, Nandakumar et al. 2006), a multi-algorithmic biometric system is considered a multibiometric system. The issue of information fusion in multibiometric systems is also discussed in (Ross and Jain 2003). The levels of fusion at which information might be combined in a multibiometric system are the feature level, matching score level and decision level.

In this chapter the multi-algorithmic fusion approach will be investigated for a colour iris recognition system. Three iris recognition algorithms are developed and the three corresponding match scores are combined at the score level by employing a weighted average. The three component algorithms employ different feature extraction techniques.

Besides the proposed multi-algorithmic colour iris recognition approach, there are other four main contributions of this chapter:

1) a versatile segmentation methodology, which is able to cope with noisy colour iris images, but also with near infrared iris images;

2) an informational theoretic iris texture analysis method which serves in finding which channels from a colour space reveal better the information from the iris texture;

3) a colour iris feature extraction methodology, based on a 3 bit encoder of the 8 neighbourhood;

4) an investigation of how the accuracy is influenced by using 50% of the available iris texture and by using 100% of the available iris texture, for the multi-algorithmic system and for the component iris recognition approaches;

The remainder of this chapter is organized as follows: Section 3.2 will present the iris segmentation methodology employed to detect the iris and the pupil in the image. In Section 3.3 the informational theoretic iris texture analysis method will be introduced. In Section 3.4 the proposed multi-algorithmic system is presented together with the feature extraction techniques corresponding to the three component algorithms. Section 3.5 will present the experimental results and the conclusions are given in Section 3.6.

3.2 A versatile iris segmentation algorithm

3.2.1 Background

At present, the research in iris recognition is focused on less cooperative and unconstrained operations of iris biometric based recognition systems, where the iris images could be captured under visible light and therefore incorporate various types of imperfections, but also under near infrared illumination. Iris recognition at a distance from wall-mounted devices or from hand-held devices, where the device could or could not have near infrared illumination, can be included in the category of less unconstrained operation scenarios. In such scenarios, the 'segmentation' stage of iris recognition plays a vital role because feature extraction from non-iris texture will be useless.

The difficulty with which a segmentation algorithm performs well in different spectrums is mentioned in (Proença and Alexandre 2005), where the UBIRISv1 database is presented. The authors of (Proença and Alexandre 2005) have implemented the most popular iris segmentation techniques at that point in time and tested them on UBIRISv1 database and on CASIA v1 database (Inst. of Automation 2004), which contains only near infrared iris images. They observed and reported numerically that the algorithms were performing well either on visible spectrum or on near infrared iris images, but not on both wavelength domains. Therefore, the necessity of a versatile iris segmentation algorithm was apparent.

Among the iris segmentation algorithms that have been reported the most popular is the integro-differential operator used in (Daugman 1993), which is implemented on most of

the commercial iris recognition systems. Another well-known iris detection method is described in (Wildes 1997), where Canny edge detector and Hough Transform were used in a 2 steps approach. Inspired by the principle of the integro-differential operator, new operators have been developed for iris segmentation in (Camus and Wildes 2002) and (Sanchez-Avila, Sanchez-Reillo et al. 2002). The winner iris segmentation algorithm of NICE I competition (Proenca and Alexandre 2012), is described in (Tan, He et al. 2010).

Usually an iris segmentation algorithm is considered robust in the literature if its performance does not decrease as the noise and distortions in the images are increased (Proenca and Alexandre 2006). However, for an iris segmentation method, the term robust has a broader meaning. For example, the robustness could include the versatility of the algorithm in segmenting both near infrared and colour iris images with comparable accuracy. Moreover, the segmentation algorithm is robust if it can be adapted to improve its throughput with a minimal reduction in accuracy. The method described in this section was designed according to this extended definition for the robustness of a segmentation algorithm.

If the eye images do not include a strong off-angle noise, both the iris and pupil have approximately the shape of a circle. Therefore a circle detection method could be used to segment the iris and pupil. The segmentation method presented in this subsection makes the assumption that the iris and pupil have circular boundaries.

3.2.2 Iris detection

The proposed iris segmentation algorithm addresses two issues: first, the lack of an iris segmentation methodology which can cope successfully with both near infrared and colour images; second, the speed of the algorithm, which can be increased significantly with a minimal reduction in accuracy.

The block diagram of the proposed segmentation algorithm is illustrated in Figure 3.1. As it is shown in the block diagram, the algorithm starts by segmenting the iris and then the pupil. Along this section, the working principle of the proposed segmentation algorithm will be explained using colour RGB images from UBIRISv1 dataset (see subsection 2.3.1). Circle detection algorithms are usually provided as parameters the upper and lower limits of

the radius of the iris and the pupil. For a certain iris images dataset, these limits are known. The algorithm depicted in this section uses the same approach.

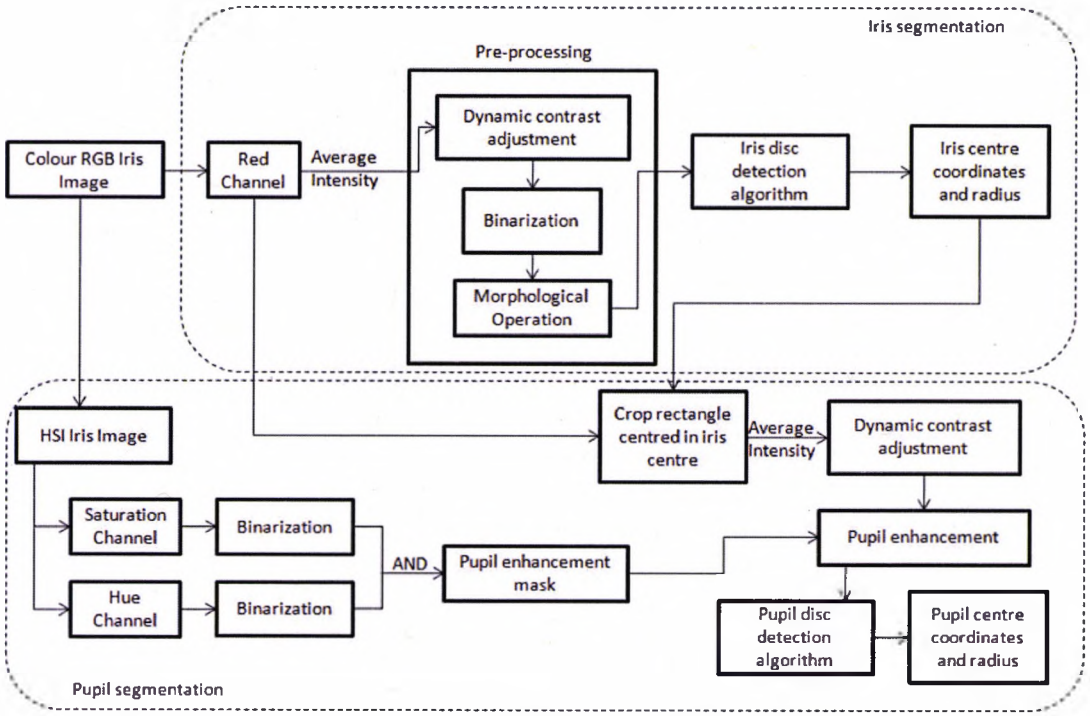

Figure 3.1. Block diagram of the segmentation algorithm

The red channel has the closest wavelength to the near infrared spectrum. For iris detection only the red channel has been used, as the sclera-iris border is more distinguishable in the red channel compared to the other channels. To cope with illumination variations of the iris image, a dynamic contrast adjustment was made (Gonzalez and Woods 2008). The adjustment parameters depend on the average intensity of all pixels from the red channel iris image. Subsequently, the iris image was binarized using a threshold depending on the average intensity of all pixels. The effects of these transformations are shown in Figure 3.2. After binarization, a spur morphological transformation (Gonzalez and Woods 2008) has been applied to the image in order to eliminate the isolated white pixels from the iris region and black pixels in the sclera.

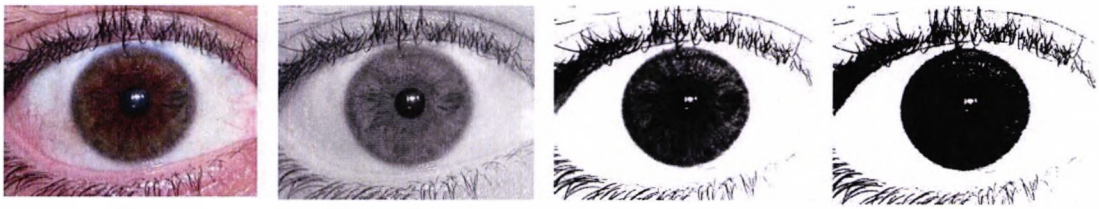

a) b) c) d)

Figure 3.2. Iris image transformations: a) original RGB image from UBIRISv1 dataset; b) red channel image; c) image after contrast adjustment; d) binarized iris image

After binarization, the iris is a black circular disc and clearly separated from the rest of the image. To determine accurately where the centre is and the corresponding radius, a simple geometrically-based method is used. A rectangle obtained by subtracting the minimum iris radius from each side of the image is considered as the search space for the iris centre. Any pixel within this rectangle is a potential candidate to the centre of the iris. The reduced search space was chosen such as the iris is not partially out of the image and for increased speed. Still, this approach enables the method to detect the iris even if it is not centred or the user is looking to the left or right.

The underlying principle behind the proposed segmentation algorithm is a simple one: the distances from the centre of the iris to its boundary should be equal. Each pixel within the isolated rectangle is considered the intersection point of 3 lines at predefined slopes. Two lines are symmetric to the horizontal direction and the third line was drawn out in the horizontal direction, as shown in Figure 3.3. The line segments are scanned along, for each pixel that is the intersection of 3 lines, starting at a distance from the maximum iris radius to the minimal iris radius, measured from the intersection. The scanning directions are from the end points of the lines towards the intersecting pixel. Then, from the intersecting pixel to the transition from white to black, the Euclidean distances are computed. The transition from white to black along a line segment is considered to be the transition from the longest white segment to black, when scanning towards the intersection pixel. In total there are 6 distances.

In the implementation, the slopes of the line segments used are within ± 30° about the horizontal. The slopes were chosen so that occlusions from the top and bottom of the iris are avoided, i.e. the eyelid partially obstructs the iris. Exact slopes of the lines are not very important and small variations do not have any significant effect on the performance of the algorithm. However, if the slope is too large, the lines will be likely to reach regions belonging to the eyelids and if the slope is too small, their corresponding terminations will be too close to the horizontal line.

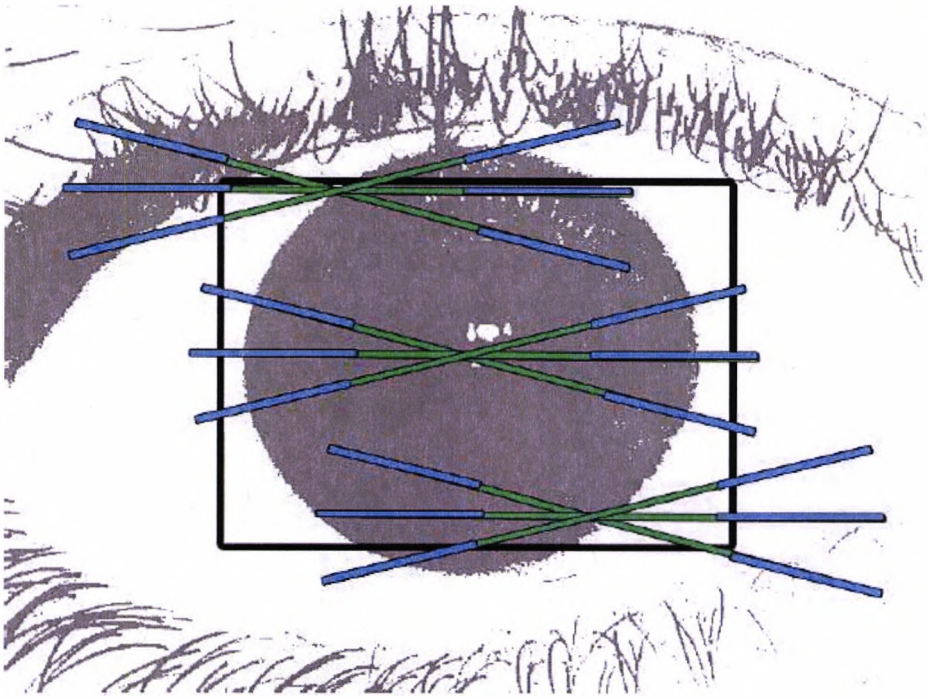

Figure 3.3. Potential iris centre locations and the corresponding intersected line segments

After computing the 6 distances, the centre of the iris is assigned to the pixel which is located at an approximately equal distance from all the 6 white to black transitions. If we denote the 6 distances with $dist_i$, where i=1,...,6, and $(k, l) \in S$, where S is the reduced search space, the coordinates of the iris centre (i_r, i_c) are chosen according to the following equation:

$$(i_r, i_c) = arg \min_{\forall (k,l) \in S} \left[\left(\sum_{i=1}^{5} \sum_{j=i+1}^{6} |dist_j - dist_i| \right) / 15 \right] \quad (3.1)$$

Once the iris centre is obtained, the iris radius is computed using the 6 distances corresponding to the centre pixel by using the following equation:

$$rad = \frac{1}{6}\sum_{i=1}^{6} dist_i \tag{3.2}$$

The rationale behind having 6 segments, respectively 3 lines is to cope with situations when black isolated regions are located in the sclera, which could confuse the algorithm. If only 2 lines are considered and some isolated black pixels are in the sclera, the method is likely to incorrectly detect the iris centre. Other variations of this method could be obtained by enlarging the number of lines and segments to be scanned. More than 3 lines could be considered to improve the segmentation accuracy, when execution speed is not essential. For this work only 3 lines were considered because a rapid segmentation of the iris images was desired.

The speed of the algorithm may be increased by enhancing the search method for the centre pixel. For example, if only the black pixels are considered in the algorithm, the number of pixels that are potential centres of the iris is significantly reduced. Another way of reducing the search space is to consider every other pixel instead of repeating the process for all the pixels within the rectangle. By starting with the pixels from the centre of the rectangle and stop when it is observed that the value returned by equation 3.1 is increasing repeatedly for the following pixels could also reduce the execution time.

3.2.3 Pupil detection

For iris images acquired in the visible spectrum, the boundary between the pupil and the iris is generally less distinguishable than in near infrared spectrum. Moreover, under visible wavelength, the pupil becomes more difficult to segment because of the reflections that are present in the image. Therefore, a segmentation algorithm designed for near infrared iris images is likely to perform worse on visible wavelength images and vice versa.

The pupil segmentation algorithm uses only the region from the image that is inside the detected iris. In this way the pupil will not be detected outside the iris. Initially, a

threshold-based technique is used to detect specular reflections inside the iris. After the specular reflections have been detected, the average of the intensity of the remaining pixels from inside the iris is calculated. This average value is then used to dynamically adjust the parameters of a contrast adjustment operation, as it is shown in the block diagram from Figure 3.1. Bearing in mind that the iris and pupil are not concentric but their centres are located close one to each other, the search area for the pupil centre can be significantly reduced. A rectangular region of interest is formed having the centre of mass the centre of the iris and the width and length obtained with equation 3.3. The parameters in equation 3.3 could take different values to make the rectangle around the iris centre larger or smaller and their exact value is not important. For this study, the numerical values used in equation 3.3 were empirically estimated by analyzing the iris to pupil ratio. For other databases, the values used in equation 3.3 need to be adjusted correspondingly. The results of these steps are shown in Figure 3.4.

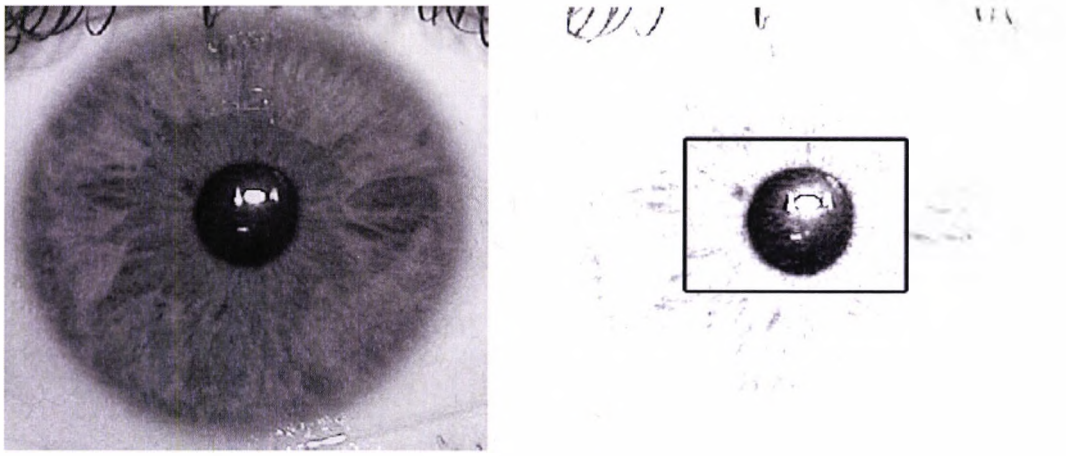

a) b)

Figure 3.4. Pupil segmentation: a) cropped iris from the red channel; b) iris after contrast adjustment

$$\begin{cases} length = irisRad * 0.4 \\ width = irisRad * 0.25 \end{cases} \tag{3.3}$$

where *irisRad* is the radius of the detected iris.

It may be observed from Figure 3.4 that after contrast adjustment the pupil became very well separated from the iris texture. For pupil segmentation, all the pixels inside the

rectangle defined with (3.3) are considered possible centres of the pupil. Each of these pixels is considered the centre of two concentric circles, one with a radius smaller with two pixels than the other. The 2 circles will have a radius ranging from the minimum to the maximum possible pupil radius. This scheme is illustrated in Figure 3.5. The difference between the values of the pixel intensities of the larger circle and the pixels of the smaller circle is computed for each pair of circles. To increase the execution speed, only 30 corresponding pixel positions along the arcs of the circles are considered, i.e. with a step of 12 degrees.

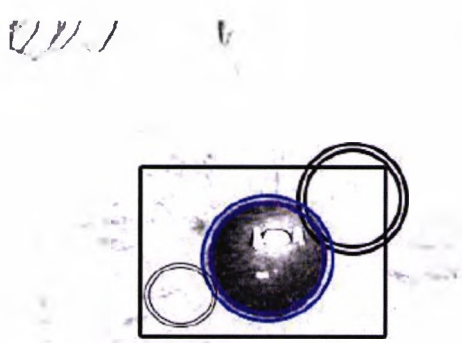

Figure 3.5. Pairs of concentric circles used for pupil segmentation

30 differences are computed for each pair of circles. Let these be denoted by $diff_i$, where i=1, ..., 30 and the centre of the pupil be (c_r, c_c). If r_{min} and r_{max} are the minimum and maximum possible radiuses of the pupil, $(k, l) \in S$ and S is the area defined by equation 3.3, the coordinates of the centre of the pupil will then be determined according to equation 3.4. The logic behind equation 3.4 is to maximize the sum of differences between pixels intensities which are positioned on two concentric circles. The centre of the circles corresponding to the maximum sum of differences will be the pupil's centre.

$$(c_r, c_c) = arg \max_{\forall (k,l) \in S} \left(\max_{r_{min} < r < r_{max}} \sum_{i=1}^{30} diff_i \right) \tag{3.4}$$

3.2.4 Near infrared operation

The proposed iris segmentation technique was developed to be a versatile tool, which can be used to segment any iris image database, regardless the wavelength under the images were acquired. The operation of the proposed segmentation algorithm in near infrared spectrum is slightly different than that in colour domain. First, the pupil is detected in a near infrared iris image, not the iris, as in colour images, because the pupil in near infrared spectrum is very dark and easy to segment. The interesting aspect is that the method described in subsection 3.2.2 for iris segmentation is used for pupil segmentation in near infrared images and the method described for pupil segmentation in subsection 3.2.3 is used for iris segmentation.

As the pupil is very dark, a simple contrast adjustment operation is sufficient to leave only the pupil, eyelashes and eyelids in the image. For pupil detection, the region of interest is restricted to a rectangle obtained by subtracting the minimum iris radius from each side of the image. Then, the method described in subsection 3.2.2 is applied to find the pupil.

After the pupil's centre and radius have been found, the search space for iris centre will be reduced only to the pixels inside the detected pupil. Those pixels will become the centres of the two concentric circles and the boundary between iris and sclera is found by applying equation 3.4.

3.2.5 Pupil segmentation improvement

Under visible wavelength, iris images could be captured under poor illumination and in this type of images, the boundary between the iris and the pupil is almost unnoticeable. Also strong reflections could have a similar effect. An iris image from UBIRISv1 dataset (Proença and Alexandre 2005), Session 2, affected by these types of noises is shown in Figure 3.6a. The effect of the contrast adjustment for pupil detection for the image from Figure 3.6a is shown in Figure 3.6b.

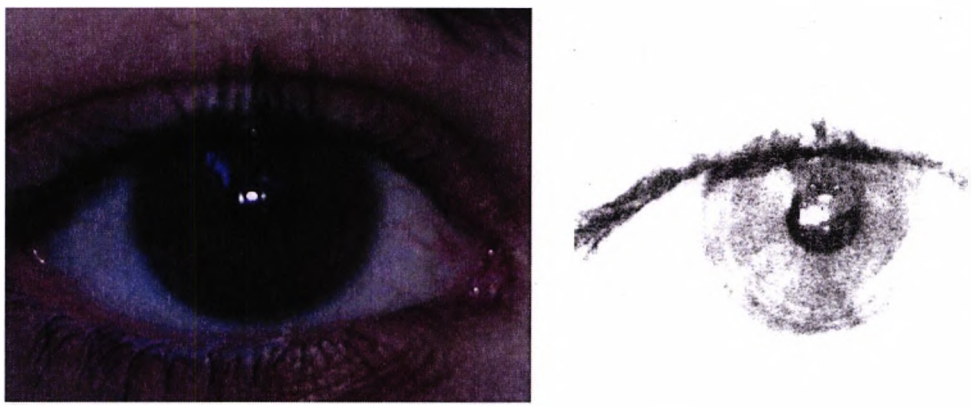

a) b)

Figure 3.6. a) Noisy iris image, where the iris-pupil boundary is difficult to distinguish;
b) Contrast adjustment for pupil detection in noisy iris images

To enhance the separation between the pupil and iris texture, additional information from HSI colour space is used. When converting from RGB colour space to HSI, it was observed that in hue and saturation channels, the area that was affected by reflections inside the pupil from the original RGB image is clearly distinguishable. Therefore, information from these channels is used to enhance the pupil segmentation. The gray-scale images of hue channel of the same image from Figure 3.6a is shown in Figure 3.7a.

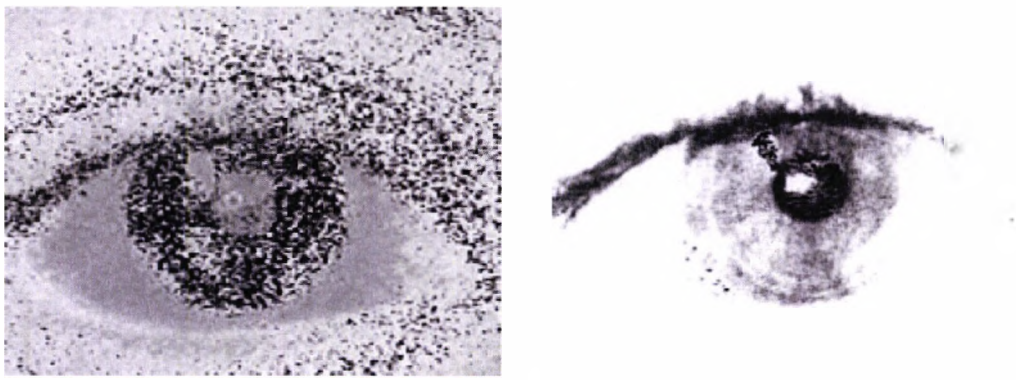

a) b)

Figure 3.7. a) Iris image in hue channel;
b) Contrast adjustment augmented with information from HSI colour space

The hue channel has also been used for pupil segmentation in (Proenca and Alexandre 2006) and in (Tan, He et al. 2010), but in the present algorithm the information from saturation channel is also used. Empirically observing that the pupil in the hue channel has pixel intensity values between 130 and 170 and in the saturation channel has values between 70 and 130, a binary mask of the pupil from both hue and saturation channels was created. A combined mask for the pupil was obtained by applying logical AND operation between the 2 masks. The combined mask was used then to assign to the corresponding pixels from the red channel a low value. The contrast adjustment from Figure 3.6b was complemented with the information from hue and saturation channels, yielding the images shown in Figure 3.7b. Using the information from HSI colour space, the pupil becomes visibly easier to segment.

3.2.6 Databases

This work is focused on the operation of iris recognition systems on colour images, but the proposed segmentation algorithm was designed to cope both with near infrared iris images and colour iris images, for future use with any iris images database. Therefore, the robustness of the proposed segmentation algorithm was assessed on near infrared and colour images. The near infrared datasets used in the experiments are CASIAv1 (Inst. of Automation 2004), which has 756 near infrared iris images from 108 individuals and CASIAv3 (Inst. of Automation 2006), the Lamp subset, which has 16213 images from 411 users. The images from CASIAv3 database, Lamp subset were acquired using a hand-held device with a lamp turned on and off to make the pupil to dilate. The colour iris images database used in the experiments is UBIRISv1. This database consists of 1877 colour RGB iris images with a dimension of 800x600 pixels. A brief description of this dataset is made in subsection 2.3.1.

Apart from the segmentation experiments, in the remainder of this work, all the experiments will be run only on the UBIRISv1 database. There are three main reasons why UBIRISv1 database was selected to benchmark the iris recognition techniques described along this work:

1. it is publicly available since 2004, containing 1877 colour iris images;

2. it contains colour iris images acquired in two sessions, in the first session the images are of good quality, while in the second session the images contain a significant amount of noise;
3. the vast majority of the colour iris recognition systems published in the literature are benchmarked on this database.

3.2.7 Segmentation results

The assessment of the segmentation algorithm was done by visually inspecting the segmented images. If both the iris and the pupil were fitted by the circles decided by the circle detection algorithms, the image is considered correctly segmented, as shown in Figure 3.8. The images have been reduced in size by a factor of 4 to increase the speed of the algorithm. One iris image is considered correctly segmented if both the iris and the pupil were segmented correctly, i.e. the circles are falling on the edges of the iris and pupil. For CASIA v3 dataset, Lamp subset, the obtained segmentation accuracy is 92.04 %. The pupil segmentation accuracy is 98.15%. For CASIAv1 dataset, similar segmentation accuracy was obtained, of 91.97 %.

For UBIRISv1, Session 1, the obtained segmentation accuracy is 95.46% and for Session 2 is 87.03%. In (Proença and Alexandre 2005) the authors have implemented a number of iris segmentation algorithms to compare with their own. In Table 3.1 their best 2 reported segmentation accuracies are presented for the most popular segmentation algorithms for UBIRISv1 and CASIAv1 datasets. The table shows that the algorithms are not performing well on both near infrared images and colour images, while the proposed algorithm does.

Methodology	UBIRISv1	CASIAv1
Daugman – tuned for colour images (Daugman 2004)	93.53 %	54.44 %
Wildes (Wildes 1997)	89.12 %	84.27 %
Proposed	92.46 %	91.97 %

Table 3.1. Iris segmentation algorithms' accuracies

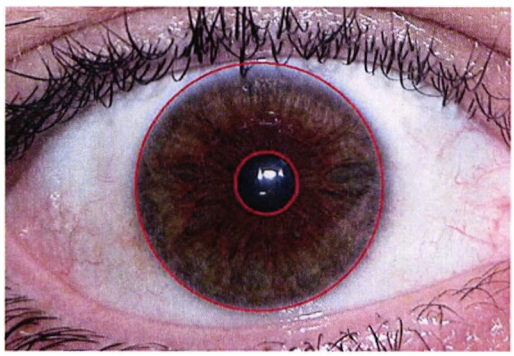

Figure 3.8. Correctly segmented UBIRISv1 iris image

The proposed algorithm was implemented in Matlab environment, due to the fact that this software has numerous pattern recognition toolboxes available. The machine used to run the experiments was an Intel Core 2 Duo running at a frequency of 2.4 GHz with 4 GB of RAM. Only one core of the Intel processor has been used. The execution time for the proposed algorithm is approximately 2.97 seconds. This time is comparable to the execution time needed by Daugman's integro-differential operator, which implementation was run in approximately 2.6 seconds. These timings were obtained by averaging the time intervals measured for 100 runs of the algorithms.

In iris images, the part of the iris texture that is closer to the pupil and in central position of the iris is richer and less redundant in radial direction than the texture close to the outer boundary (Daugman 2004). Therefore, the computational efforts in detecting with a high accuracy the iris-sclera boundary could be minimized by detecting it less accurately when speed is a critical requirement of the application. The segmentation algorithm proposed in this subsection can be adapted to work faster with a minimal reduction in accuracy by resizing the iris image. For UBIRISv1 dataset, the image is reduced in size by a 10 times for iris edge detection, and for pupil segmentation, the image is downsized 6 times.

The proposed iris segmentation algorithm detects the outer iris boundary in the smaller image when the iris image is resized 10 times. When the circle coordinates are multiplied by 10 to get to the original iris centre position, some of the circles do not fit exactly the outer iris boundary. However, in pupil segmentation, the downsizing factor used was 6, as the pupil segmentation accuracy is much more important in extracting useful features. In this size reduction, the pupillary boundary can still be detected with a high accuracy in most of UBIRIS v1 images, which have an original dimension of 800 by 600 pixels. After these modifications, the segmentation accuracy obtained for Session 1 iris

images is 92.36% and for Session 2 is 83.96%. The average segmentation time is only 0.48 seconds, approximately 6 times less than the original segmentation time. Therefore, with approximately only 3% decrease of accuracy, the segmentation algorithm is suitable for real time scenarios implementations.

A mobile phone implementation of the proposed segmentation algorithm is presented in (Oprea 2012). The implementation was done on Android 2.3 platform and has been optimised so that the algorithm is able to run in real time on a mobile phone. The algorithm was subsequently deployed on an HTC Desire mobile phone (HTC 2012), equipped with a processor running at 1 GHz and 512 MB of memory.

3.3 Information theoretic analysis of iris texture

After the iris images are segmented and unwrapped, the information needs to be extracted from the iris texture. There are a number of colour spaces available to represent digital colour images and their component channels could potentially all be used to extract information from iris texture, but such an approach is not a practical one. The issue that appears is how to select the most discriminative few channels from various colour spaces and to find a fusion mechanism to enhance the system's accuracy. In this section a methodology of selecting the most discriminative colour channels from a colour space is proposed, based on an informational theoretical analysis of iris texture.

As shown in (Boyce, Ross et al. 2006), an iris recognition system performs best using features extracted from the red channel, followed by the green channel. On the blue channel, the system performed poorly. These results could be possibly due to the fact that the red channel has the closest wavelength to the near infrared spectrum, where the reflections are not captured. However, a theoretical explanation of the fact that red channel is the best performing channel has not been formulated.

A statistical measure which may be used to characterize the randomness of the texture is the Shannon entropy E. The Shannon entropy E of a grayscale digital image is expressed by equation 3.5, where $p(i)$ is the normalized histogram count for the gray level i and n is the total number of bins. The larger the value of the entropy is, the more random information is present in the image texture.

Channel	Mean	Standard deviation
Red	5.89	0.34
Green	5.82	0.41
Blue	6.12	0.32
Hue	5.35	0.50
Saturation	6.78	0.53
Intensity	5.82	0.36

Table 3.2. Mean and standard deviations of the entropy distributions for RGB and HSI colour spaces

$$E = -\sum_{i=1}^{n} p(i) \cdot \log\left(p(i)\right) \tag{3.5}$$

To observe how the entropy of the iris texture varies in different colour channels, all the 1205 images from UBIRISv1, session 1 are processed. The images from session 1 have a reduced amount of noise and a more objective characterization of the iris texture may be performed. The entropy is computed for all the channels from RGB and HSI colour spaces. The range of the entropy distributions for the six colour channels are presented in Table 3.2.

According to the entropy statistics from Table 3.2, all the channels reveal a similar amount of discriminative information in the iris texture. This contradicts the experimental results obtained in the literature, where the performance of some channels was clearly worse than the performances obtained using other channels. Therefore the Shannon entropy is not a reliable measure to decide on which channel the system's performance improves. A clearer separation between the quality measurements of the iris texture in different colour channels is needed.

By visually observing iris images, it may be concluded that the iris texture has a radial direction. The most prominent texture structures start from the pupil and head towards the sclera following mainly a straight direction, as shown in Figure 3.9a. When the iris image is unwrapped, the radial trend of the texture will become a vertical one, as it may be observed in Figure 3.9b and Figure 3.9c. In the blue channel of the unwrapped image (see Figure 3.9d), the vertical patterns of the texture are not clearly distinguishable, compared to red and green channels.

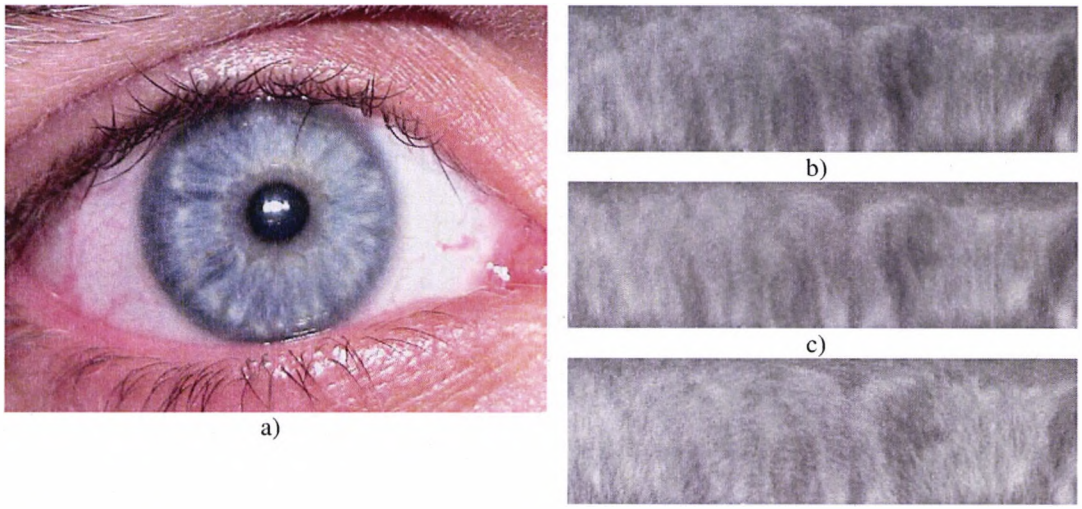

a) b) c) d)

Figure 3.9. a) Iris image from UBIRISv1 dataset; corresponding unwrapped iris image in b) red channel; c) green channel; d) blue channel;

A generic edge detection technique may be employed to locate texture edges. For this investigation, the unwrapped images in red, green and blue channels were filtered with Sobel masks for edge detection in the horizontal and vertical directions. The 2 Sobel masks G_x and G_y are given in equation 3.6. By applying Sobel edge detection on the y axis, where y axis corresponds to 0^o, the vertical orientation of the texture structure is highlighted.

$$G_x = \begin{matrix} -1 & 0 & 1 \\ -2 & 0 & 2 \\ 1 & 0 & 1 \end{matrix} \qquad G_y = \begin{matrix} -1 & -2 & -1 \\ 0 & 0 & 0 \\ 1 & 2 & 1 \end{matrix} \tag{3.6}$$

The result obtained after applying Sobel edge detection on red channel unwrapped iris image for horizontal and vertical edge directions is shown in Figure 3.10. The Sobel filter is applied on the same iris image that is illustrated in Figure 3.9a. It may be observed that there are no edges detected by applying the filter in the vertical direction.

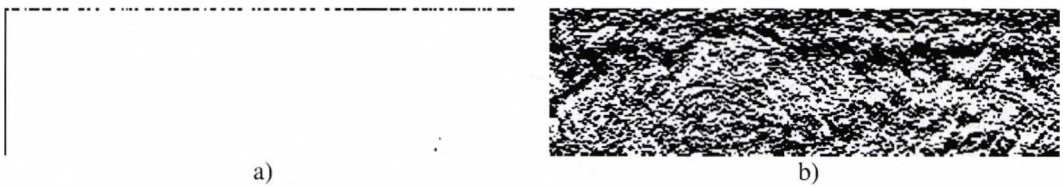

a) b)

Figure 3.10. Red channel unwrapped iris image filtered with Sobel edge detector for a)horizontal edges; b)vertical edges.

The texture edges' direction is given by the gradient obtained from the 2 edge detectors. The histograms of the gradients converted in degrees for the red, green and blue channels of the unwrapped iris image from Figure 3.9 are shown in Figure 3.11.

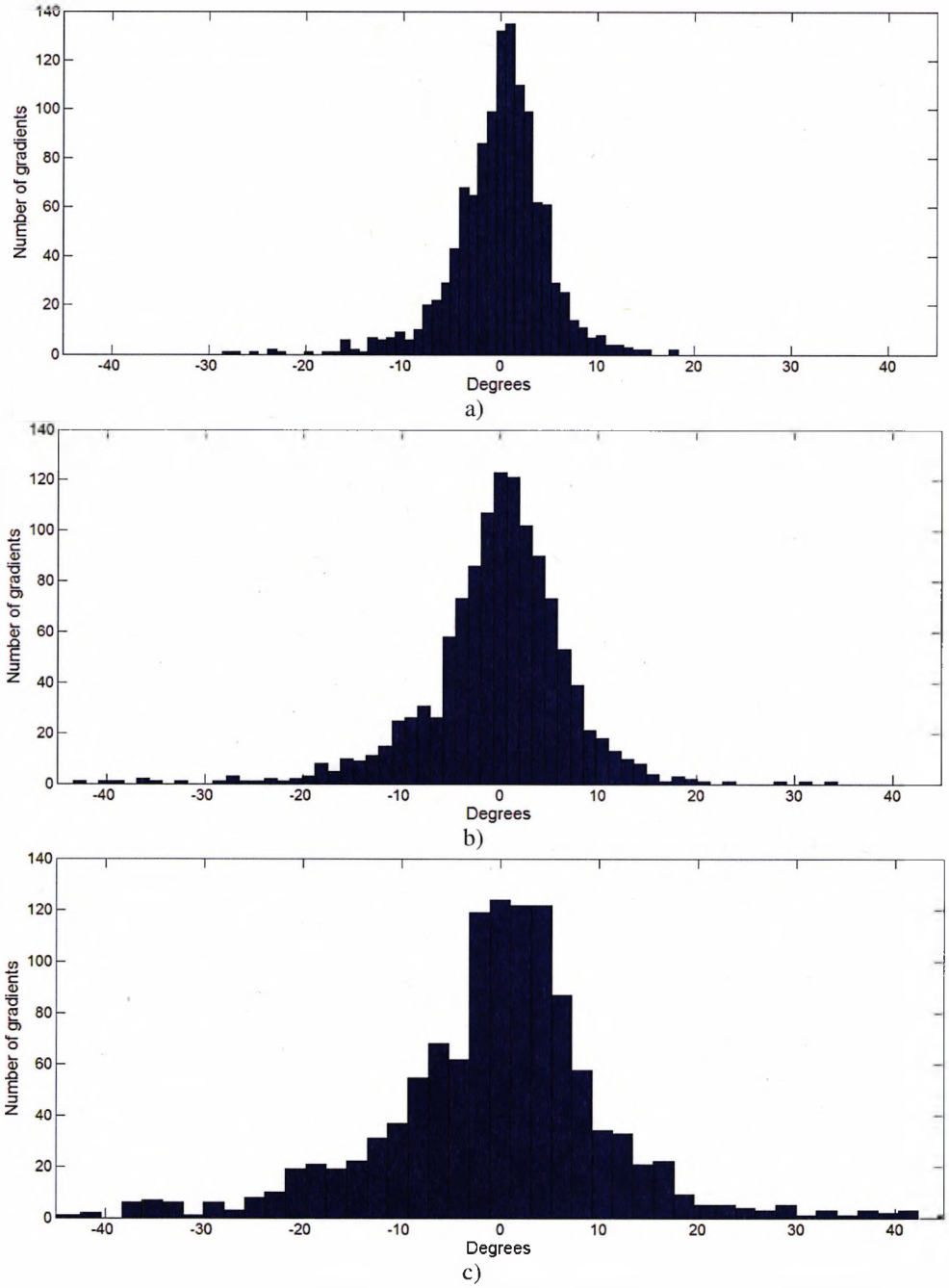

Figure 3.11. Distributions of gradients for a) red channel; b) green channel; c) blue channel

From Figure 3.11 it may be observed that the three distributions have a mean approximately equal to 0, which is the main direction of the iris texture edges. Also, the gradients of the blue channel are significantly spread compared to the gradients of the red and green channels. This fact indicates that the blue channel contains noisy orientations of the iris texture.

By computing the entropy of the gradient distributions, the amount of noisy directions present in the iris texture in a particular channel is measured. For narrow distributions of the gradients, the entropy will have a small value and for a wider spread distribution of the gradients, the entropy will increase. The Shannon entropies were computed for all gradients from UBIRISv1, session1 images and for all the RGB and HSI colour spaces' channels. The spreads of the gradient entropies for all the channels from RGB and HSI colour spaces are illustrated in Figure 3.12. From Figure 3.12 it may observed that the entropy values for blue, hue and saturation channels are higher than those in the red, green and intensity channels. This approach could be used for other colour spaces to analyse which channels contain most discriminant information from the iris texture.

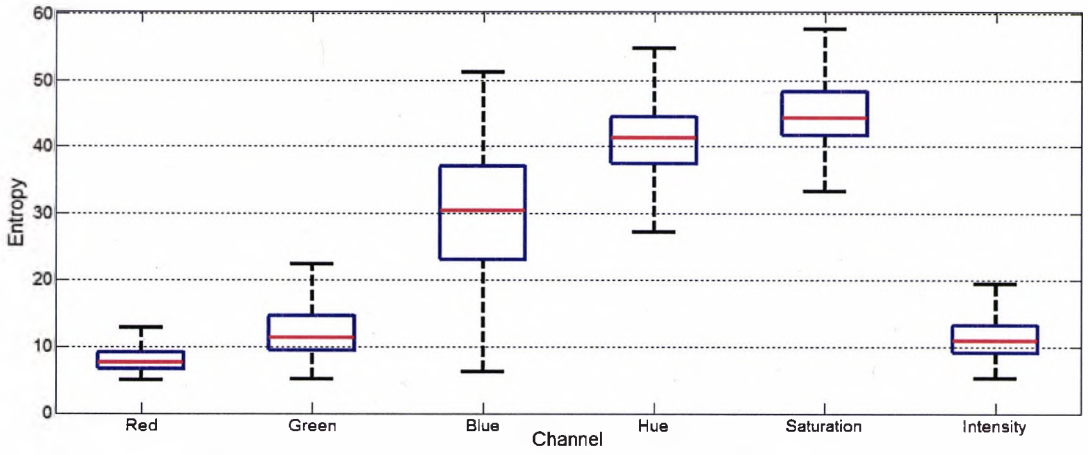

Figure 3.12. Entropies of the gradients computed for RGB and HSI colour spaces' channels

After the iris images are segmented using the proposed segmentation algorithm

described in Section 3.2 and the channels which exhibit more discriminant information are selected, the multi-algorithmic biometric system may be further developed.

3.4 Multi-algorithmic iris recognition system

The segmentation and colour channel selection are the prerequisites of any iris recognition system that operates on colour images. These steps were described in the previous sections. In this section, a multi-algorithmic approach is explored for iris recognition systems working on visible spectrum images. The multi-algorithmic approach is explored first in this thesis, because it involves a basic fusion mechanism between the scores generated by the component algorithms. The colour iris recognition approaches described in Chapter 4 and Chapter 5 will employ more complex fusion techniques.

The proposed multi-algorithmic iris recognition system uses three different feature extraction methodologies. The first one uses the gray levels of the 8 neighbourhood of a pixel from the iris texture and is proposed in this study. The second one employs wavelet transform to extract the information from the iris texture. Finally, the third one uses the classical 2D Gabor filters (Daugman 2004) for feature extraction. All three types of features are binary strings. The block diagram of the proposed multi-algorithmic iris recognition system is presented in Figure 3.13. As may be observed, the system only uses the red channel to extract the information from the iris texture. By using only the red channel, the investigation separates the benefits of the multi-algorithmic approach from the benefits of fusing data from multiple colour channels.

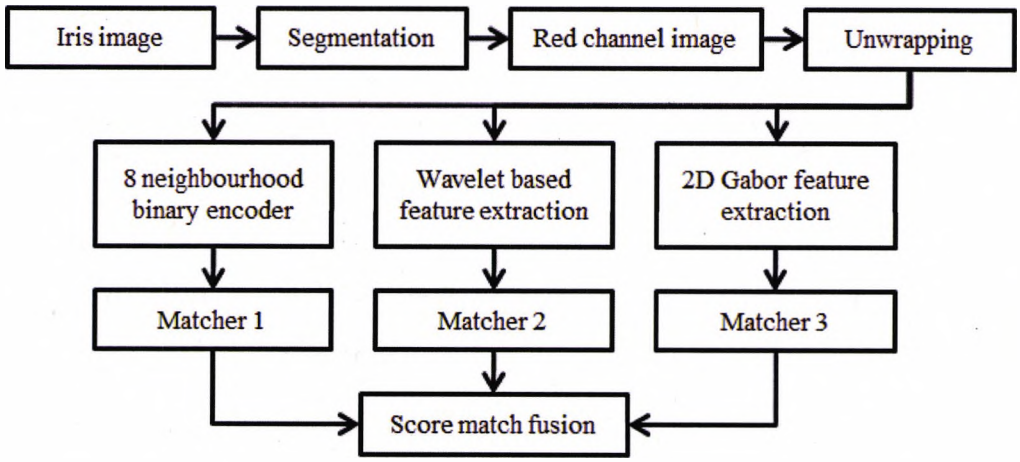

Figure 3.13 Multi-algorithmic iris recognition system architecture

The iris images unwrapping was done using the rubber sheet model proposed in (Daugman 1993). To avoid including the eyelashes in the unwrapped image, the circle sector defined between -45° and +45° of vertical axis was not considered. The unwrapped image dimension initially is 120 by 50 pixels. Then, 100 pixels are considered around the pupil and the resulting unwrapped image dimension is 120 by 100 pixels. As the iris width for UBIRISv1 images is approximately 100 pixels, the 50 pixels and 100 pixels around the pupil represent roughly 50% and 100% of the available information in the iris texture. A comparison of how the iris recognition system's performance increases when 100% of the available information is used over the case when only 50% of the information is used will be presented in the experimental results subsection.

3.4.1 8-neighbourhood binary encoder

The pixel relationships are the basis of the least computationally demanding texture analysis techniques, as there is no filtering operation necessary. By using the 8 neighbourhood of a pixel, a computationally efficient iris feature extraction method is proposed which is therefore suitable to be implemented on embedded or mobile devices.

The working principle of the proposed feature extraction method is a simple, yet effective one: the 8 positions of the 8-neighborhood of a pixel may be encoded on 3 bits, as

shown in Figure 3.14. An offset of 1 is obtained when the center pixel is immediately near its neighbours, but the offset may be higher. Considering the values of the 8 neighbours of a pixel, the 3 bits corresponding to that pixel are the binary code corresponding to the position of the highest intensity value of the 8 neighbour pixels. The choice of the highest intensity value was made in order to capture the orientation of the iris texture.

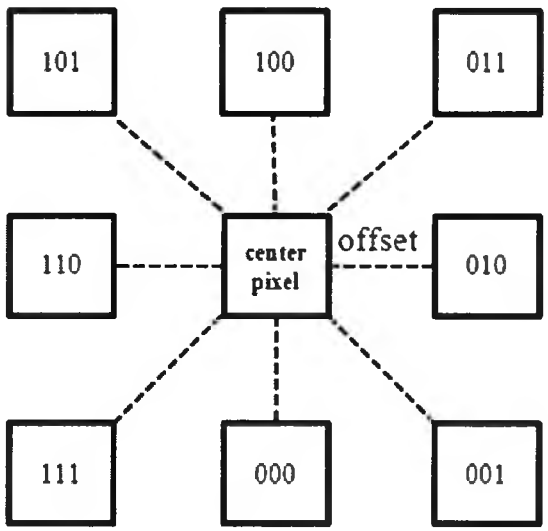

Figure 3.14. Binary encoding of 8 neighbourhood of a pixel

Additionally to encoding the position of the maximum pixel value of the 8-neighborhood, the value of the center pixel is compared to the average of the 8-neighborhood. If the center pixel has a value greater than the mean, a logical 1 is concatenated to the 3 bits corresponding to the position of the maximum neighbour, otherwise a logical 0 is concatenated.

The 8-neighborhood doesn't necessarily have to be considered for all pixels, it may be considered with a step for the vertical scan and one for the horizontal scan. In this way this feature extraction method becomes even more computationally efficient. A direct search investigation was carried to observe how the performance varies with the step size. The HD is used as a matching algorithm (Daugman 1993).

This feature extraction method has three parameters: the offset, the horizontal scanning step and the vertical scanning step. These parameters were found empirically, by taking the first 40 classes from UBIRISv1 Session 1 dataset and computing the decidability index (Daugman 1993), which is a measure of the separation between the authentic and impostor score distributions (see subsection 2.2). The maximum DI was obtained for an offset of 7 pixels, a horizontal step of 1 pixel and a vertical step of 5 pixels. The resulting feature size is 3392 bits for the 120 by 50 pixels unwrapped image and 7632 bits for the 120 by 100 pixels image.

3.4.2 Wavelet based feature extraction

Wavelet transforms were proposed by the mathematician Alfred Haar in 1909, but the concept was defined only in 1981 by the geophysicist Jean Morlet. Wavelet transforms were introduced to overcome the limitation of Fourier transform, which can only analyse stationary signals, i.e. signals which do not change their frequency in time. Wavelets are able to locate the change in frequencies of non-stationary signals. A reference work on wavelets may be found in (Daubechies 1992). While the basis functions for Fourier transform are sinusoids, in wavelet transform the basis functions are small waves, called *wavelets*, which are limited in duration and of varying frequency.

The continuous wavelet transform (CWT) $\Psi(\tau, s)$ may be defined as the convolution of a 1D signal $x(t)$ with a mother wavelet function $W(t)$, which may be dilated or compressed, as it may be observed from equation 3.7. τ defines the translation and s is the scale of the wavelet. The scale s is inverse proportional to the frequency of the signal. The wavelet transform produces a good time resolution and poor frequency resolution at high frequencies and good frequency resolution and poor time resolution at low frequencies.

$$\Psi(\tau, s) = \frac{1}{\sqrt{s}} \int_{-\infty}^{\infty} x(t) \cdot W\left(\frac{\tau - t}{s}\right) dt \tag{3.7}$$

The CWT may be practically computed by sampling the time-scale plane. A popular wavelet discretization technique is to employ a dyadic scale (power of two) for the wavelet

scale and shifting parameters, s and τ respectively. In such a manner, a discrete wavelet transform (DWT) of the signal $x(t)$ is obtained.

For two dimensional signals, such as digital images, the DWT is computed using a four-band filter bank subband coding technique. Initially, the rows of the images are processed, then a dyadic down-sampling is made and subsequently the columns of the image are filtered. This process is illustrated in Figure 3.15.

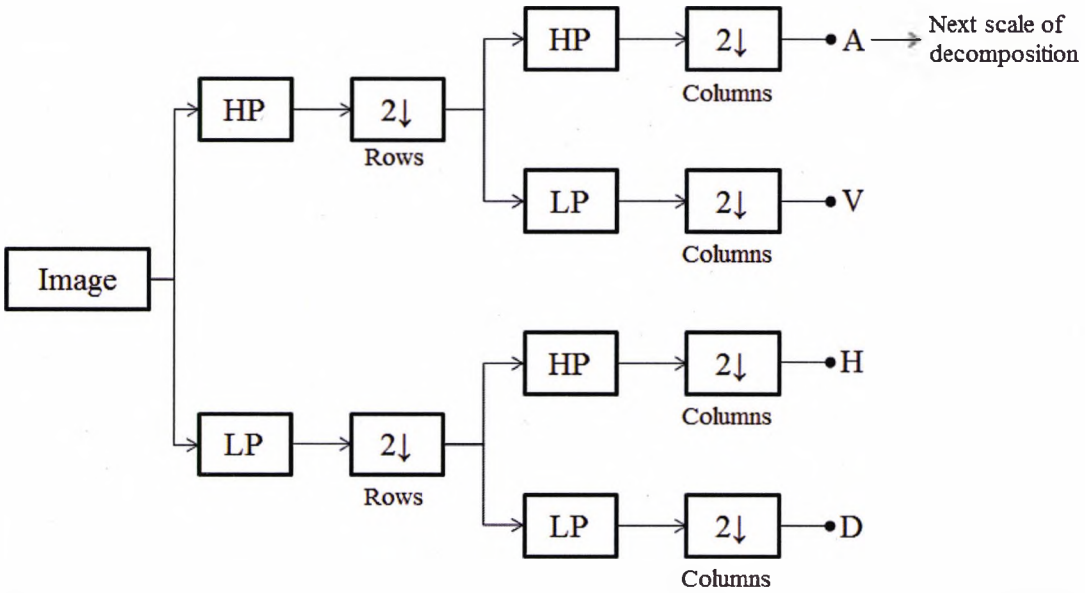

Figure 3.15. The wavelet decomposition scheme. HP – highpass filter; LP – lowpass filter; 2↓ - dyadic down-sampling; A – approximation coefficients; V – vertical detail coefficients; H – horizontal detail coefficients; D – diagonal detail coefficients.

To extract the most discriminative iris features using wavelets, the best performing wavelet family has to be found together with the optimum level of decomposition. An empirical study which shows which wavelet family is best to be used for colour iris images feature extraction is made in (Szewczyk, Grabowski et al. 2012). The study was done on iris images from UBIRISv2 database on unwrapped iris images of size 512 by 256 pixels. For one level of decomposition, only the vertical detail coefficients were used to generate the features. The vertical detail coefficients were binarized by comparing them to the median value of the coefficients. The performance criteria used to rank the wavelet families was the

EER and the DI. The study was conducted for 73 wavelets with 5 levels of decomposition. According to the results of the empirical analysis, the best wavelet choice for iris feature extraction is the reverse biorthogonal wavelet with 2 vanishing moments, i.e. the wavelet scaling function is linear. The authors of the empirical study report that for UBIRISv1 dataset, the optimum wavelet family to be used for iris feature extraction is reverse biorthogonal wavelet with 3 vanishing moments. The different vanishing moments of the best performing wavelet is due to the fact that irises from UBIRISv1 are of higher dimension and quality than those acquired in UBIRISv2 dataset (see subsection 2.3.1).

Wavelets are one of the main feature extractors used in iris recognition research. In the proposed multi-algorithmic iris recognition system, the wavelet-based features were extracted using the reverse biorthogonal wavelet with 3 vanishing moments, as indicated in the empirical analysis described in the above paragraph. The vertical detail coefficients of various levels of decomposition were computed and the corresponding binary features were extracted by comparing them to their median value. The first 40 classes from UBIRISv1 dataset, Session 1 were considered for finding the optimum level of decomposition. In Table 3.3 the DI corresponding to the features extracted from different wavelet decomposition levels are given.

Level of decomposition	Feature size	Decidability index
1	3224	1.81
2	924	2.75
3	304	3.09
4	120	2.58
3 and 4	424	3.21
2, 3 and 4	1348	3.07

Table 3.3. DI for features obtained from different wavelet decomposition levels

As it may be observed from Table 3.3, the maximum DI is obtained when the features extracted from the 3rd and 4th wavelet decomposition levels are concatenated. The resulting feature size is 424 bits for the 120 by 100 pixels iris images and only 274 bits for the 120 by 50 pixels iris images.

3.4.3 Classical phase-based feature extraction

This method extracts information from iris texture by employing the classical 2D Gabor filters (Daugman 1993). 2D Gabor filters are obtained by modulating a sinusoid with a Gaussian. 2D Gabor filters are complex-valued filters and have the formula given in equation 3.8:

$$g(x,y) = \exp\left(-\frac{x^2+y^2}{\sigma^2}\right) \cdot \exp\left(2\pi f i(x\cos\theta + y\sin\theta)\right) \tag{3.8}$$

where σ is the standard deviation of the Gaussian kernel, Θ is the orientation of the complex sinusoid and f the frequency of the complex sinusoid. The real part of a 2D Gabor filter is shown in Figure 3.16.

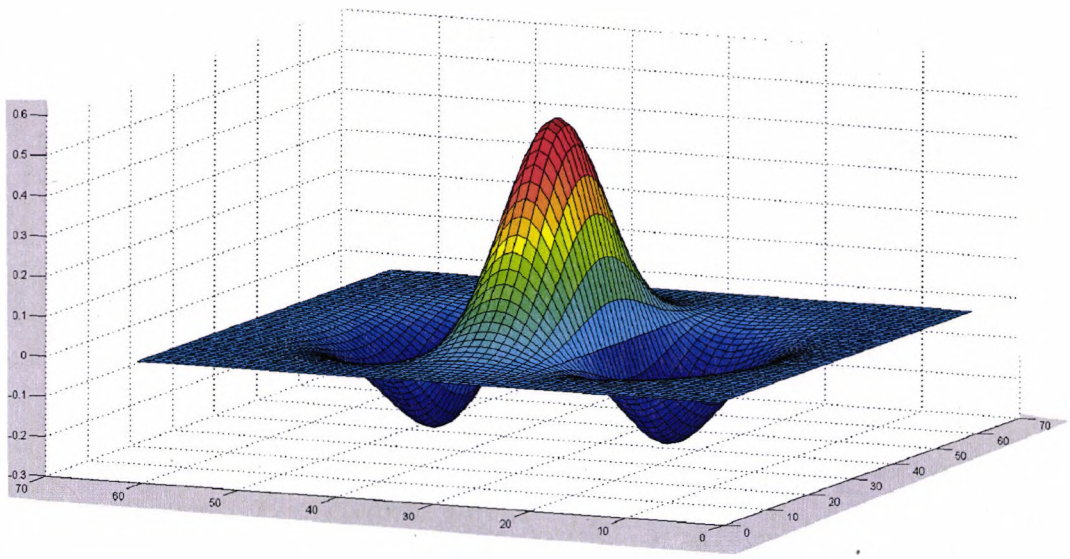

Figure 3.16. Real part of a 2D Gabor filter

The convolution of a 2D Gabor filter with an image $I(x,y)$ is given by the equation 3.9:

$$G(x,y) = \iint I(m,n) \cdot g(x-m, y-n) dm\, dn \tag{3.9}$$

The parameters of the 2D Gabor filter that need to be found are the frequency and orientation of the sinusoid and the filter size. Although the 2D Gabor filters are the basis of the most popular iris feature extraction methodology, the parameters of the filters are not standardized. The vast majority of the published works that use 2D Gabor filters for iris feature extraction do not discuss the values of the parameters.

For each pixel of the unwrapped image, 2 bits of information are extracted, corresponding to the sign of the real and imaginary part of the filtered iris image. The values of the three parameters of the 2D Gabor filters were found by employing a direct search. The orientation of the complex sinusoid was fixed to 90°, as the orientation of the iris texture in the unwrapped image is vertical. The fact that the 90° orientation yields the best accuracy among the directions of the complex sinusoid will be shown in an empirical study from Chapter 4. With a fixed orientation, the search space of the filter parameters became a two dimensional one. The size of the filter is an integer number and in the direct search it was searched from 3 to 30, with a step of 1. The frequency of the complex sinusoid ranged from 0.001 to π, with a step of 0.001. The performance criterion was the maximum DI. The first 40 classes from UBIRISv1 were used in finding the parameters, comprising 5 images per class.

It was observed that if the information is extracted from every other pixel of the unwrapped image, the drop in performance is negligible. The feature size is 3000 bits for the 120 by 50 pixels unwrapped iris image and 6000 bits for the 120 by 100 pixels image. The issue of rotation is addressed by shifting one binary string 4 bits to the left and 4 bits to the right and the minimum HD out of the 9 computations is stored. The same shifting methodology is applied for the other two types of features to overcome the effects of image rotation on the calculated HD.

3.5 Experimental Results

In UBIRISv1 database, Session 1, 10 images out of the total of 1205 are strongly or totally occluded and therefore no useful information can be extracted from them. From the second session, 13 iris images are occluded. The experiments were conducted on all the images from the dataset, including the occluded ones. Examples of images from UBIRISv1, Session 1 and Session 2 are shown in Figure 3.17.

The experimental setup consists of the classical one vs. one score generation for all possible combinations between same class images and different class images. The fusion between the scores produced by the 3 algorithms was done by using weighted average. The weighted average was selected as a fusion method by conducting an empirical study on how some basic fusion methods affect the accuracy of the multi-algorithmic biometric system on the first 40 classes of UBIRISv1, session 1. The benchmarked fusion mechanism were the sum, average, minimum, maximum, median and weighted average. The weighted average is also shown to yield the best accuracy as a score level fusion in the colour iris recognition system described in (Caitang, Melgani et al. 2008).

The weights for the 3 algorithms were determined using the first 40 classes via a direct search. Initially, the weights were selected by maximizing the DI, but a weight of 0.96 was assigned to the score generated by the 2D Gabor features. A weight close to 1 for one of the three algorithms will produce results which are not significantly different than those obtained by the algorithm corresponding to the large weight. Subsequently, the weights of the 3 algorithms were calculated by minimizing the EER. The obtained weights were 0.75 for the 8-neighbourhood feature score, 0.08 for the wavelets features HD and 0.17 for the 2D Gabor features HD. The obtained weights are database specific and they need to be recalculated if another database is to be used.

For session 1 iris images the experimental results are reported for the last 201 users left after the weights were determined using the first 40 classes and also for all 241 users. There are a total of 2410 authentic scores and 723000 impostor scores for session 1 iris images. For session 2 iris images, there are 1320 authentic scores and 216150 impostor scores. Initially, the results for the case when 50 pixels around the pupil are used will be reported and then the results when the whole of the iris is used will be presented.

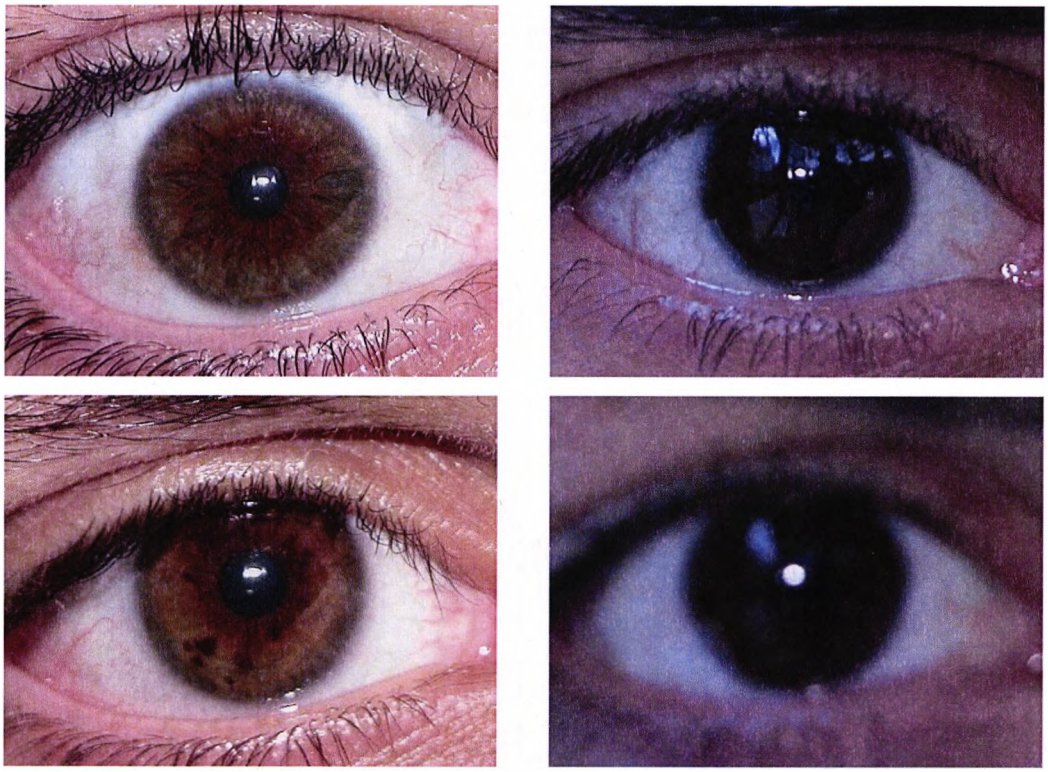

a) b)

Figure 3.17. UBIRISv1 images from a) Session 1; b) Session 2

3.5.1 Using 50 pixels around the pupil

In Table 3.4, the DI and EER are reported for the scores obtained by using the last 201 users and subsequently for all 241 users of session 1 images, for the 3 algorithms and for the fusion. It may be observed from Table 3.4 that although the 2D Gabor filter based features yield the highest DI among the three algorithms, the lowest EER is obtained by the 8-neighborhood based features. This fact indicates that a higher DI of an iris recognition algorithm does not imply that the algorithm performs better than algorithms which have a lower DI. By fusing the three algorithms at the score level, the EER of the system was decreased by approximately 8%, from 4.05% to 3.73%.

Algorithm	UBIRISv1 Session 1 - 201 classes		All UBIRISv1 Session1 images	
	DI	EER [%]	DI	EER [%]
8-neighborhood	3.34	3.71	3.22	4.05
Wavelets	2.92	7.43	2.86	7.64
2D Gabor	4.00	3.53	3.93	4.20
Fusion	3.78	3.27	3.64	3.73

Table 3.4. DI and EER for UBIRISv1 Session 1, when 50 pixels around the pupil are used

The Receiving Operator Characteristic (ROC) curves for all Session 1 images for the three algorithms and the fusion are plotted in Figure 3.18. It may be observed from Figure 3.18 that the 2D Gabor filter based features yield the best ROC curve out of the three component algorithms. Also, the score level fusion of the three algorithms improves the ROC curve of the 2D Gabor filter based algorithm for a large range of FARs.

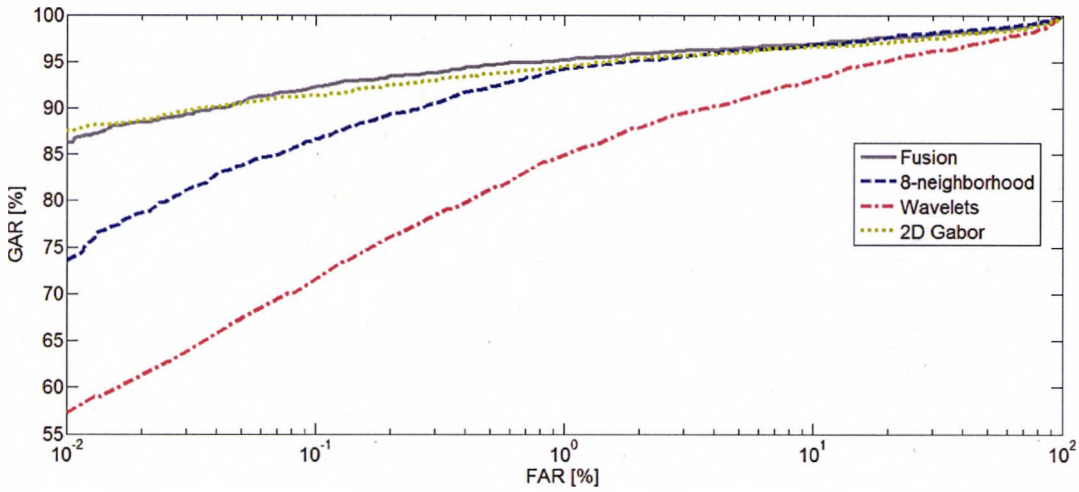

Figure 3.18. ROC curves for the three component algorithms and the multi-algorithmic approach for UBIRISv1 Session 1 images, when 50 pixels around the pupil are used

For Session 2 iris images, which contain a significant amount of noise, the DI and EER obtained are presented in Table 3.5. The same weights found for session 1 iris images were used in the weighted average. It may be observed from Table 3.5 that 2D Gabor filter

based algorithm and 8-neighborhood based algorithm yield superior accuracy to the wavelet based algorithm. Also, the score fusion of the three algorithms is not able to improve the EER of the 2D Gabor filter based algorithm. The ROC curves obtained for Session 2 images for the three component algorithms and the fusion are plotted in Figure 3.19. The ROC curve corresponding to the 2D Gabor filter based algorithm is superior to the ROC curves of the other 2 algorithms and also to the score fusion approach.

Algorithm	All UBIRISv1 Session 2 images	
	DI	EER [%]
8-neighborhood	1.50	23.49
Wavelets	1.32	26.26
2D Gabor	1.66	22.03
Fusion	1.62	22.49

Table 3.5. DI and EER for UBIRISv1 Session 2, when 50 pixels around the pupil are used

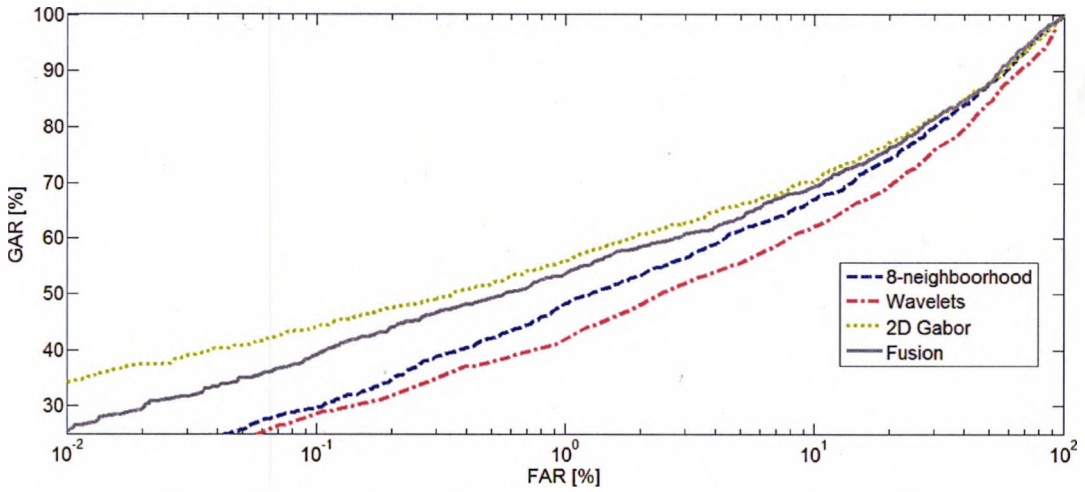

Figure 3.19. ROC curves for the three component algorithms and the multi-algorithmic approach for UBIRISv1 Session 2 images, when 50 pixels around the pupil are used

As mentioned previously, for UBIRISv1 database the width of the iris band is roughly 100 pixels, therefore 50 pixels around the pupil represent approximately 50% of the available iris texture. After investigating how the fusion of the three individual iris

recognition systems performs when only approximately 50% of the iris texture is used, it is interesting to observe how the multi-algorithmic iris recognition system performs when 100% of the iris texture is used.

3.5.2 Using 100 pixels around the pupil

In Table 3.6, the DI and EER are reported for the scores obtained by using the last 201 users and subsequently for all 241 users of UBIRISv1 session 1 iris images, for the 3 algorithms and for the fusion, when 100 pixels around the pupil are used. It may be observed from Table 3.6 that the 8-neighborhood based algorithm has the lowest EER, although the 2D Gabor filter based algorithm has a significantly higher DI. By fusing the three algorithms at the score level, the EER of the system was decreased by approximately 10%, from 3% to 2.67%. A similar improvement of the EER was obtained for UBIRISv1 session 1 iris images when 50 pixels around the pupil were used (see Table 3.4).

Algorithm	UBIRISv1 Session 1 - 201 classes		All UBIRISv1 Session1 images	
	DI	EER [%]	DI	EER [%]
8-neighborhood	3.80	2.40	3.73	3.00
Wavelets	3.96	3.75	3.79	4.10
2D Gabor	4.83	2.45	4.58	3.03
Fusion	4.47	2.25	4.19	2.67

Table 3.6. DI and EER for UBIRISv1 Session 1, when 100 pixels around the pupil are used

The Receiving Operator Characteristic (ROC) curves for all Session 1 images for the three algorithms and the fusion are plotted in Figure 3.20. From Figure 3.20 it may be observed that the 2D Gabor filter based algorithm has the best ROC curve out of the three component algorithms. Also, the score level fusion of the three algorithms improves the ROC curve of the 2D Gabor filter based algorithm for a large range of FARs.

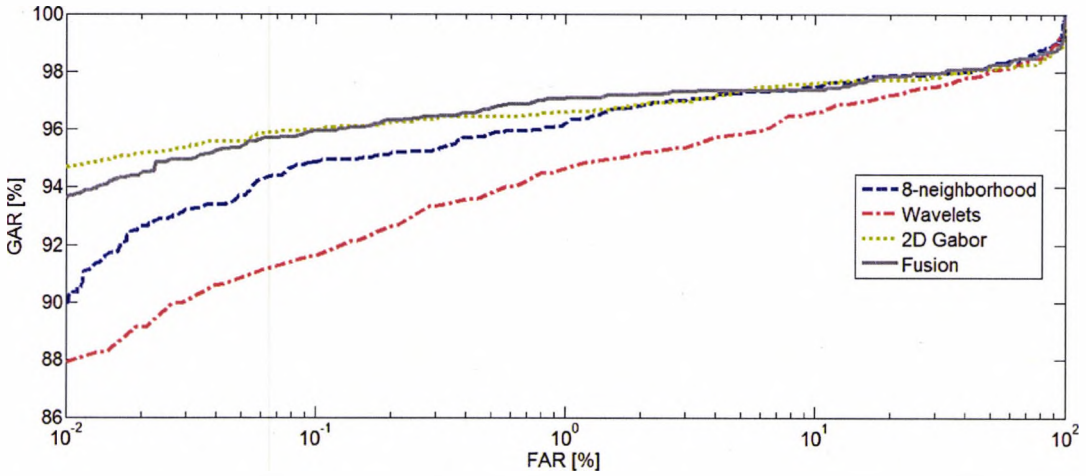

Figure 3.20. ROC curves for the three component algorithms and the multi-algorithmic approach for UBIRISv1 Session 1 images, when 100 pixels around the pupil are used

For Session 2 iris images, the DI and EER obtained are presented in Table 3.7 for the case when 100 pixels around the pupil are used. It may be observed that the lowest EER among the three component algorithms is obtained by the 8-neighborhood based approach. The score level fusion does not improve the EER of the 8-neighborhood algorithm. However, the ROC curve for the 8-neighborhood approach is not the best one, as it may be observed from Figure 3.21. The ROC curve corresponding to the 2D Gabor filter based algorithm is superior to the ROC curves of the other two algorithms and of the fusion approach for low values of the FAR. The score fusion together with the 8-neighborhood based approach have a superior ROC curve compared to that of 2D Gabor filter approach for higher values of FAR.

Algorithm	All UBIRISv1 Session 2 images	
	DI	EER [%]
8-neighborhood	2.05	15.29
Wavelets	1.85	18.84
2D Gabor	2.12	16.65
Fusion	2.13	16.14

Table 3.7. DI and EER for UBIRISv1 Session 2, when 100 pixels around the pupil are used

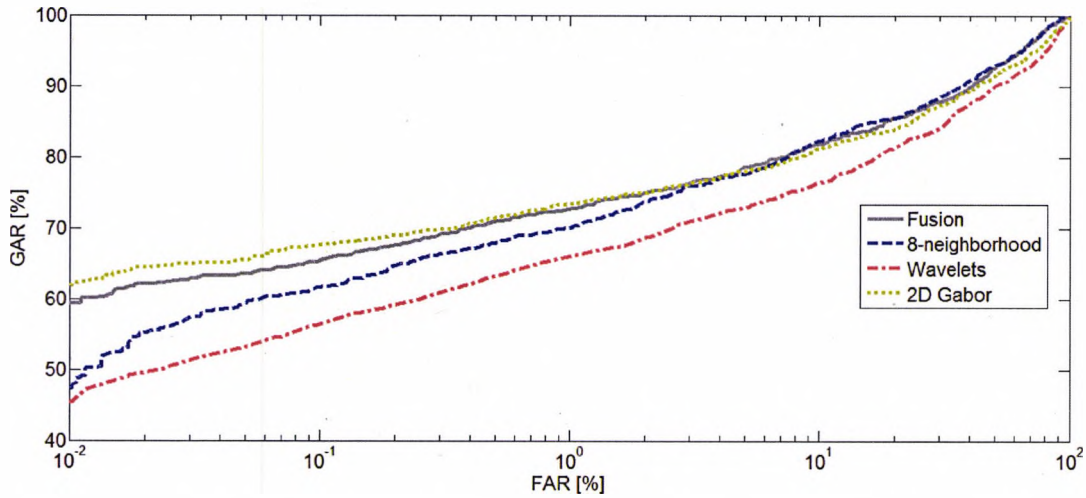

Figure 3.21. ROC curves for the three component algorithms and the multi-algorithmic approach for UBIRISv1 Session 2 images, when 100 pixels around the pupil are used

In Table 3.8, the FRRs for given thresholds of the FAR are given for both session 1 and session 2 iris images. It may be observed from Table 3.8 that when the multi-algorithmic iris recognition system has working points corresponding to low values of the FARs, the 2D Gabor filter based approach is performing best. For working points corresponding to higher values of the FAR, the score fusion of the algorithms performs best, but only for the good quality iris images from UBIRISv1 session 1.

Algorithm	All UBIRISv1 session 1 images			All UBIRISv1 session 2 images		
	FRR [%], FAR=0.01%	FRR [%], FAR=0.1%	FRR [%], FAR=1%	FRR [%], FAR=0.01%	FRR [%], FAR=0.1%	FRR [%], FAR=1%
8-neighborhood	9.98	5.10	3.63	53.58	38.33	29.92
Wavelets	11.95	8.35	5.45	54.62	43.21	35.94
2D Gabor	5.31	4.04	3.40	38.03	32.35	26.69
Fusion	6.35	4.07	2.84	41.68	34.55	27.27

Table 3.8. FRR for different values of FAR for the 3 algorithms and the fusion approach when 100 pixels around the pupil are used

In Table 3.9 the accuracy of the 8-neighborhood approach, 2D Gabor filter approach and score fusion approach are compared to the accuracies reported in literature. As may be observed, the 2 proposed individual systems and the multi-algorithmic approach perform significantly better than the results reported in literature, but only on session 1 iris images, which are of high quality. However, the accuracies reported for the proposed iris recognition systems are obtained using all the images from UBIRISv1 database, while the accuracies reported in (Hosseini, Araabi et al. 2010) are obtained only on non-occluded iris images. The work from (Hosseini, Araabi et al. 2010) was chosen for comparison because the results are reported using most of the iris images from UBIRISv1 database using a classical distance based decision module.

Method	GAR for FAR=1%	
	Session 1	Session 2
Hosseini et al (Hosseini, Araabi et al. 2010)	81.70	81.37
Proposed 8-neighborhood approach	96.37	70.08
2D Gabor filters approach	96.60	73.31
Proposed fusion approach	97.16	72.73

Table 3.9. Performance comparison of proposed approaches with published works

To observe the improvement brought by using 100 pixels around the pupil over the case when only 50 pixels are used, in Figure 3.22 and Figure 3.23 the authentic and impostor distributions of the multi-algorithmic approach are plotted, produced for all images of UBIRISv1 session 1 and session 2 respectively. The EER for session 1 iris images when using 100 pixels around the pupil is improved by 28.41% compared to the case when only 50 pixels are used. For session 2 iris images, the EER is improved by 28.23 % when using 100 pixels around the pupil.

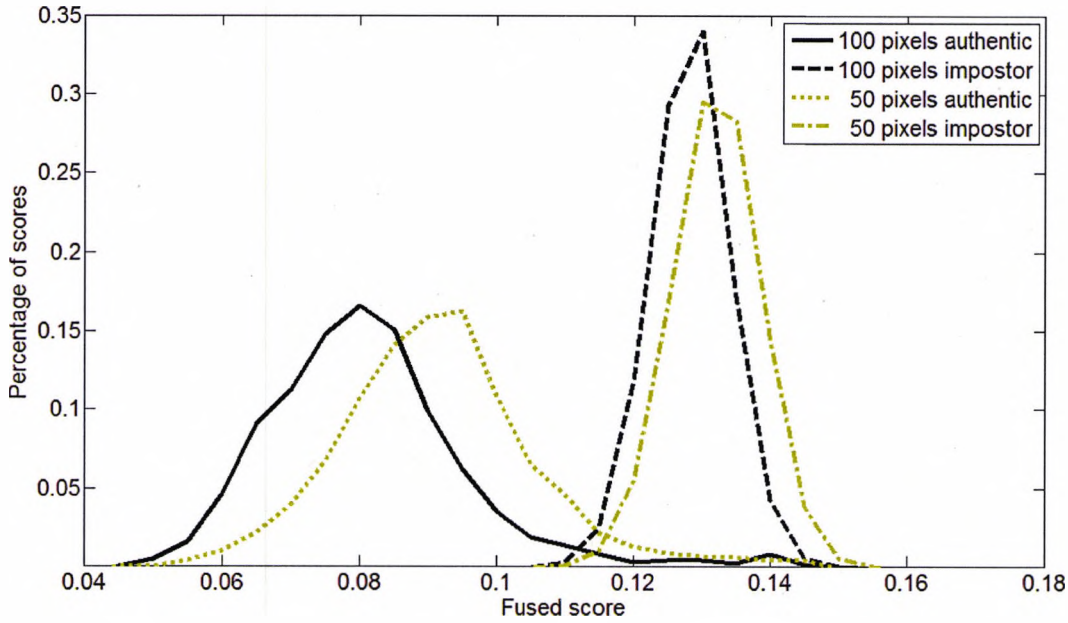

Figure 3.22. Authentic and impostor fused score distributions for UBIRISv1 session 1, when using 50 pixels and 100 pixels around the pupil

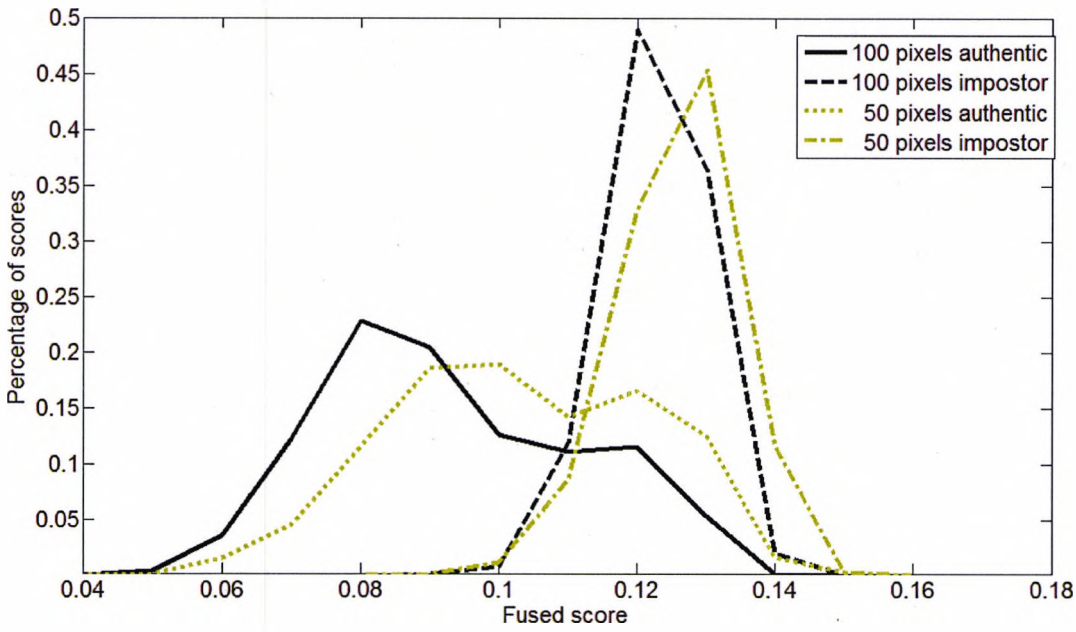

Figure 3.23. Authentic and impostor fused score distributions for UBIRISv1 session 2, when using 50 pixels and 100 pixels around the pupil

3.6 Chapter conclusions

Iris recognition on colour images is a challenging task, due to the large amount of noise that affects the iris image quality in the visible spectrum. In this chapter, a multi-algorithmic approach was developed for iris recognition, which aims to cope with noisy colour iris images. A novel iris segmentation method is proposed, which may be applied on both colour and near infrared iris images, yielding similar accuracies in the two spectrums.

Before the features are extracted, one needs to find out which colour channels reveal better the information from the iris texture. An information theoretical iris texture analysis method is proposed to find which colour channels to extract iris features from. Using this methodology, it was shown that from RGB colour space, the red and green channel reveal best the iris structure and from HSI colour space, the intensity channel is the most discriminative one. The proposed multi-algorithmic iris recognition system uses information extracted only from the red channel.

An iris feature extraction is proposed, based on the 8-neighborhood of the iris texture. This feature extraction method is a highly efficient computational one, because it does not involve image filtering or image transformations. The other two component algorithms of the multi-algorithmic biometric system employ feature extraction methods based on wavelet transform and 2D Gabor filters. The fusion of the three individual iris recognition algorithms is done at the score level by employing weighted average.

The experimental results show that the 2D Gabor filters perform best among the three component iris recognition algorithms. By fusing the three iris recognition algorithms at the score level, the EER of the system is improved by approximately 8%. It was also investigated how the performance of a colour iris recognition system is affected when using only 50 pixels around the pupil compared to the case when 100 pixels around the pupil are used. It was found that the EER is improved by roughly 28% when 100 pixels around the pupil are used compared to the case when only 50 pixels around the pupil are used.

Overall, the experimental results show that a multi-algorithmic approach for colour iris recognition is beneficial, even when the accuracy of some component algorithms is significantly poorer compared to the best performing algorithm from the ensemble. A multi-algorithmic approach for colour iris recognition is appropriate to be used when the robustness and reliability of the biometric system represent critical aspects of the scenario.

However, if the application of an iris recognition system requires a working point corresponding to low values of the FAR, the 2D Gabor filter based approach exhibits a superior accuracy to the proposed multi-algorithmic approach. This fact is an indication that a highly optimized 2D Gabor filter based iris recognition algorithm is desirable for low values of the FAR rather than a multi-algorithmic approach. Such an iris recognition algorithm based on many 2D Gabor filters will be developed in the following chapter.

Chapter 4
Fusing texture and colour for less constrained iris recognition systems

In this chapter features will be extracted from iris texture and eye colour and a fuzzy logic fusion is employed to combine at score level the scores generated by the two features extraction methodologies. A technique for optimising the parameters of multiple 2D Gabor filters to be useful for features extraction from the iris texture is also proposed.

4.1 Introduction

The fusion of information from eye colour or periocular region with the iris texture data has been shown to improve significantly the accuracy of colour iris recognition systems, as concluded from the literature review made in Chapter 2. In Chapter 3, a multi-algorithmic iris recognition system was proposed, which uses three iris features extraction methodologies, to obtain information from the iris texture. From the experimental results reported in Chapter 3, it may be observed that the classical 2D Gabor filter based algorithm performs best among the three algorithms, although only one set of parameters of the 2D Gabor filters was used for feature extraction. For working points of the iris recognition system corresponding to low FAR the 2D Gabor filter based algorithm yield a better ROC curve than the multi-algorithmic approach.

The pioneering iris recognition system (Daugman 1993) based on the 2D Gabor filters employs "many filter sizes, frequencies and orientations". However, indications about the number or values of the filter parameters are not given in (Daugman 1993). A methodology of finding the parameters of many 2D Gabor filter feature extractors to jointly analyse the iris texture is a highly desirable one. For colour iris images, the information extracted from the texture may be augmented with information extracted from the eye colour. The eye colour could be considered a subjective characteristic of the human body and a methodology of numerically describing the iris colour is therefore necessary.

The motivation of the work described in this chapter was given by the fact that the best algorithms from NICE II competition (Lab 2009) were using a fusion approach between multiple sources of information, but the main two sources were the iris texture and eye colour. In this chapter a fusion approach between the information extracted from the iris texture and the eye colour is explored. The main idea behind the texture – colour fusion is to complement the properties of the HD authentic and impostor distributions generated by the 2D Gabor filters based features. As mentioned in Chapter 1, the reliability of the classical iris recognition approach is given by the low FARs that is capable to achieve due to the rapid termination of the impostors' HD distribution. Thus, an iris feature extraction methodology which will generate a rapid terminating authentic score distribution will complement the property of the 2D Gabor filter based impostor distribution.

There are three main contributions of this chapter:

1) a methodology of using many sets of optimized 2D Gabor filters parameters to enhance the iris recognition system's accuracy;
2) an eye colour feature extraction methodology, adapted from a colour feature extraction technique available in the literature;
3) an investigation of how a Fuzzy logic score fusion between texture and colour is enhancing the iris recognition system's accuracy, especially when the low quality colour iris images generate poor performing texture features.

The remainder of this chapter is organized as follows: Section 4.2 will present the proposed methodology of using multiple sets of optimal 2D Gabor filter parameters to extract features from the iris texture. In Section 4.3 the eye colour feature extraction technique is described. Section 4.4 describes the proposed fuzzy logic score level fusion methodology that was employed for fusing the information from colour and texture. The results from the experimental investigation are reported in Section 4.5 and the conclusions are given in Section 4.6.

4.2 Iris texture feature extraction

The texture feature extraction methodology developed in this subsection proposes a technique of extracting classical phase based iris features by using multiple sets of optimized 2D Gabor filter parameters. 2D Gabor filters are a powerful tool in analysing the texture because they provide spatial-frequency information, similar to the human visual cortex (Daugman 1980). The 2D Gabor filters are a product between a Gaussian and a complex sinusoid. Their formula (Daugman 1988) was given in equation 3.8, but for ease of reading, the formula is rewritten in equation 4.1:

$$g(x,y) = \exp\left(-\pi\frac{x^2+y^2}{\sigma^2}\right)\cdot\exp\left(2\pi fi(x\cos\theta + y\sin\theta)\right) \tag{4.1}$$

where σ is the standard deviation of the Gaussian kernel, Θ is the orientation of the complex sinusoid and f the frequency of the complex sinusoid. A visualization of 2D Gabor filter composition is illustrated in Figure 4.1.

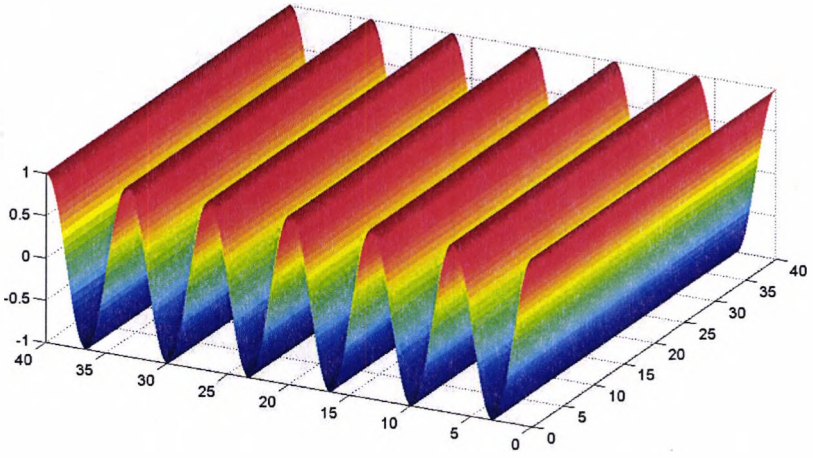

a)

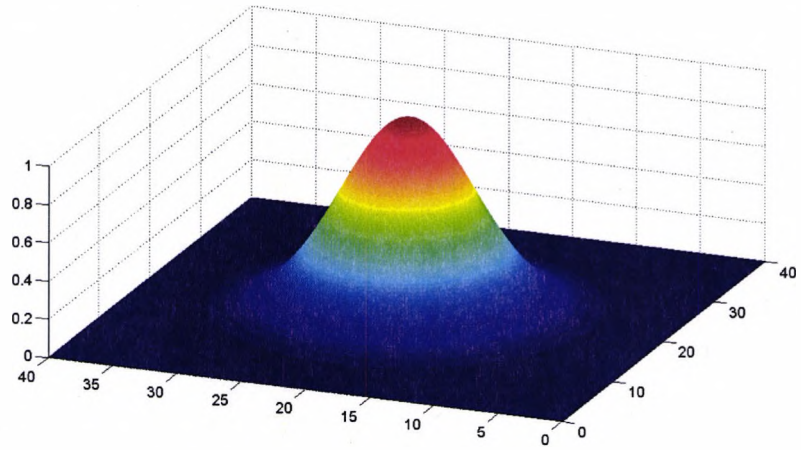

b)

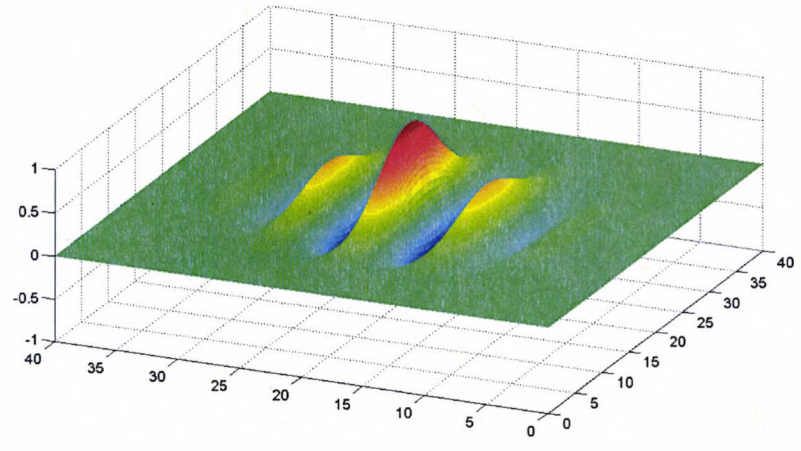

c)

Figure 4.1. Gabor filter composition: a) 2D sinusoid orientated at 90°; b) Symmetric Gaussian kernel; c) the real part of the resulting 2D Gabor filter

By choosing appropriate values for the 2D Gabor filter parameters, the filters have similar behaviour to multi-resolution analysis (Kyrki, Kamarainen et al. 2004), such as wavelet transform. The 2D Gabor filter frequencies and sizes correspond to the scale of the wavelet transform. For lower frequencies of the analysed signal, the size of the filter has to be large and the value of the frequency has to be similar to that of the analysed signal. For higher frequencies of the signal to be analysed, the size of the 2D Gabor filter will decrease.

The randomness and richness present in the iris texture make the 2D Gabor filter bank analysis a suitable technique to be used for iris recognition systems. The iris recognition system proposed in (Daugman 1993) based on 2D Gabor filter bank analysis is implemented in most of the commercially available iris recognition devices. The features used in this pioneering iris recognition approach are the binarized signs of the real and imaginary components of the filter responses. For each pixel of the unwrapped iris image, 2 bits of information are extracted, binary ones corresponding to positive signs and binary zeros corresponding to negative signs. However, details about how the filter bank should be designed were not given in Daugman's publications.

To accurately characterize complex texture structures using 2D Gabor filters it is necessary to use multiple sets of parameters. Using only one set of parameters of the 2D Gabor filter does not lead to the highest accuracies of an iris recognition system, as indicated in (Chia-Te, Sheng-Wen et al. 2006). The filter parameters have to be fine-tuned for various regions of the unwrapped iris image. The filter bank will enhance the relationship between filter responses of various textures as more distinct filter parameters are used for analysis (Kyrki, Kamarainen et al. 2004).

In the present study, the employed 2D Gabor filters have 3 parameters: the orientation of the sinusoid, the frequency of the sinusoid and the filter size. The problem that has to be solved is how to apply 2D Gabor filters with various parameters to improve the iris recognition system's accuracy gradually, by adding more components to the filter bank. For the selection of filter orientations it is shown in the literature (Kyrki, Kamarainen et al. 2004) that the orientation have to be spaced uniformly, by respecting equation 4.2.

$$\theta_k = \frac{k2\pi}{n}, \quad k = \{0, \dots, n-1\} \tag{4.2}$$

where Θ_k is the k-th orientation of the filter and n is the number of orientations to be used. The range of the orientations may be reduced to half, since filter responses on orientations between [π, 2π] are phase shifted from filter responses on orientations between [0, π] in case of real valued inputs (Kyrki, Kamarainen et al. 2004).

For the filter frequency selection, in (Daugman 1988) and (Kyrki, Kamarainen et al. 2004) is suggested that an exponential sampling is beneficial to be used, that is:

$$f_k = a^{-k} f_{max}, \quad k = \{0, \dots, m-1\} \tag{4.3}$$

where f_k is the k-th frequency, f_0 is the highest frequency to be used and a is the scaling factor. When octave spacing between filter frequencies is used (one octave contains 12 frequencies), the value of a is equal to 2 and when half-octave spacing is desired, $a=\sqrt{2}$. The octave spacing between frequencies and also filter sizes is suggested in (Daugman 1988) to be beneficial for designing 2D Gabor filter banks. However, the selection of frequency and filter sizes in octave steps is not suggested in Daugman's publications on iris recognition.

The randomness of the iris texture makes it difficult to define a maximum frequency to be used in the design of the 2D Gabor filter bank. As may be observed from Figure 4.2, the spatial frequency of the iris texture is higher towards the pupil and lowers towards the sclera, due to its radial orientation. For a better understanding, the reader may consider a point in the centre of the pupil as the origin of multiple lines in a radial direction. Near the origin, the lines will have a small distance between them and further away from the origin, the distance between the lines will gradually increase. Therefore, a search technique is a safe solution to find the optimum sets of parameters to be used in designing the iris feature extractor.

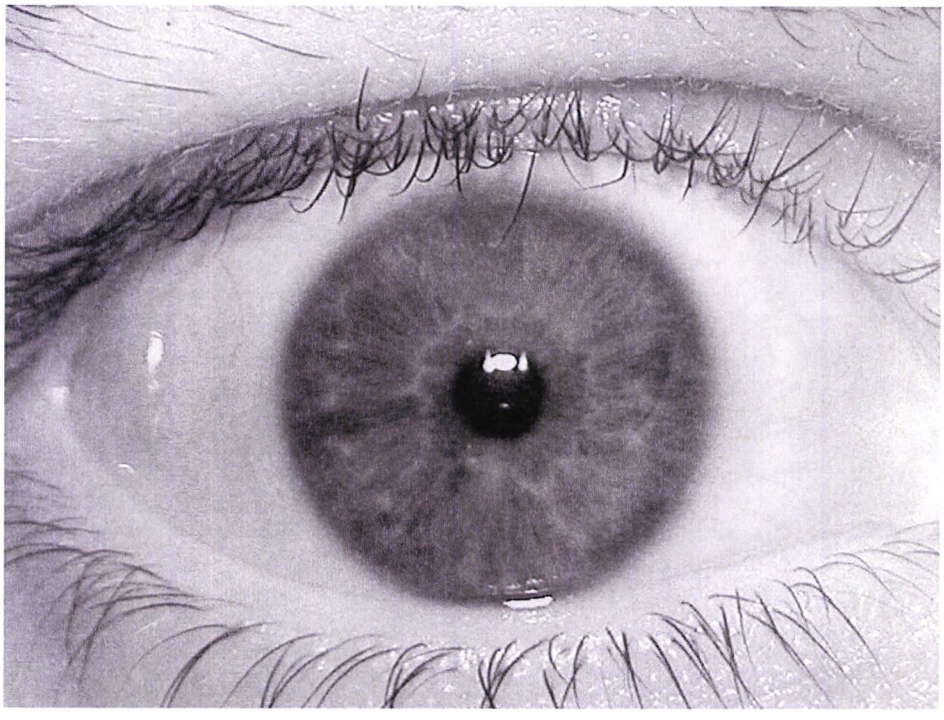

Figure 4.2. Red channel of an eye image from UBIRISv1 Session 1 database

A genetic algorithm approach is proposed in (Chia-Te, Sheng-Wen et al. 2006) to search for optimum 2D Gabor filter parameters in designing an iris recognition system. The fitness function of the genetic algorithm consisted of the DI, i.e. the separability between authentic and impostor HD distributions for a fixed number of classes. The approach from (Chia-Te, Sheng-Wen et al. 2006) does not sample the parameters space with the rules mentioned above and there is no certainty that the genetic algorithm has found the best sets of parameters.

In the present investigation the 2D Gabor filter parameters were found by performing a direct search in the two-dimensional space defined by the size and frequency parameters, for a fixed orientation of the filter. The values of the filter orientations are sampled according to equation 4.2. The range [0, π] was spaced uniformly at 12 fixed intervals, with a step of 0.261 radians, which correspond to 15°. For each value of the orientation, a direct search was performed to find the filter size and frequency. The filter size is an integer value and it was searched in the [3; 30] interval, with a step of 1. The filter

frequency was searched in the [0.001; π] interval, with a step of 0.001. The 100 iris images corresponding to the first 20 classes from UBIRISv1, Session 1 database are used in the direct search. The parameters which correspond to a maximum DI for one orientation are saved. The features are extracted from the 120 by 100 pixels red channel unwrapped iris images. The binary features will have 2 bits of information for every pixel, resulting in a final feature size of 24000 bits. The maximum DI obtained for different filter orientations for the first 20 classes of UBIRISv1 Session 1 database are summarized in the bar plot from Figure 4.3.

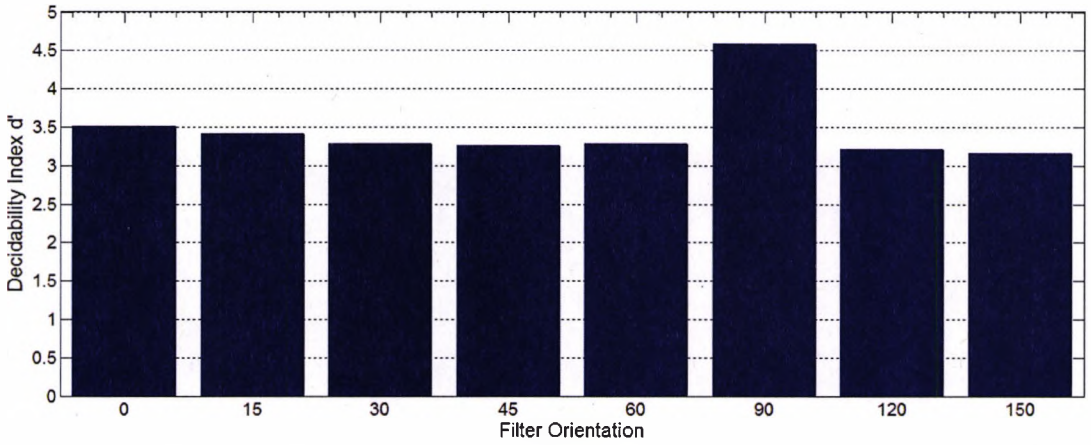

Figure 4.3. Maximum DI obtained for different 2D Gabor filter orientations when first 100 iris images from UBIRISv1 Session 1 are used

As may be observed from Figure 4.3, the DI for the orientation of π/2 of the 2D Gabor filter is significantly higher than the DI obtained for all other 7 orientations of the filter. This is due to the fact that in the unwrapped iris image, the main orientation of the texture is 90°, as shown in Figure 3.8 from subsection 3.3. It was observed that by extracting information only from every other pixel on lines and columns, the DI of the biometric system remains approximately the same, but the feature size is reduced from 24000 bits to 6000 bits. The feature size reported for Daugman's pioneering iris recognition system is only 2048 bits.

The problem that has to be solved is how to use other filter orientations, in addition

to $\pi/2$ orientation to increase the accuracy of the iris recognition system. In finding a solution to this problem, the features are extracted only from one line of pixels from the unwrapped image. As mentioned in (Daugman 1993), there is a radial redundancy in the iris texture, as the structure of the texture does not change considerably from one line of pixels to the next one. Therefore, by sampling the iris texture of the unwrapped iris image along the lines, most of the redundant bits are eliminated and the feature size is reduced in the same time. After optimizing the parameters of the 2D Gabor filter bank for one line of pixels, an identical optimization algorithm should be applied for the sampled lines of the unwrapped iris image and the final binary code will be the concatenation of the binary codes corresponding to all the sampled lines.

The most straightforward method to use other orientations in addition to the 90^{o} one is to concatenate the bits extracted using 90^{o} orientation with the bits extracted using another orientation of the filter. For the optimization procedure, features were extracted from line 50 of the first 200 images from UBIRISv1 Session 1 database, which correspond to 40 users. In Table 4.1, the obtained DI for different approaches of augmenting the bits extracted using 90^{o} and 45^{o} are reported. It may be observed that the DI is maximized for one line of pixels by concatenating the bits extracted using 90^{o} and every other 4^{th} bit extracted using another orientation.

Feature extraction methodology	DI
Using only $\pi/2$	3.07
Using $\pi/2$ and $\pi/4$	2.96
Using $\pi/2$ and $\pi/4$ with every other pixel extracted using $\pi/4$	3.11
Using $\pi/2$ and $\pi/4$ with every 3^{rd} pixel extracted using $\pi/4$	3.18
Using $\pi/2$ and $\pi/4$ with every 4^{th} pixel extracted using $\pi/4$	3.31
Using $\pi/2$ and $\pi/4$ with every 5^{th} pixel extracted using $\pi/4$	3.19

Table 4.1. DI maximization approaches by using 2 orientations of the 2D Gabor filter

After finding how to concatenate the bits from 90^{o} with the bits extracted using another filter orientation, a method of using multiple orientations has to be devised. An algorithm that dynamically chooses the next best orientation from a pool of orientations was developed. Its working principle is shown in the flowchart from Figure 4.4. A pool of 12

orientations was created, from 0 to π, with a step of 0.261, excluding π/2. After the parameters are optimized for 90° orientation, the algorithm loops through all other 12 orientations and finds the orientation which maximizes the DI d'. Then, the binary feature vector is updated by concatenating to the bits extracted using 90° every 4th bit of the binary code corresponding to the new optimum orientation. The algorithm uses the new concatenated binary code to find the next optimal orientation from the pool. The algorithm stops when a pre-defined number of orientations are added to the 2D Gabor filter bank.

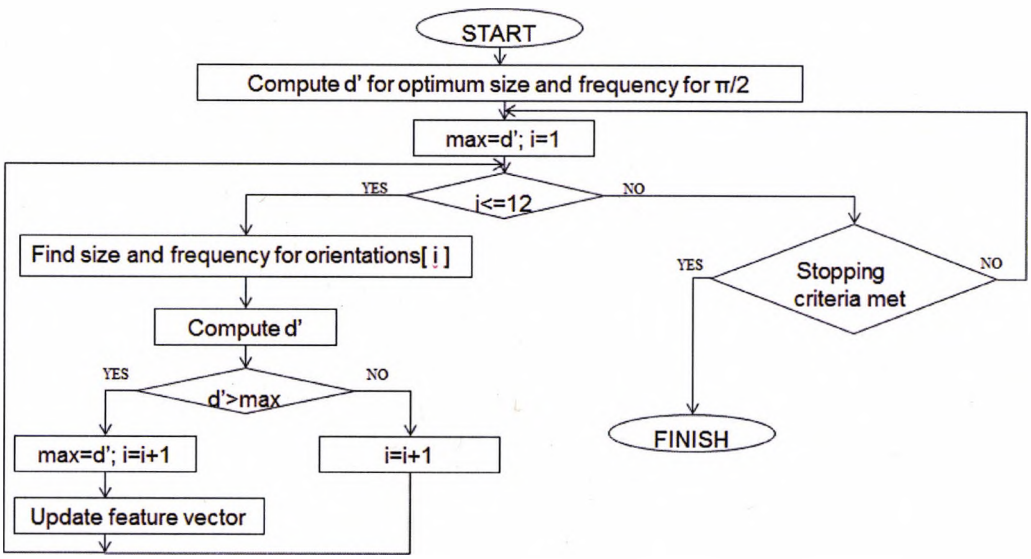

Figure 4.4. Flowchart of the 2D Gabor filter bank parameters optimization algorithm for one line of pixels

The results of the optimization algorithm may be observed in Figure 4.5, where the same 50th line of the unwrapped iris images from the first 40 users of UBIRISv1 session 1 database was used. The DI has increased by more than 30% by adding 8 orientations to the original 90° orientation. By adding more than 8 orientations to the original 90° orientation, the DI was increasing with a step lower than 0.03, which is considered too small.

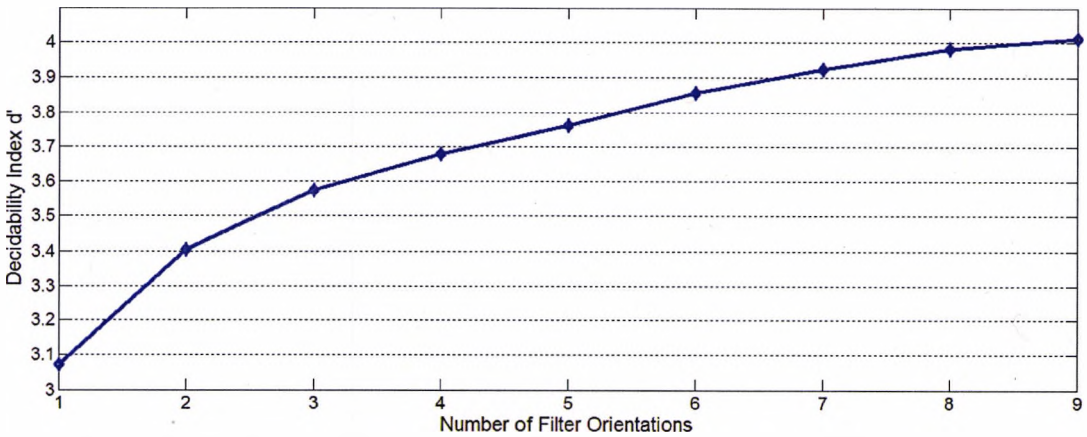

Figure 4.5. DI maximization by adding additional orientations to the 2D Gabor filter bank

The optimization algorithm for one line of pixels of the unwrapped iris image described above is applied to multiple lines of pixels of the unwrapped image. The lines are sampled with a fixed step of 10 pixels in the implementation done in this study. The sampling step may be decreased if a higher accuracy of the iris recognition is required, but the trade-off is a larger feature size and higher computational demand for optimizing the 2D Gabor filter bank parameters.

The solution proposed in this subsection to optimize and use multiple parameters for the 2D Gabor filters based feature extraction process produces a feature size for the iris similar to the feature size reported by Daugman (Daugman 1993), which was 2048 bits. One advantage of colour iris recognition systems over classical near infrared iris recognition systems is that the former may benefit from the eye colour features to avoid false matches of irises when they have different colours.

4.3 Iris colour feature extraction

The eye colour could be considered a subjective characteristic of the human body, due to various factors which influence the observations, e.g. eye colour observed under artificial lightning could be different than the colour observed under natural lightning for the same eye. Therefore, a numerical characterization of the eye colour is desirable.

In (Fu, Caulfield et al. 2005) it is suggested that the colour of the eye may be used as additional information to the texture features for an enhanced discrimination of the iris biometric. An iris database indexing method based on eye colour is proposed in (Qin 2011). In (Dantcheva, Erdogmus et al. 2011) a separation of eye colours in 4 classes is made, but the benchmarking was done on a small number of users.

In the present study, a method of retrieving images containing similar colours is employed. The method is described in (Ciobanu, Costin et al. 2013) and uses the CIELAB colour space. This method was chosen for iris colour feature extraction due to the following two reasons:

1) it has a low computational complexity, as the original feature vector proposed in the method contains only 96 real valued components;

2) yields a high rank 1 accuracy in retrieving the images containing similar colours.

The CIE L*a*b* colour space has a cubic form. The L (lightness axis) runs from top to bottom and has a maximum value of 100. The minimum value for L is 0, which represents the black colour. The a and b axes correspond to green/red and blue/yellow respectively, as shown in Figure 4.6.

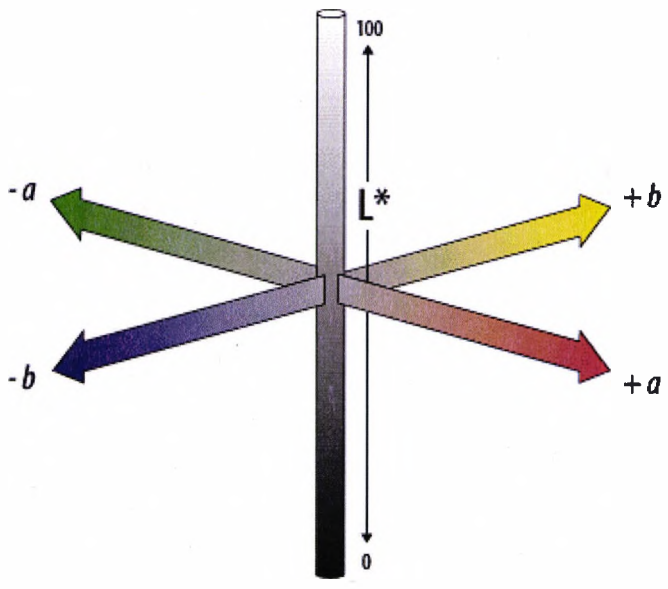

Fig. 4.6. CIELAB colour space axes[1]

The CIE L*a*b* colour space representation is obtained from RGB colour space in

[1] Image from http://dba.med.sc.edu/price/irf/Adobe_tg/models/cielab.html

two steps: first, the RGB values are converted to an intermediate CIEXYZ colour space using the formulas from equation 4.4. Then, the CIE L*a*b* values are obtained from CIEXYZ colour space using the formulas from equation 4.5.

$$\begin{bmatrix} X \\ Y \\ Z \end{bmatrix} = \begin{bmatrix} 0.412453 & 0.357580 & 0.180423 \\ 0.212671 & 0.715160 & 0.072169 \\ 0.019334 & 0.119193 & 0.950227 \end{bmatrix} \cdot \begin{bmatrix} R \\ G \\ B \end{bmatrix} \tag{4.4}$$

$$\begin{cases} L^* = 116 \cdot \left(\frac{Y}{Y_n}\right)^{\frac{1}{3}} - 16 \\ a^* = 500 \cdot \left(\left(\frac{X}{X_n}\right)^{\frac{1}{3}} - \left(\frac{Y}{Y_n}\right)^{\frac{1}{3}}\right), \quad for\ \frac{X}{X_n}, \frac{Y}{Y_n}, \frac{Z}{Z_n} > 0.00856 \\ b^* = 500 \cdot \left(\left(\frac{Y}{Y_n}\right)^{\frac{1}{3}} - \left(\frac{Z}{Z_n}\right)^{\frac{1}{3}}\right) \end{cases} \tag{4.5}$$

$$\begin{cases} L^* = 903.3 * \frac{Y}{Y_n} \\ a^* = 3893.5 \cdot \left(\frac{X}{X_n} - \frac{Y}{Y_n}\right), \quad otherwise \\ b^* = 1557.4 \cdot \left(\frac{Y}{Y_n} - \frac{Z}{Z_n}\right) \end{cases}$$

where X_n, Y_n and Z_n are the standard tristimulus values of the reference white.

The CIE L*a*b* colour space has the closest representation to the human perception of colours (Ciobanu, Costin et al. 2013). The CIEL*a*b* colour space was also used in (Melgosa, Rivas et al. 2000) to characterize the colour of the eye.

If the L* axis is quantized in 256 values, there will be 256 a*b* planes to represent the colours. A reduction of the number of a*b* planes is made in (Ciobanu, Costin et al. 2013) by sampling the 1-256 interval with a step of 32. The sampled colour planes are shown in Figure 4.7. A total of 12 a*b* planes are obtained.

The sampled planes contain a reduced number of colours of a digital image. The reduction in the number of colours is achieved by replacing each pixel value from the original image with the closest value from the sampled L*a*b* colour space. The colours

are not significantly changed by this transformation, but the reduction in size is significant.

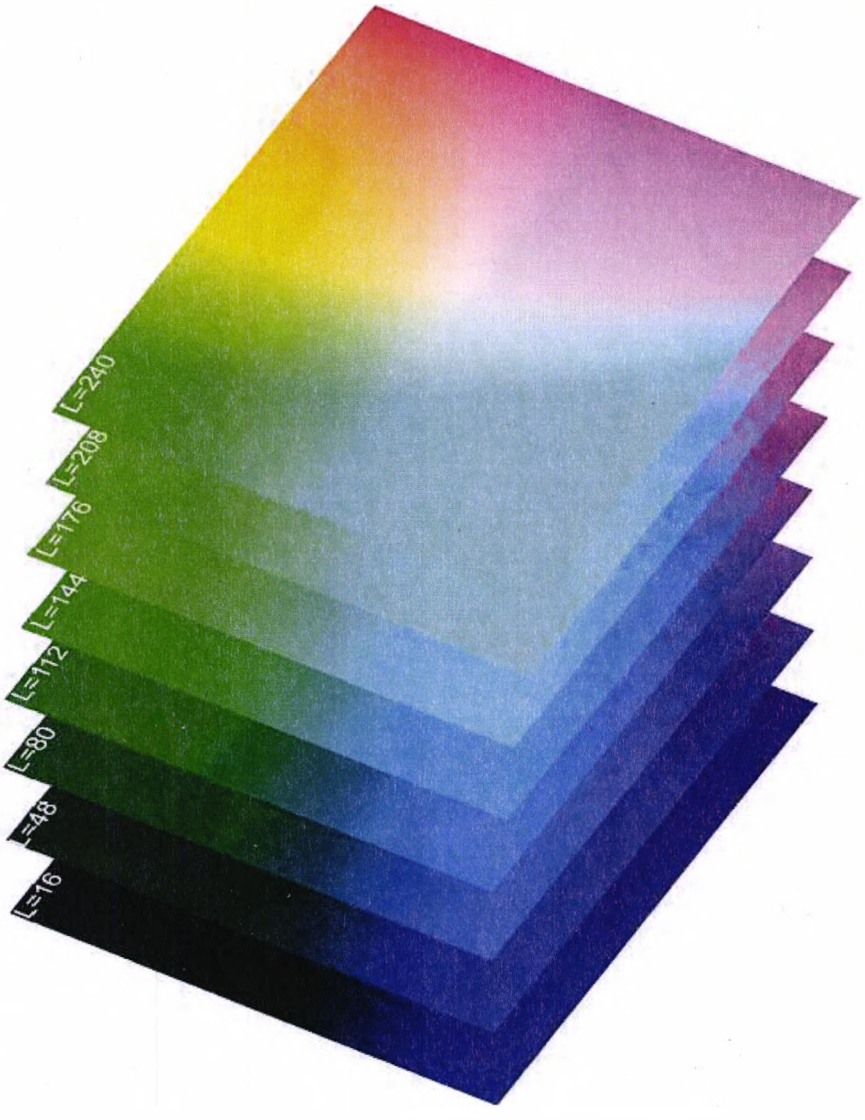

Figure 4.7. L*a*b* planes for sampled values of the lightning

Further, each L*a*b* plane is divided into 12 regions such as one region contains mainly one uniform colour. The splitting of the L*a*b* planes is illustrated in Figure 4.8. Figures 4.7 and 4.8 are taken from (Ciobanu, Costin et al. 2013). After dividing the 8 planes

in 12 regions, a number of 96 major colour components are obtained. The colour features are extracted by taking every pixel from the input image and placing its value into one of the 96 regions. A 96 bins histogram is generated therefore with a computationally efficient algorithm. For an image I, the feature vector has the form given in equation 4.6.

$$F(I) = (n_1, n_2, n_3, \ldots, n_{96}) \tag{4.6}$$

where n_1, n_2, ..., n_{96} are the pixel counts corresponding to each colour region.

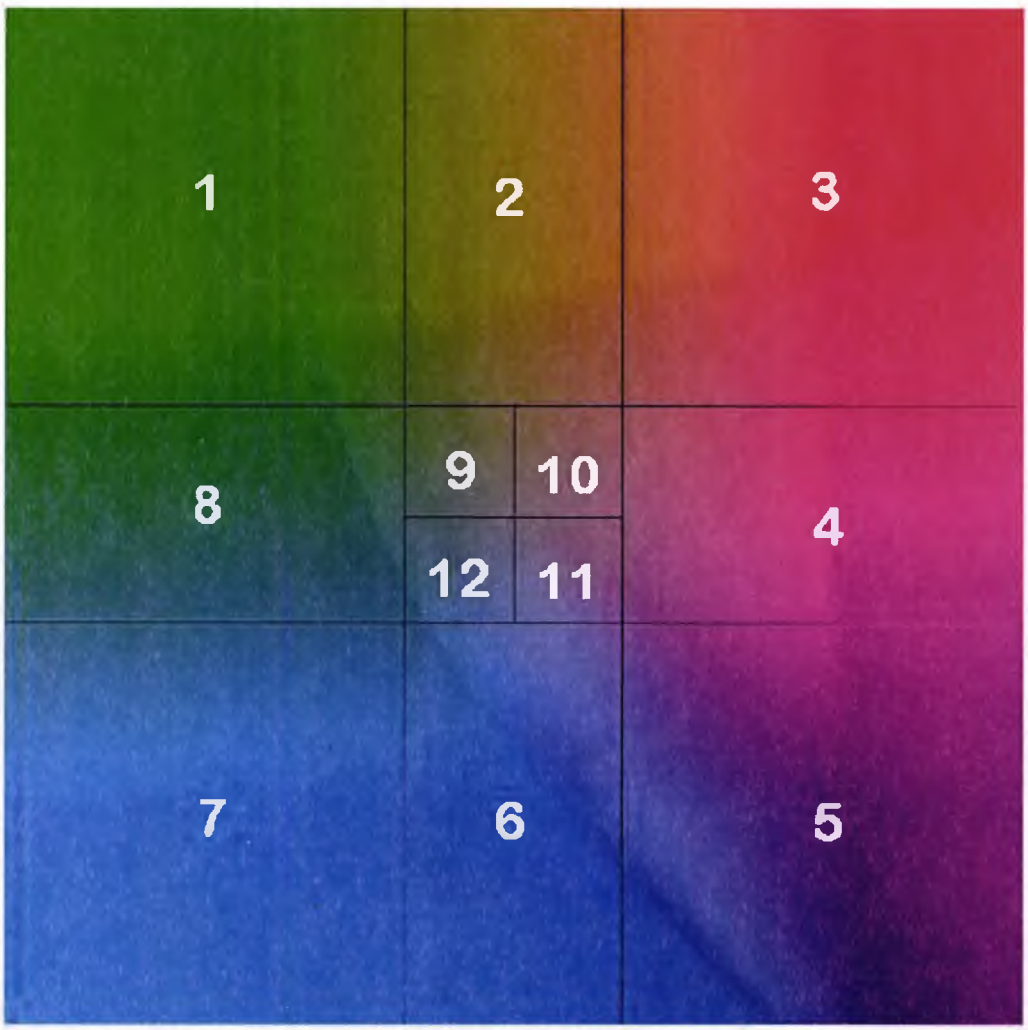

Figure 4.8. The choice of splitting an a*b* plane in 12 regions

The features extraction process described above is adapted in the present study to match the characteristics of an iris recognition algorithm. A methodology to further process the 96 component feature vector will be described below.

The 96 component colour feature vectors were generated using the implementation from (Ciobanu, Costin et al. 2013). Since the classical phase-based features extracted from the iris texture are binary features, it is desirable to have binary features for the colour features as well. For this purpose, the 96 component colour feature vector generated from a colour unwrapped iris image from UBIRISv1 Session 1 database (Proença and Alexandre 2005) is plotted in Figure 4.9.

As may be observed from Figure 4.9, if the histogram is considered a signal, this signal has abrupt changes in frequency. For short intervals, the signal has very high values, but most of the 96 components of the signal are 0. The peaks of the signal correspond to the colours present in the iris image. For non-stationary signals, which have high values for short periods of time, the Discrete Wavelet Transform (DWT) is an appropriate tool to be used for analysis (Daubechies 1992).

Similar to the DWT empirical analysis performed in (Szewczyk, Grabowski et al. 2012), various wavelet families were tested in the present study to analyse the iris colour features. The wavelet coefficients were binarized by comparing them to their median value. If the value of the coefficient is higher than the median, a binary 0 is stored, otherwise a binary 1 is stored.

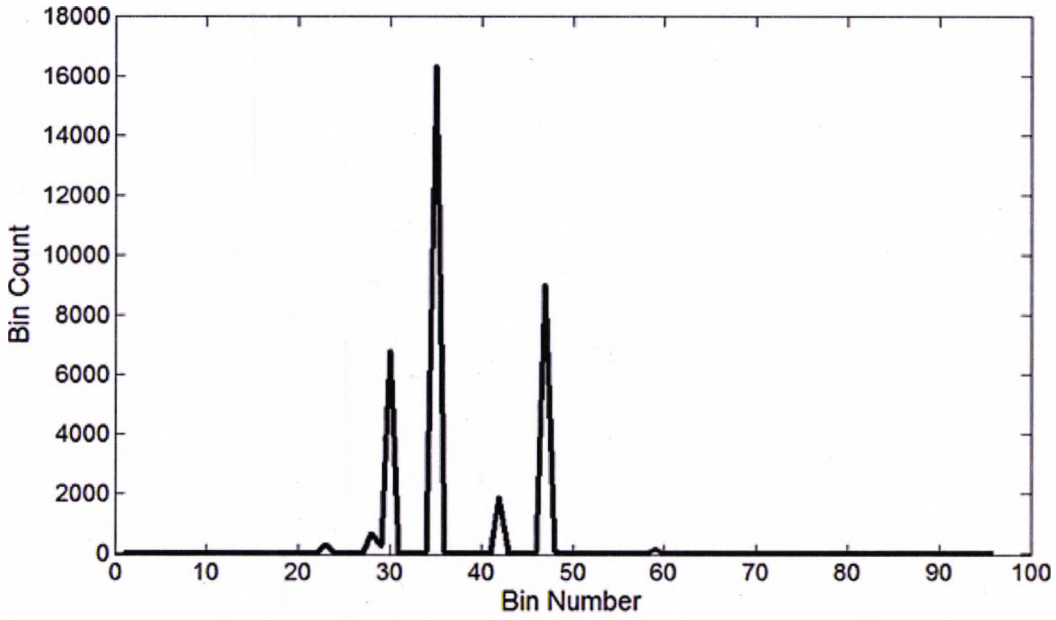

Figure 4.9. 96 component colour feature vector for an unwrapped iris image

For the empirical analysis, the first 200 images from UBIRISv1 session 1 were used. After the 96 component colour feature vectors were analysed using DWT, the coefficients were binarized and HD was used as a distance measure. The performance criterion was the separation between the authentic and impostor distributions, measured by the DI. The family of Daubechies wavelets produced the best separation between the authentic and impostor distributions. A feature size of 300 bits was obtained.

The authentic distribution of HD produced by the colour features terminates rapidly, around the value of 0.18, as shown in the experimental results subsection. This is due to the fact that two images belonging to the same eye cannot produce a high colour based score. The rapid termination of authentic HD distribution corresponding to the colour features complements the rapid termination of impostors HD. Therefore, an effective fusion methodology between the texture and colour data has to be developed. A fuzzy Logic based fusion technique that was developed to combine the information extracted from the texture and the colour will be described in the next subsection.

4.4 Fuzzy Logic fusion of texture and colour data

The concept of fuzzy logic was introduced by Lotfi Zadeh in a paper published in 1965 (Zadeh 1965), that was the basis of fuzzy computer chips produced 20 years later. Fuzzy logic was introduced to overcome the difficulties of crisp sets, where the data could either belong to one set or another set. Nowadays, fuzzy logic has a wide range of applications, being implemented in microcontrollers, computer networks, data acquisition and control systems.

The choice of fuzzy logic as a fusion mechanism is based on the analysis made in (Popescu-Bodorin, Balas et al. 2011), where the overlapping between the impostors and authentic score distribution was modelled using fuzzy logic. The HDs ranging between 0.37 and 0.55 are considered to increase the discomfort and decrease the usability of the iris recognition system developed in (Popescu-Bodorin, Balas et al. 2011). Also, in the iris recognition system depicted in (Babu and Vaidehi 2011), fuzzy logic was used in to serve as a similarity-based classifier. Features are extracted from UBIRISv1 database images using DWT and further processed using Independent Component Analysis.

The fuzzy logic relies on *if-then* rules for solving problems and is based on the knowledge of the system designer, who will define membership functions of the input and output variables of a problem. The robustness of the fuzzy logic is given by the fact that the membership functions parameters do not have fixed critical values, they are modelled by the system user according to previous empirical observations. In other words, there are no given mathematical formulas for modelling the membership functions, and slight modifications of their parameters do not affect significantly the system's performance.

The fuzzy logic system developed for the present study has the structure shown in Figure 4.10. As may be observed from Figure 4.10, the inputs of the fuzzy logic system are the HDs produced by the texture and the colour features. The type of the fuzzy inference system is Mamdani. Mamdani inference system is the most common type of fuzzy logic mechanism (Mamdani and Assilian 1975).

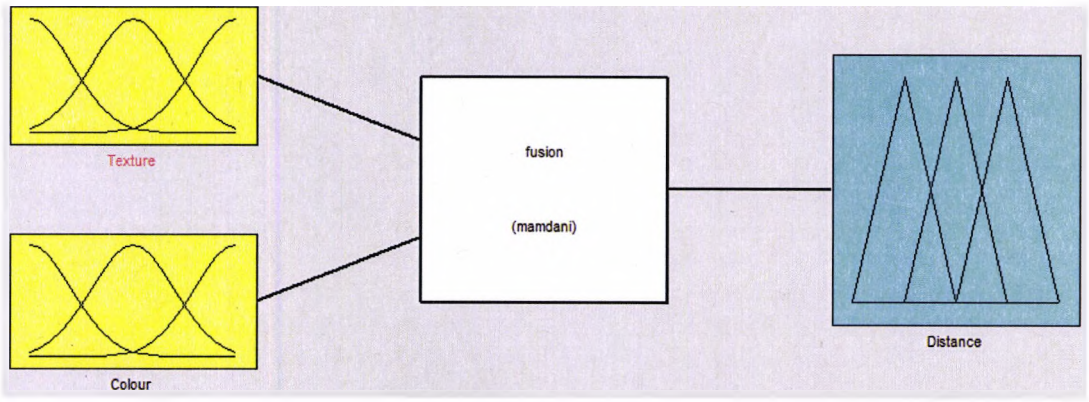

Figure 4.10. The fuzzy logic inference system for the iris texture and colour score level fusion

The membership functions for the HD scores inputs for both texture and colour have a Gaussian shape termination. The membership functions for the texture score input variable are shown in Figure 4.11. The Gaussian shape termination was used because it has a similar shape to the HD distributions and its parameters may be adjusted to skew or stretch the shape of the membership function. As the HDs produced by the texture and colour features do not go above 0.55, the range of coordinates for which the membership functions were created was [0; 0.55].

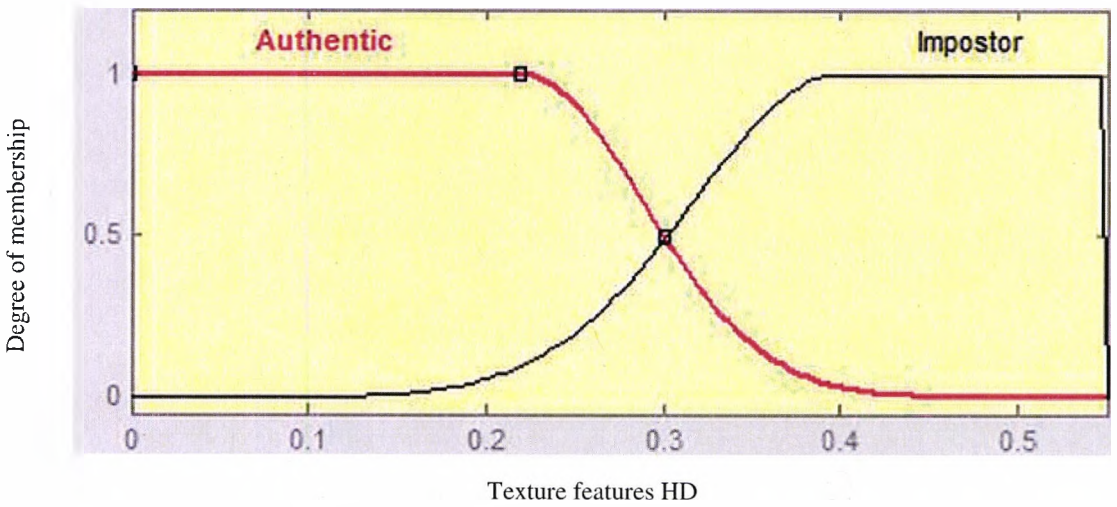

Figure 4.11. Texture information membership functions

To set the parameters of the Gaussian membership functions, the mean and standard deviation of the authentic and impostor scores' distributions obtained using the first 40 classes from UBIRISv1 were used. For the membership functions of the texture HDs, the intersection of the authentic and impostor functions occurs at 0.3. The mean of the Gaussian type termination of the authentic membership function is 0.21 and the standard deviation is 0.069. The mean of the Gaussian type termination of the impostor membership function is 0.4 and the standard deviation is 0.08. These values were selected by observing the HD distributions generated by the phase based features extracted using the methodology described in subsection 4.2. Therefore, if a HD generated by texture features is lower than 0.21, the degree of membership for the authentic curve is maximum. If the HD generated by texture features is higher than 0.4, the degree of membership for the impostor curve is maximum. The "uncertain" range of HDs generated by the texture features is between 0.21 and 0.4 and the fuzzy logic inference system is a suitable technique to model this uncertainty.

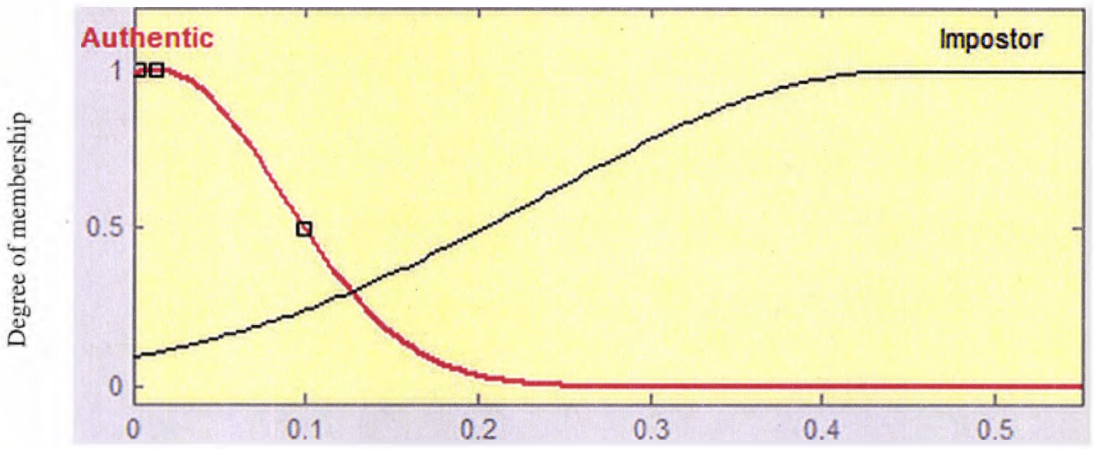

Figure 4.12. Colour information membership functions

The membership functions for the colour score input variable are plotted in Figure 4.12. By observing the HD distributions generated by the colour features, it was observed that the authentic HD distribution terminates before 0.2 and contains the vast majority of the HDs around the value of 0.02. Thus, the Gaussian membership function of the authentic

colour HDs has a mean value of 0.02 and a standard deviation of 0.07. The Gaussian membership function for the impostor HDs has a mean value of 0.44 and a standard deviation of 0.2. The large standard deviation of the impostors' membership function was selected according to the data observed when the colour features were extracted. The authentic and impostor membership functions intersect at 0.13. The "uncertain" range of values for the colour features HDs lies in the [0.02; 0.2] interval.

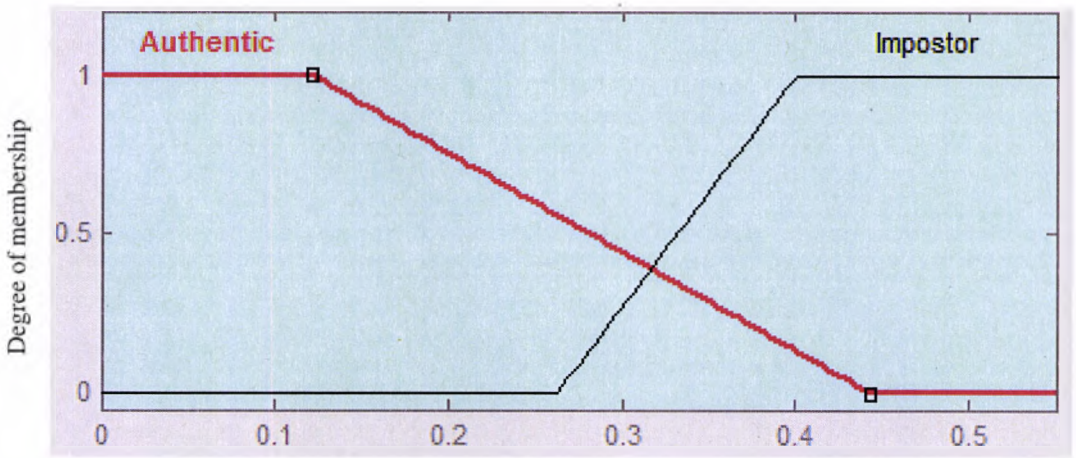

Figure 4.13. Distance output membership functions

The membership functions of the output of the fuzzy inference system are shown in Figure 4.13. They have a rectangular trapezoidal shape. For the authentic membership function, the slope of the trapezoid descends starting at a fused score of 0.12 and terminates at 0.44. The slope for the impostor membership function's trapezoid starts at a fused score of 0.4 and terminates at 0.27.

The Fuzzy inference system was designed by adding 2 rules:

1) *If* (Texture is Authentic) *then* (Distance is Authentic)
2) *If* (Colour is Impostor) *then* (Distance is Impostor).

The first rule relies on the fact that if the texture HD is low (0.21 in the present implementation, as it may be observed in Figure 4.11), based on the rapid termination

property of the impostor HD distribution for texture features(Daugman 1993), the output should be an authentic score. The second rule was added based on the rapid termination of the authentic score distribution for the colour features. In the rest of the cases, the fuzzy inference system will calculate the output score using the membership functions. The defuzzyfication is done using the centroid method.

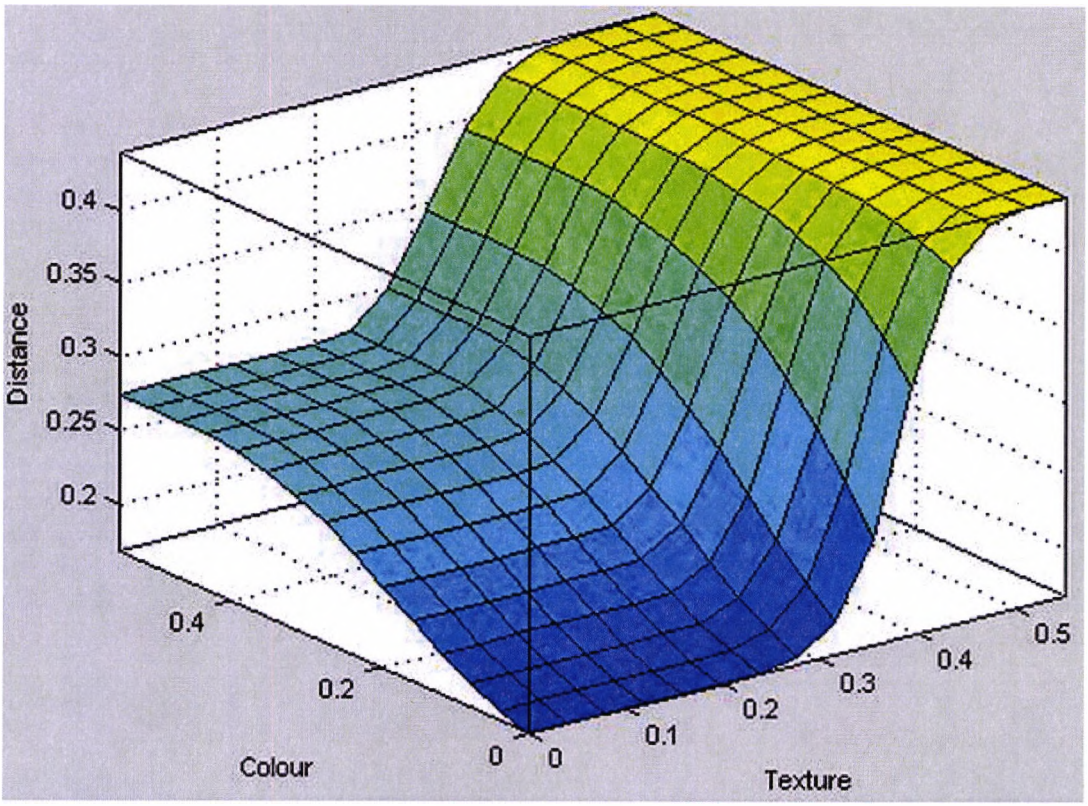

Figure 4.14. Decision surface generated by the fuzzy logic inference system

The decision surface of the proposed fuzzy inference system is illustrated in Figure 4.14. As it may be observed, for low values of the texture score and low values of the colour score, the fused distance is low. For high values of the texture score and low values of the colour score, it may be observed how the slope of the surface is not so high, and it gradually increases when the colour score is larger. This is due to the inference rule number 2. Also, for low texture scores, the high value of the colour scores do not increase the fused distance, due to inference rule number 1.

The effictiveness of the proposed texture and colour fusion approach is illustrated by a concrete example in Figure 4.15. As mentioned in the previous chapters, the issue with the classical iris recognition systems based on 2D Gabor filters is the large scores of an authentic attempt, when the image quality is poor. A HD score of 0.335 of authentic attempt will not be considered as authentic in a highly secure verification (i.e. 1 to 1) scenario. The value of 0.335 is used in the example from Figure 4.15 as it is the suggested threshold to be used in (Daugman 2004). Bearing in mind that the iris image is noisy, the colour based HD will have a higher value as well; assume that the colour based distance is 0.1. In this case, the fused score will be 0.274 and therefore, the user will be correctly recognized as an authentic.

An enhancement of the practicability of state of the art iris recognition technology is brought by the proposed approach. First, the feature extraction from colour images reduces significantly the set of constraints that have to be put on the user. Secondly, the proposed fusion between the texture and colour make the system more robust to noises without using image enhancement techniques, which often times are computationally expensive. The experimental results of the proposed fuzzy logic fusion are reported in the following subsection.

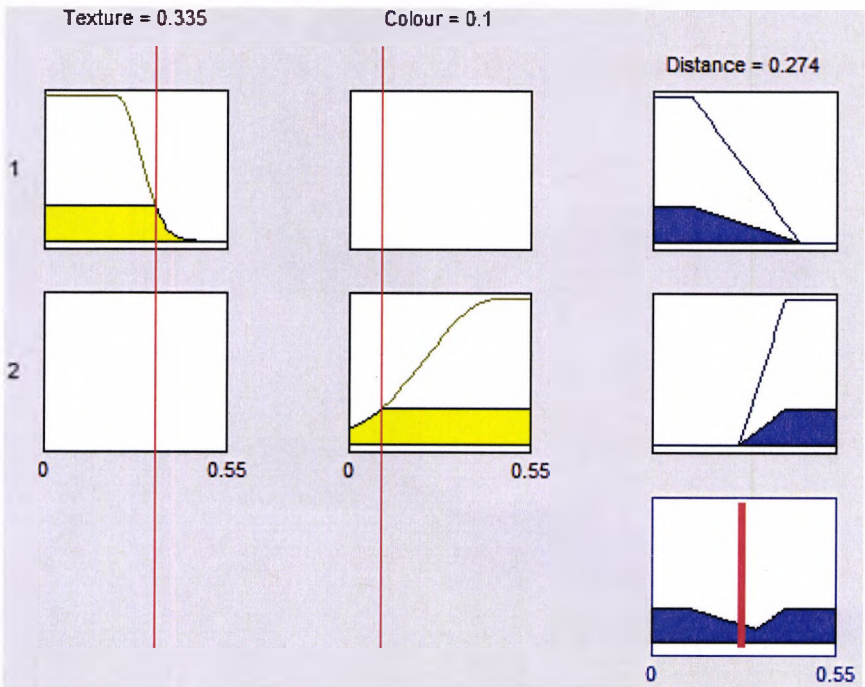

Figure 4.15. Example of Fuzzy score fusion

4.5 Experimental results

The database used for the experiments is UBIRISv1. This colour iris images database is described in subsection 3.2.6. All 1875 images of the dataset were used in the experiments. Examples of images from UBIRISv1 dataset may be observed in Figure 3.16. The experimental setup consists of the classical one vs. one score generation for all possible combinations between same class images and different class images.

Initially, for all 1205 iris images of the first session, the DI was computed using texture features extracted from one line of pixels using 6 orientations of the 2D Gabor filters. The unwrapped image dimension is 120 by 100 pixels. The number of pixel lines across the unwrapped iris image was then increased, by adding lines sampled at every 10 pixels. The lines of pixels processed were 20, 30, 40, 50, 60 and 70. The DI improved with every lines of pixels processed, as it may be observed in Figure 4.16.

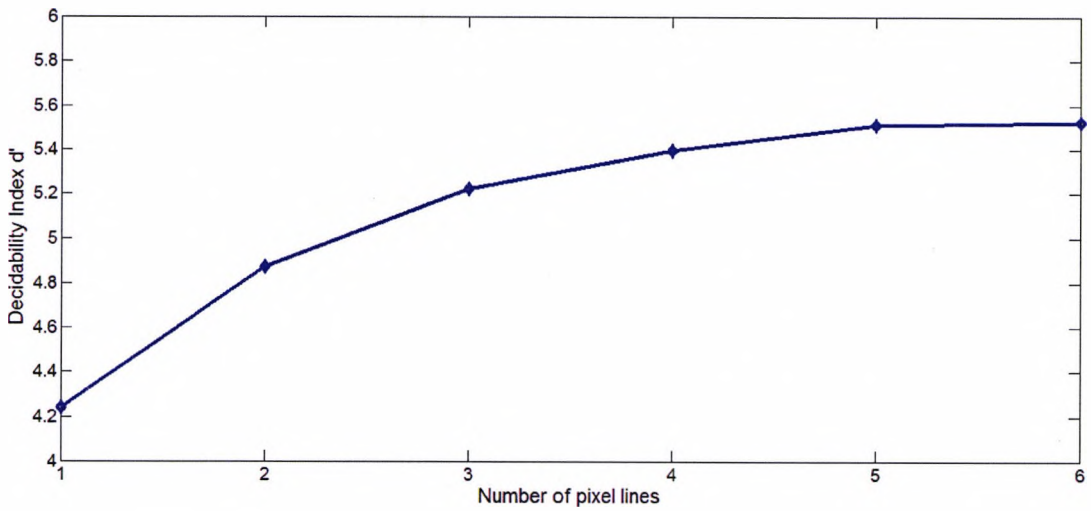

Figure 4.16. Decidability index vs number of processed pixel lines for all images of UBIRISv1 session 1

The length of a line of pixels is 120 pixels. For the 90° orientation, the features were extracted from all the pixels of a line. For the other orientations, only every fourth bit was kept. For 6 orientations of the 2D Gabor filter, the resulting feature size for one line of

pixels has a size of 270 bits. The obtained texture feature size for one iris image is therefore 270*6 = 1620. In total, the texture features are extracted from an unwrapped iris image using 36 sets of parameters of the 2D Gabor filter bank. The accuracy of the texture features based iris recognition system can be enhanced by adding more orientations of the 2D Gabor filter for processing one line of pixels and by decreasing the sampling step.

In Figure 4.17 the HD distributions generated by the texture features are plotted and in Figure 4.18 the HD distributions corresponding to the colour features are plotted for all images of UBIRISv1 session 1 database. There are a total of 2410 authentic scores and 723000 impostor scores for session 1 iris images. The DI obtained using the texture features is 5.54. The EER corresponding to the texture features is 1.69 %. For the HD distributions corresponding to the colour features, the DI and EER are not relevant to be reported, as the images of different users might have similar colours. The aim of using the colour features is to observe when the distance between the two eyes colour is large.

In Figure 4.19 the fused score distributions are plotted for all the UBIRISv1 session 1 images. It may be observed from Figure 4.19 that both authentic and impostor distributions are considerably improved compared to the distributions generated by the texture features. The DI of the fused approach is 7.71, which corresponds to an improvement of 39.16 % compared to the DI generated by the texture features. The EER for the fused approach is 1.39 %, a value that is 29% lower than the EER obtained using the phase based features.

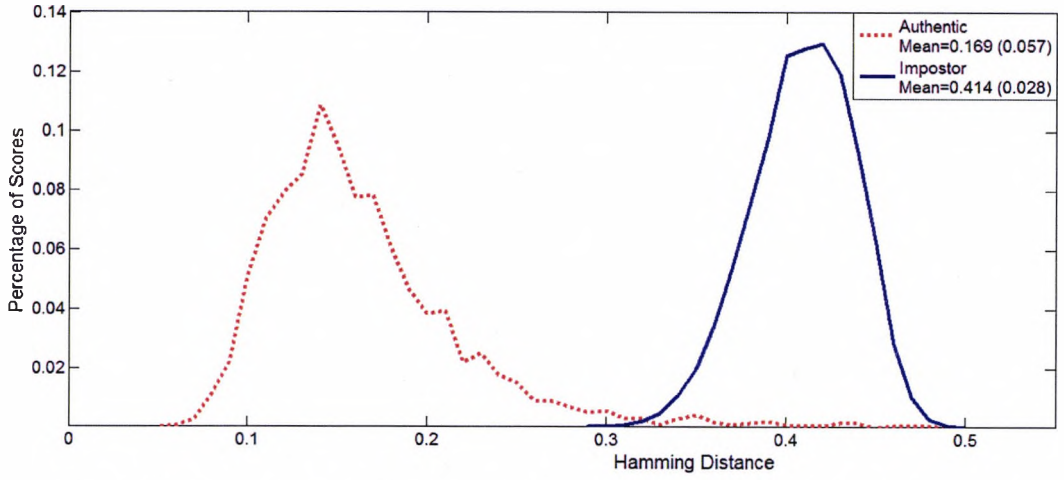

Figure 4.17. Texture features HD distributions for all images of UBIRISv1 session 1 database

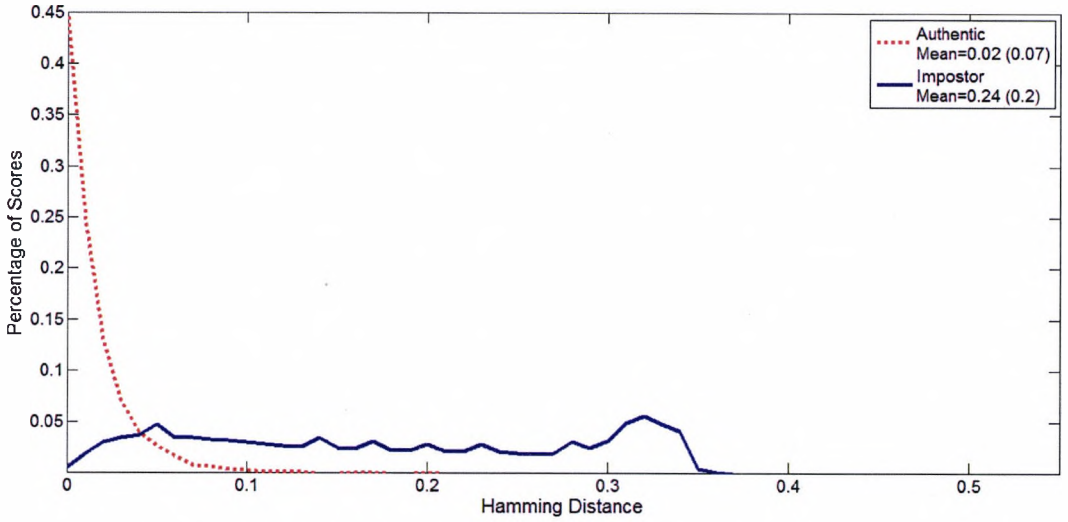

Figure 4.18. Colour features HD distributions for all images of UBIRISv1 session 1 database

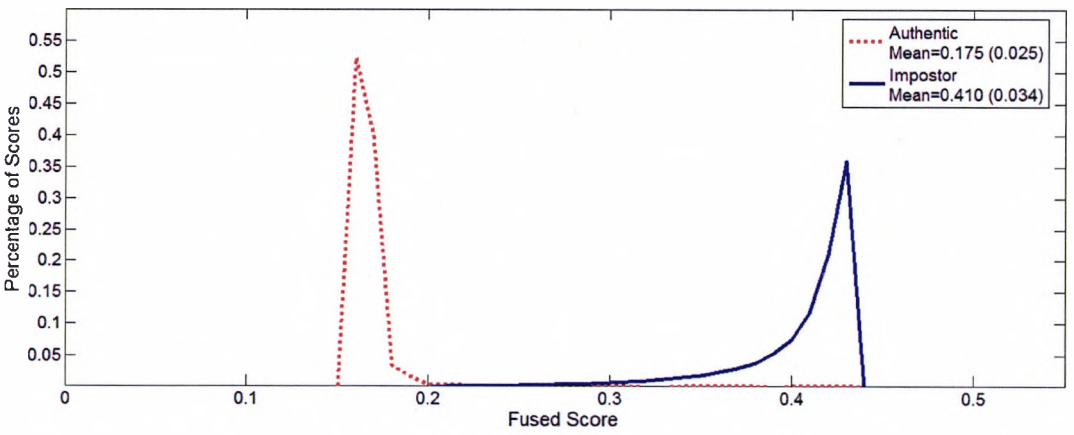

Figure 4.19. Fused score distributions for all images of UBIRISv1 session 1 database

All iris images from UBIRISv1 session 2 were included in the experiments. For session 2 iris images, there are 1320 authentic scores and 216150 impostor scores. In Figure 4.20 the authentic and impostor HD distributions for texture features are plotted. The distributions for the fused scores obtained using the proposed Fuzzy Logic fusion are plotted in Figure 4.21. The DI for the texture generated distributions is 2.33 and for the fused score distributions is improved by 47.78 %, being equal to 3.34. The EER for the texture based scores is 13.62 % and for the fused scores is 8.84%, roughly 30% lower.

By comparing the authentic and impostor score distributions from Figure 4.17 and Figure 4.20 it may be observed how the classical 2D Gabor filter based iris recognition approach proposed in (Daugman 1993) cannot cope with noisy images. The rapid termination of the impostor score distribution is still occurring for the UBIRISv1 session 2 images, but the authentic distribution overlaps significantly with the impostors' distribution. The overlap will generate a high FRR when the iris recognition system is deployed.

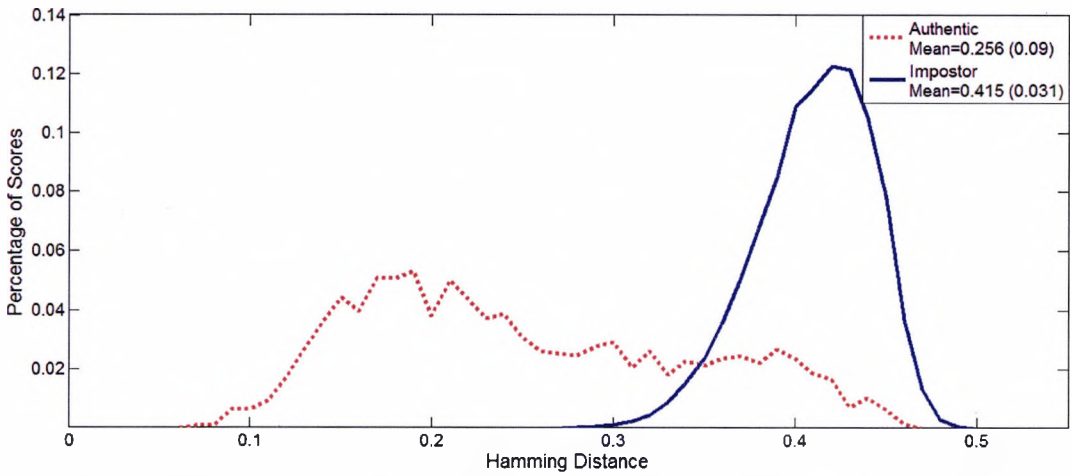

Figure 4.20. Texture features HD distributions for all images of UBIRISv1 session 2 database

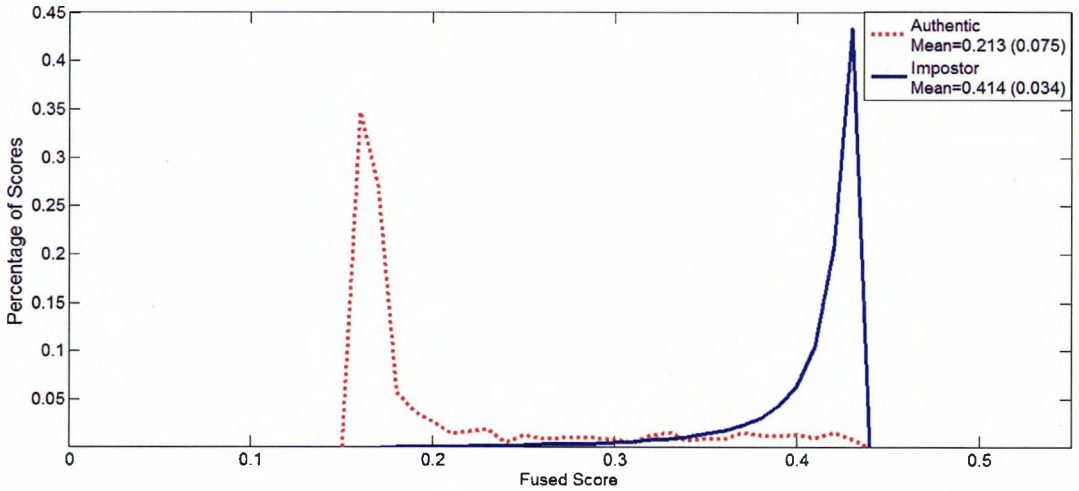

Figure 4.21. Fused score distributions for all images of UBIRISv1 session 2 database

The results of the proposed texture-colour fusion methodology for iris recognition are compared to those found in the published literature for UBIRISv1 database in Table 4.2. There are a small (or zero) number of papers published that report accuracies on all the iris images from UBIRISv1. Most of the papers that report experimental results for UBIRISv1 dataset do not use the noisy images. For comparison purposes, the distributions were generated without the occluded images. In session 1 there are 10 occluded images and in session 2 13 images are strongly occluded. Table 4.2 compares accuracies obtained using distance based algorithms, not statistical approaches, where training is needed prior to testing.

Algorithm	UBIRISv1 session 1		UBIRISv1 session 2	
	DI	EER [%]	DI	EER [%]
Proposed using texture for all images	5.54	1.69	2.33	13.62
Proposed fusion for all images	7.78	1.29	3.34	8.84
Szewczyk (Szewczyk 2007)[2]	6.3	0.6	-	-
Hosseini et al (Hosseini, Araabi et al. 2010)[3]	-	8	-	9
Fengua et al(Fenghua and Jiuqiang 2009)[4]	-	0.63	-	-
Proposed fusion excluding occluded images	8.21	0.93	3.68	7.92

Table 4.2. Performance comparison of the proposed iris recognition system with published works

[2] Occluded images were replaced by good quality images from session 2
[3] Occluded images were not included and EER estimated from ROC curves
[4] 206 subjects with good quality iris images from UBIRISv1 session 1 are used

It proves interesting to find whether the accuracy obtained by the proposed colour iris recognition system is comparable to the accuracy reported for near infrared iris images, when a similar number of images are used. NIST (Technology 2012) organized in 2005 an iris recognition competition called Iris Challenge Evaluation (ICE 2005) (Phillips, Bowyer et al. 2008), where algorithms from industry and academia were benchmarked on a dataset containing 2953 near infrared images from 132 users enrolled with both eyes. The UBIRISv1 session 1 dataset contains 1205 iris images of 241 users enrolled with the right eye. In ICE 2005 dataset, there are 1425 right eye near infrared images. Examples of near infrared iris images from ICE 2005 dataset are shown in Figure 4.22.

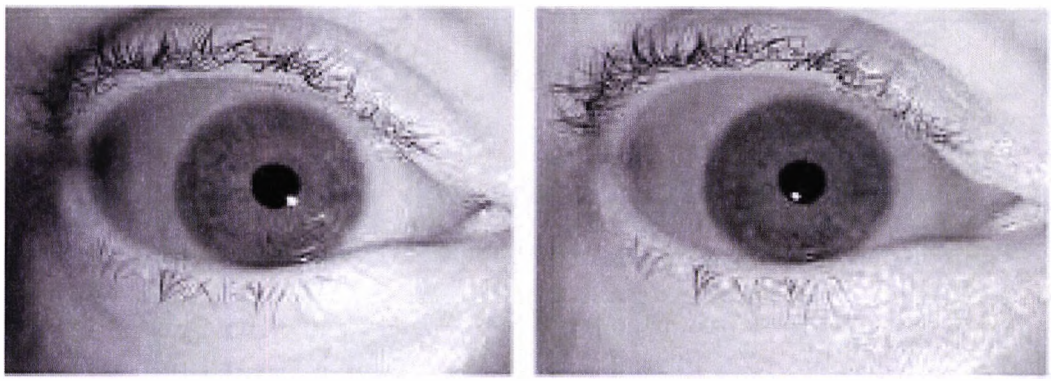

Figure 4.22. Near infrared iris images from ICE 2005 dataset

As may be observed from Figure 4.22, the iris images from ICE 2005 dataset are of high quality. Their texture is visible due to the near infrared illumination and there are no noise factors present, such as reflections, motion blur or darkness. They were acquired using a dedicated iris camera, namely LG EOU 2200. This acquisition device has automatic image quality control software that does not accept images which do not meet certain quality criteria (Phillips, Bowyer et al. 2008). Unlike the ICE 2005 dataset, the iris images from UBIRISv1 were acquired using a commercial Nikon E5700 camera, with a 5 mega pixels RGB sensor. No image quality checks are performed for UBIRISv1 dataset images.

The ROC curves obtained for the proposed iris recognition algorithm using 1195 non-occluded UBIRISv1 session 1 images are plotted in Figure 4.23. The ROC curves

reported for the algorithms submitted by the ICE 2005 participants, when the right eye is used are plotted in Figure 4.24. By comparing the ROC curves from Figure 4.23 and Figure 4.24, it may be observed that the proposed iris recognition approach performs similarly to the 6th ranked algorithm from ICE 2005 competition, which is denoted CAS 1 in Figure 4.24. Moreover, the accuracy of the proposed iris recognition approach may be improved if more optimized filter parameters sets are added to the 2D Gabor filter bank.

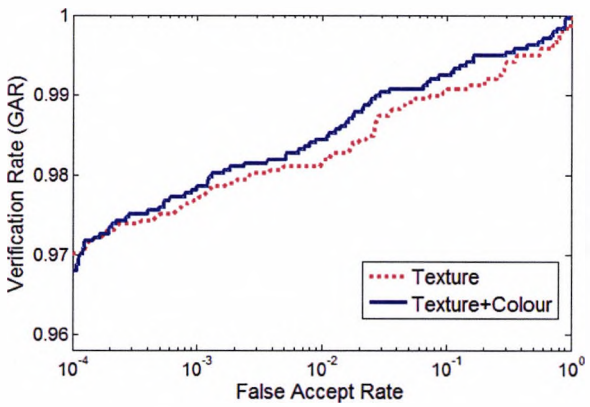

Figure 4.23. ROC curves obtained using the proposed iris recognition approach for UBIRISv1 session 1

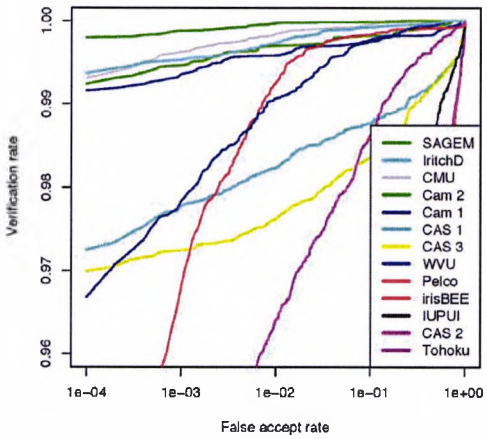

Figure 4.24. ROC curves obtained by the ICE 2005 participants on right eye iris images

For the poor quality images of UBIRISv1 session 2 dataset, the ROC curves obtained by the proposed iris recognition approach are plotted in Figure 4.25. 13 occluded images from the second session were not used in obtaining the ROC curves from Figure 4.25. For comparison purposes, the ROC curves reported for the algorithms submitted to ICE 2005 competition is plotted in Figure 4.26, but with the range of verification rate extended from 0.6 to 1. By comparing the ROC curves from Figure 4.25 and Figure 4.26, it may be observed that the proposed iris recognition algorithm performs comparably to the last 2 ranked algorithms published for ICE 2005 competition.

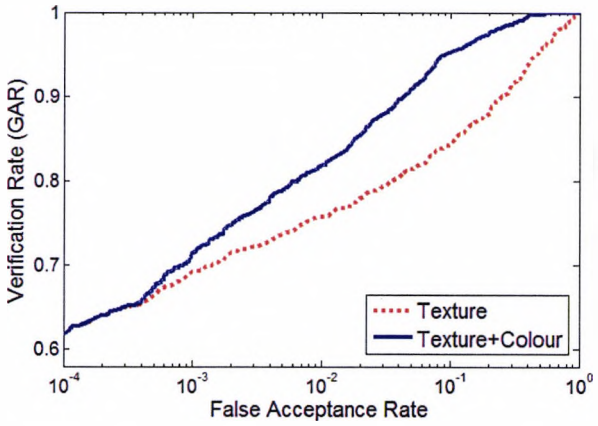

Figure 4.25. ROC curves obtained using the proposed iris recognition approach for UBIRISv1 session 2

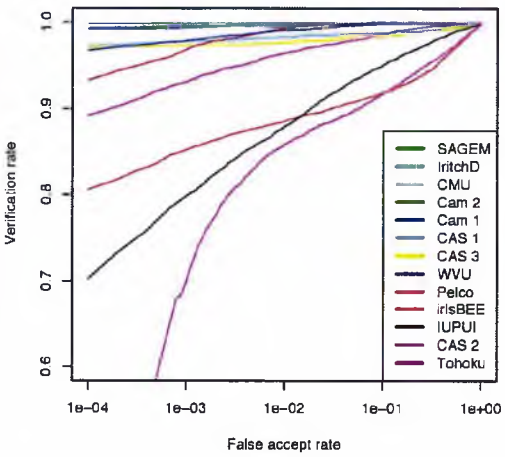

Figure 4.26. ROC curves obtained by the ICE 2005 participants on right eye iris images

4.6 Chapter conclusions

One of the major advantages of colour iris recognition systems over those operating on near infrared iris images is that they are able to use the colour of the eye to enhance their accuracy.

Although the reported accuracies for the classical 2D Gabor filter based iris recognition approach are almost perfect, it is not yet clear from the published works how to optimize the parameters of the filter bank to extract useful iris features. In this chapter, a methodology of finding sets of optimized 2D Gabor filter parameters is proposed. It is also shown that the 90° orientation of the 2D Gabor filter yield the best accuracy among other orientations, due to the radial structure of the iris texture.

The classical 2D Gabor filter based approach for iris recognition has shown to be reliable due to the rapid termination of impostors' score distribution. A low FAR may be achieved for large datasets, if a corresponding threshold for HD score is set. This fact led to the worldwide deployment of iris recognition technology in high secure scenarios, such as airport border control. However, if the iris image is not of high quality, then the biometric system produces a high FRR. In this chapter it is shown that the 2D Gabor filter based

approach is efficient in colour spectrum if the iris images are of good quality, not only in near infrared spectrum. Further, this chapter shows how the FRR of the classical iris recognition system increases when the quality of iris images drops.

When using colour iris images, the colour of the eye may be used as an additional source of information to the texture features. Colour feature extraction methodologies that are available in the literature may be used to complement the information extracted from the iris texture. In this chapter a colour feature extraction methodology is introduced by adapting a published colour retrieval technique to be suitable for iris recognition. The resulted colour features are binary and a HD is used for matching. The distributions of authentic and impostors' colour based scores complement the texture based distributions due to the rapid termination of authentic colour score distribution.

The fusion between the texture and colour data is done at score level using a fuzzy logic inference system. The fusion of colour and texture data improves the EER by approximately 29% over the case when only the texture information is used. The accuracies obtained by the proposed colour iris recognition approach are among the best in the literature for UBIRISv1 dataset. For UBIRISv1 session 1 images, which are of good quality, the ROC curves obtained by the proposed biometric system are comparable to the curves obtained by the benchmarked algorithms in ICE 2005 competition on near infrared iris images.

Another advantage of the proposed fusion methodology between texture and colour for iris recognition in less constrained environments is its computational efficiency. The unwrapped iris image has a dimension of only 120 by 100 pixels and no image enhancement techniques are employed. Therefore, the proposed iris recognition system is suitable to be implemented on mobile or embedded devices. Such implementations will have a major contribution to sustainable social development by enabling more secure communication of personal data.

Although the accuracy of the proposed colour iris recognition system is high for good quality iris images, the 2D Gabor filter approach is not the appropriate one to be used when colour iris images acquired in less constraints environment are presented to the biometric system. It appears that the classical distance based matchers for iris recognition could be replaced by more complex matchers, such as statistical classifiers. The statistical based classifiers, however, will need a number of training samples and they are more

challenging to be designed. The following chapter will investigate how the accuracy of the colour iris recognition system can be enhanced on poor quality colour iris images by using statistical based approaches.

Chapter 5
Enhanced information fusion for colour iris recognition

In this chapter statistical approaches are employed for the design of the colour iris recognition system. Features are extracted from various colour channels and a feature selection procedure keeps only the most discriminant subset of features. A Multiple Classifier System architecture is proposed to increase the robustness of the colour iris recognition system.

5.1 Introduction

Iris recognition technology is achieving a mature stage under constrained environments, but significant progress still needs to be made in iris recognition when the constraints are relaxed. One of the most significant drawbacks of the currently deployed iris recognition systems is their requirement of near infrared illumination. Under near infrared illumination, the melanin pigment, where all the reflections are captured in the visible spectrum, is not stimulated, thus the iris structure is revealed. By addressing the limitation of near infrared light necessity, and developing solutions for visible spectrum iris recognition, a major milestone of biometric authentication will be reached.

As mentioned in Chapter 2, there are three main approaches for the matching or classification stage of an iris recognition system:

1) distance-based matching, generally used in near infrared iris recognition;
2) multi-algorithmic approach, using a score level or feature level fusion;
3) statistical-based approach, where a number of images is required for training.

The distance-based matching was explored in Chapter 3 for UBIRISv1 dataset together with a simple multi-algorithmic approach. It was observed from the experimental results that the multi-algorithmic approach based on score level fusion does not improve significantly the accuracy of the best component algorithm. In Chapter 4 an optimized 2D Gabor filter based feature extractor was developed and the texture information was fused with colour information using a fuzzy logic approach. The colour iris recognition approach developed in Chapter 4 yields comparable accuracy to those reported for near infrared iris images, but only on high quality colour iris images.

This chapter will investigate how statistical-based approaches may be applied to colour iris recognition to enhance their accuracy on iris images which are affected by various distortions. After extracting the iris features, the proposed iris recognition system employs Multiple Classifier Systems (MCS) (Kuncheva 2004) to fuse the information from different colour channels. Unlike the phase-based features, which are binary strings, the features used by the MCS are real-valued.

In addition to achieving superior accuracies to what is published in the literature for

UBIRISv1 database, the approach developed throughout this chapter brings the following contributions to the state of the art in colour iris recognition:

1) Detailing the design steps of the MCS to be used in the proposed colour iris recognition system;

2) An iris recognition system which is able to operate without the enrolled dataset being available, once the MCS is trained. This enables the system to be deployed in remote locations where there is no network connection available.

3) Comparing the experimental results when 50% of the iris texture is used and the results obtained when 100% of the iris texture is used.

The remainder of this chapter is organized as follows: Section 5.2 will present a background of the classification techniques and MCS. The design of the proposed MCS architecture will be described in Section 5.3. Experimental results will be reported in Section 5.4 and the conclusions will be given in Section 5.4.

5.2 Background on classification techniques

5.2.1 Introduction

The *classification* is the process of assigning the features of a pattern into a class. Pattern recognition problems are divided in two main categories :

1) Supervised classification, where the objects have a pre-assigned class label;

2) Unsupervised classification, where the classes have to be deduced from the common characteristics.

The distinction between supervised/unsupervised learning and classification is made by the type of the outputs the learning process possesses. The outputs could be quantitative (numeric values), qualitative (finite set of words) or a class label (Hastie 2009). The class

labels may also be considered as qualitative variables. Thus, when the learning process has a class label as output, it is called classification. When the output is of quantitative type, the process is called *regression*.

A *classifier* is a method that realises the mapping between the input features and the corresponding output class labels by modelling various discriminant functions. The input feature is assigned to the class generating the highest value of its discriminant function (or to the class corresponding to the smallest distance, if it is a distance-based classifier). For the evaluation of the performance of a classification process, researchers usually refer to two characteristics: classification error and classification accuracy (Kuncheva 2004). The typical structure of a classification system may be observed in Figure 5.1.

The classifiers need to be trained before they can assign a class label to an unseen input pattern. The learning paradigm involves the approximation of a function f(x), which is making the correspondence between the feature space and the set of class labels (Palade 2006). The features used in classification are of two types: quantitative (numerical) and qualitative (categorical). Furthermore, the quantitative features are divided into continuous-valued features and discrete features.

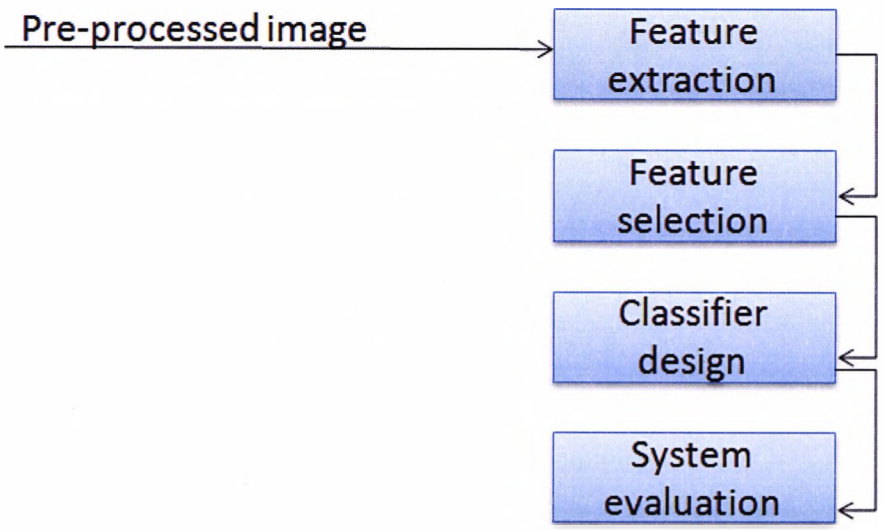

Figure 5.1. Classification system flowchart

The combination of multiple classifiers often improves the classification accuracy than that obtained by any of the individual classifiers (Dietterich 2000). In the literature, a variety of terms are employed to denote a set of classifiers whose decisions are fused: MCS, ensemble methods, classifier fusion, mixture of experts, classifier ensembles, etc. The key conditions that have to be accomplished by an MCS in order to have a greater accuracy than any of the individual classifiers are that the errors made by each individual classifier are independent and the recognition rate of each individual classifier of the ensemble is greater than chance (Dietterich 1997). The individual classifiers are known as base classifiers (Kittler, Hatef et al. 1998; Kuncheva 2004).

5.2.2 Base classifiers

In classification the input-output correspondences are obtained with a class of methods that model *discriminant functions* to label each class. An input is labelled to the class with the higher value of its discriminant function (Kuncheva 2004). In the literature, *Bayes classifiers* are considered those classifiers that classify the features to the most probable class. In a Bayesian classifier, a probabilistic model of the feature space is built, based on prior information about the data and conditional probability density functions.

Linear and quadratic classifiers are named after the type of discriminant functions they use. In a two-class example, the classification boundaries corresponding to class labels are obtained with lines and quadratic shapes respectively. In this approach the class conditional probability density functions are known, therefore these classifiers are parametric classifiers. The method used to model their discriminant functions is called *linear discriminant analysis* (Hastie 2009).

Multinomial and Parzen classifiers are nonparametric classifiers which estimate the probability density function of a feature X being in a certain region of the feature space (Duda, Hart et al. 2001).

For the *multinomial classifiers*, the feature space is divided into cells (bins). The multinomial classifier is also called the "histogram method" because each cell has the same

label as the majority of the points falling into it. When a new input X has to be classified, the *histogram classifier* automatically assigns the label of the cell in which the new input falls. Intuitively, the larger the number of bins, the better accuracy is achieved.

The *Parzen Classifier* uses Parzen Windows (or kernel functions) for which the simplest model is to define an n-dimensional hypercube, with edge 1, centred at the origin. If we consider N hyper-boxes each centred in a training point X, a new feature will have the class label corresponding to the centre of the hypercube. An often choice for the kernel function is the multidimensional Gaussian Kernel. The Parzen classifier has the disadvantage of being time consuming since it needs all the available data for training and also the difficulty of correctly choosing the value of the edge of the hypercube.

The *k-NN (k-Neareast Neighbor)* assigns a class label to an input feature according to the class label that the majority of a reference set, or *prototypes features* have (Hastie 2009). This reference contains k nearest points in the feature set, using a specified distance metric.

If Parzen Classifier uses a fixed volume around a point and labels a new feature according to the class label of that fixed point, for k-NN the roles will be reversed. A number k of points (called prototypes) are fixed and the volume surrounding a new feature will be adjusted to include all k prototypes. To reduce the computational complexity, it is recommended to find a smaller set of prototypes.

Fisher Linear Discriminant projects the data to a line so that samples from different classes become better separated. The projection maximizes the between class scatter matrix and minimizes the within class scatter matrix.

Tree classifiers are part of the *instable* classifiers group because they are capable of memorizing the training data so that a different structure of the tree classifier will be obtained if the training data suffers minor alterations. Tree classifiers are usually described in graph terminology (root, intermediate nodes, leafs). At a certain node, the proportion of points from a class within the data set is called the *impurity* of the node (Kuncheva 2004).

Artificial Neural Networks (ANN) are used as base classifiers in multiple classifier systems and are also instable. One of the most popular NN models is the Multilayer Perceptron. The multilayer perceptron has one input layer of neurons, one or more intermediate layers of neurons and output neurons. Each neuron has a corresponding set of

weights which are used to connect to the neurons from the next layer. The training process of an ANN consists of finding the correct values of the weights. Once the optimum weights are found through learning examples, the ANN is able to classify unseen input features.

The *Support Vector Machines (SVM)* classifier was introduced in 1995 (Cortes and Vapnik 1995) to address the limitations of ANN. An ANN stops the training procedure when all the training features are correctly classified, while a SVM classifier finds the maximum margin between the training examples and the boundary between the classes. The margin of the SVM is defined as the perpendicular distance between the decision boundary and the closest training features. The training feature points lying on the margin are called support vectors.

5.2.3 Multiple Classifier Systems

There are two main strategies in building a MCS: *fusion* and *selection* (Kuncheva 2004). In classifier fusion, each individual classifier is supposed to have knowledge of the whole feature space, while in classifier selection, each classifier only knows well a part of the feature space. The notion of *diversity* refers to the property of a set of classifiers which can be exploited to construct a MCS that has a better accuracy than any of its component classifiers (Partridge and Griffith 2002). If all the classifiers are of the same type or they have almost the same accuracy, the MCS built upon them may not provide a significant improvement to the recognition process.

The output of a classifier can be of three types (Xu, Krzyzak et al. 1992):

1) *Abstract level* (Level 1), when the classifier outputs a single unique class for a given feature.

2) *Rank Level* (Level 2), when the output of the classifier is an array with the classes ranked in order of plausibility of being the correct label classes.

3) *Measurement Level* (Level 3), where the output consists of a vector with the belief values of the classifier for each class label that can be assigned to the input feature. These classifiers are known as *probabilistic classifiers*.

A fourth type of classifier output may be defined as the *Oracle Level* (Level 0)

(Kuncheva 2004), where the output of the classifier can only take the values 0 or 1. This is an ideal situation, when the labels of the data set are known a priori. Different types of combiners use different outputs of the individual classifiers (Jain, Duin et al. 2000).

5.2.3.1 MCS Topologies

A very important aspect of MCS is their topology. In the literature, there are four well-known topologies of MCS (Lam 2000):

1) *Conditional Topology.* One classifier is selected. If the classifier cannot correctly assign a class label to the presented feature, another classifier is selected. The selection of the next classifier can be either static or dynamic. Each classifier has knowledge of the whole feature space.

2) *Hierarchical (Serial) Topology.* In this topology, classifiers are applied in succession. Each classifier is applied to reduce the number of possible classes of the presented feature. There should be insurance that the classes selected by any classifier will always contain the correct class.

3) *Hybrid Topology.* Based on the fact that the different pattern recognition algorithms are suitable for particular type of patterns, in this topology a single classifier is selected for a given input feature.

4) *Multiple (Parallel) Topology.* All the classifiers operate in the same time on the input (parallel) and the decision is a consensus agreement between the classifiers.

5.2.3.2 Combination of class label outputs

When the individual classifiers give label outputs and not continuous-valued outputs, there are several possible fusion techniques for constructing the MCS:

- *The majority vote* (Lam and Suen 1997) is a fusion technique in which the MCS output is the class label assigned by the majority of the individual classifiers. The decision may rely on unanimity voting (all individual classifier outputs are the same), simple majority (50%+1) or plurality (most

votes).

- *Weighted majority vote* (Kuncheva 2004) is a fusion technique in which the more competent classifiers are more important in taking the final decision.
- *Borda count method* is applied in case of level 2 (rank level) classifier outputs and is a generalization of the majority vote. For each class, the sum of the number of classes ranked below it represents the Borda count. Then the classes are arranged in descending order according to Borda count value. Therefore, Borda count method is a decision group technique, measuring the agreement level of the classifiers that an input pattern belongs to a specific class.
- *Naïve Bayes combination* (Xu, Krzyzak et al. 1992) scheme assumes that the classifiers are mutually independent given a class label (conditional independence). The method computes a support value for each possible class and assigns to the input feature the class corresponding to the maximum support value. The support values are the posterior probabilities computed using Bayes' rule (Kuncheva 2004).
- *Multinomial methods*, in which the posterior probabilities of the final output, given the outputs of the individual classifiers are estimated. The class label is determined by the highest posterior probability. Two multinomial methods are *Behavior Knowledge Space (BKS) Method* (Huang and Suen 1995) and *Wernecke's Method* (Wernecke 1992).
- *Probabilistic approximation* method constructs a dependence tree for each possible output class label (Kuncheva 2004).
- *Singular Value Decomposition* (SVD) (Kuncheva 2004) combination method uses *correspondence analysis* to map the space spanned by the classifier outputs to a real space with a smaller dimension. The reduction in dimensionality is done by using SVD.

5.2.3.3 Combination of continuous-valued outputs

In these methods the individual classifiers outputs are Level 3 outputs (see subsection 5.2.3.1). The *degrees of support* (vector components) are usually confidences in the suggested labels or estimates of the posterior probabilities for the classes (Kuncheva 2004).

There are 2 categories of combination techniques when the outputs of individual classifiers are continuous-valued (Kuncheva, Bezdek et al. 2001):

1) *Class-conscious combination methods*, which uses the degrees of support of each classifier for a single possible class label output;

2) *Class-indifferent combination methods*, in which a new feature space is obtained from the degrees of support of the individual classifiers. This is called *intermediate feature space*. Another classifier then receives as input the features from the new space and outputs the final class label.

The class-conscious combination methods may have trainable combiners or non-trainable combiners. From the non-trainable MCS the most popular are: *simple mean (average), maximum/minimum/median, trimmed mean, product, generalized mean* (Kuncheva 2004).

In the class-conscious trainable combiners' category the most representative MCS architectures are:

- *The weighted average*, with various forms: *L weights* (L is the number of individual classifiers), *c x L weights* (c is the number of class labels), *c x c x L weights* (Kuncheva 2004).
- *Fuzzy Integral* (Kuncheva, Bezdek et al. 2001) (Kuncheva 2003).

In the class-indifferent combination methods are included:

- *Decision Templates (DT)* (Kuncheva, Bezdek et al. 2001).
- *Dempster-Shafer Combination* (Rogova 1994).

5.2.3.4 Diversity of MCS

A possible definition of the diversity of the MCS could be: the measurement of how different the outputs of the base classifiers in an ensemble are.

When a classifier does not assign the correct label to an input feature its decision is complemented with the decision of another classifier that correctly identifies the label for the same input. Therefore the errors made by the base classifiers within the MCS have to be independent. Two errors e_1 and e_2 corresponding to the misclassifications of a random input feature of two base classifiers are independent if the probability of e_1 *and* e_2 equals to the probability of e_1 multiplied by probability of e_2.

The diversity of MCS seems to be more important than the accuracy of individual base classifiers when designing an ensemble method (Kuncheva 2004). Therefore the best trade-off between the diversity and accuracy has to be found. The process of choosing base classifiers can lead to a very small performance improvement over one single base classifier if it is not done properly. Thus, when designing an ensemble method, one may wish to consider the complexity of the MCS for a possible implementation while trying to achieve a high degree of diversity among the base classifiers. The diversity in MCS may be obtained in three ways:

1) Changing the parameters of the individual classifiers;
2) Changing the classification algorithms;
3) Changing the training data used by the individual classifiers. This is possible by either using learning strategies (e.g. bagging, boosting) or feature selection methods.

The measures of diversity in ensemble methods are divided in two important categories (Kuncheva 2004):

1) Pairwise measures, which for a number of N base classifiers will compute N(N-1)/2 values and the measure for the whole MCS is obtained by averaging all pairwise computed measures.

2) Nonpairwise measures are computed considering all base classifiers together.

5.3 Colour iris recognition system employing MCS

Classical phase-based features proposed for iris recognition are binary strings and they are matched against other binary strings using a HD. The majority of the iris recognition approaches available in the literature rely on a distance-based matching algorithms, as shown in the survey made in (Radu, Sirlantzis et al. 2012). The advantage of this approach is that a new user enrolment does not require a retraining procedure for the biometric matcher. However, for colour iris images, where the amount of noise present in the images is increased, a simple distance based matching algorithm does not yield a high accuracy, as it was shown in Chapter 4.

To deal with noisy colour iris images, more complex classification techniques are necessary. As MCS have been shown to be robust in dealing with noisy data, in this section an iris recognition system is developed by exploring this powerful pattern recognition tool. The proposed iris recognition system is able to cope with noisy colour iris images by employing MCS for information fusion between different colour channels. The details of the MCS design will be detailed along this section. The proposed colour iris recognition system has the block diagram illustrated in Figure 5.2.

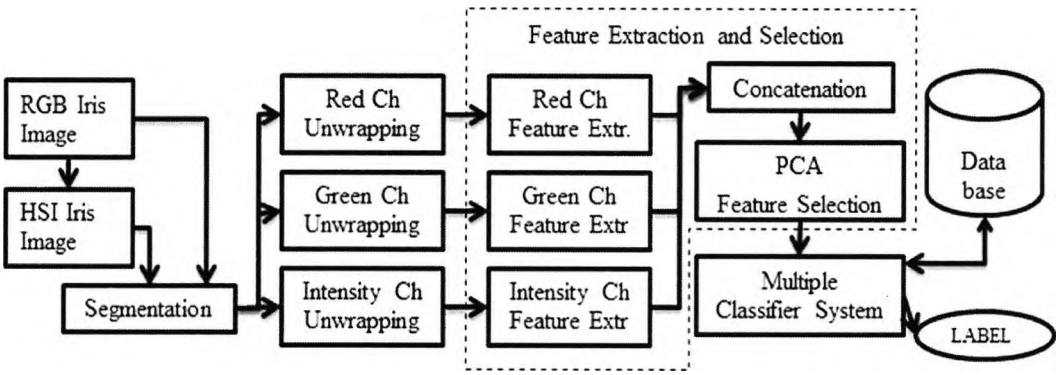

Figure 5.2. Colour iris recognition system using MCS

5.3.1 Iris image preprocessing

In colour iris recognition algorithms, a significant part of the computational effort is expended for segmentation and noise detection (Tan, He et al. 2010). If the feature

extraction and classification stages of the system are computationally demanding too, the usability of the system is considerably diminished, especially if it has to be deployed on embedded or mobile devices. Therefore, a simple method for feature extraction and a robust classification stage are essential for a practical implementation of a colour iris recognition system, especially in mobile platforms.

The colour iris images from UBIRISv1 database were segmented using the algorithm described in Chapter 3. The segmentation algorithm uses the red channel for iris detection and the red channel together with hue and saturation channel for pupil detection (Radu, Sirlantzis et al. 2011). As mentioned in Chapter 3, the iris images that could not be automatically segmented were manually segmented. Then, the iris images were unwrapped to a dimension of 360 by 100 pixels. The transformation from raw coordinates in the original image to polar coordinates in the unwrapped image was performed using the method proposed by Daugman in (Daugman 1993). To avoid including the eyelids and eyelashes in the unwrapped image, the sector defined between -45° and +45° of vertical axis in the top half of the iris was discarded in the normalization process.

According to the information theoretical analysis of the iris texture made in Chapter 3, the red and green channel from RGB colour space and intensity channel from HSI colour space contain the most discriminant information. The iris images were unwrapped therefore from the red, green and intensity channels and all the three channels were further used for feature extraction and classification.

No image enhancements techniques were applied on the unwrapped iris image, in order to reduce the computational demand for a possible embedded or mobile implementation. In the system's block diagram from Figure 5.2 the preprocessing steps may be observed.

A bank of circular symmetric filters is used in (Ma, Wang et al. 2002) to create an iris feature vector of a fixed size of 384 real valued components. The experimental results reported using these features were comparable to the best results reported in the literature on near infrared iris images. In the present work the feature extraction methodology proposed in (Ma, Wang et al. 2002) is adapted to be effective on colour iris images and a MCS framework was developed to be used with this type of feature. The adaptation of the feature extraction stage consists of fusing at the feature level the information obtained from various colour channels. The features extracted from various colour channels are

concatenated and subsequently, a feature selection method is employed (Radu, Sirlantzis et al. 2012).

5.3.2 Feature extraction

For feature extraction, circular symmetric filters were employed (Ma, Wang et al. 2002). These filters are similar to 2D Gabor filters (Daugman 1993), being the product of a Gaussian function and a sinusoidal function. The difference between the two is that 2D Gabor filters have an orientation for the sinusoidal function, while circular symmetric filters have an isotropic modulating sinusoidal function. The circular symmetric filters have the form given by equation 5.1:

$$G(x,y,f) = \frac{1}{2\pi\delta_x\delta_y} e^{-\frac{1}{2}\left(\frac{x^2}{\delta_x^2}+\frac{y^2}{\delta_y^2}\right)} \cos\left(2\pi f\sqrt{x^2+y^2}\right) \tag{5.1}$$

where δ_x and δ_y are the space constants of the Gaussian function, f is the frequency of the modulating sinusoid. The window size of the filter to be applied is the fourth parameter necessary to be found. The reason why circular symmetric filters are used over classical 2D Gabor filters is that in a small rectangle of the iris texture, the orientation of the texture is not relevant, as explained in (Ma, Wang et al. 2002). Moreover, 2D Gabor filters are less computationally efficient than circular symmetric filters because they have an imaginary part, while circular symmetric filters only have the real part. The shape of the circular symmetric filters may be observed from Figure 5.3.

As for 2D Gabor filters, the challenge in designing an iris recognition system that uses circular symmetric filters is to find the optimum parameters of the filter bank. In the work of Ma et al the parameters of the circular symmetric filter were tuned for horizontal bands of the unwrapped iris image. Details about the filter bank parameters or the size of the horizontal bands are not given in (Ma, Wang et al. 2002). Unlike the original method, in the present investigation the parameters are optimized on the entire unwrapped iris image and a feature selection methodology is employed to keep only the most discriminant features.

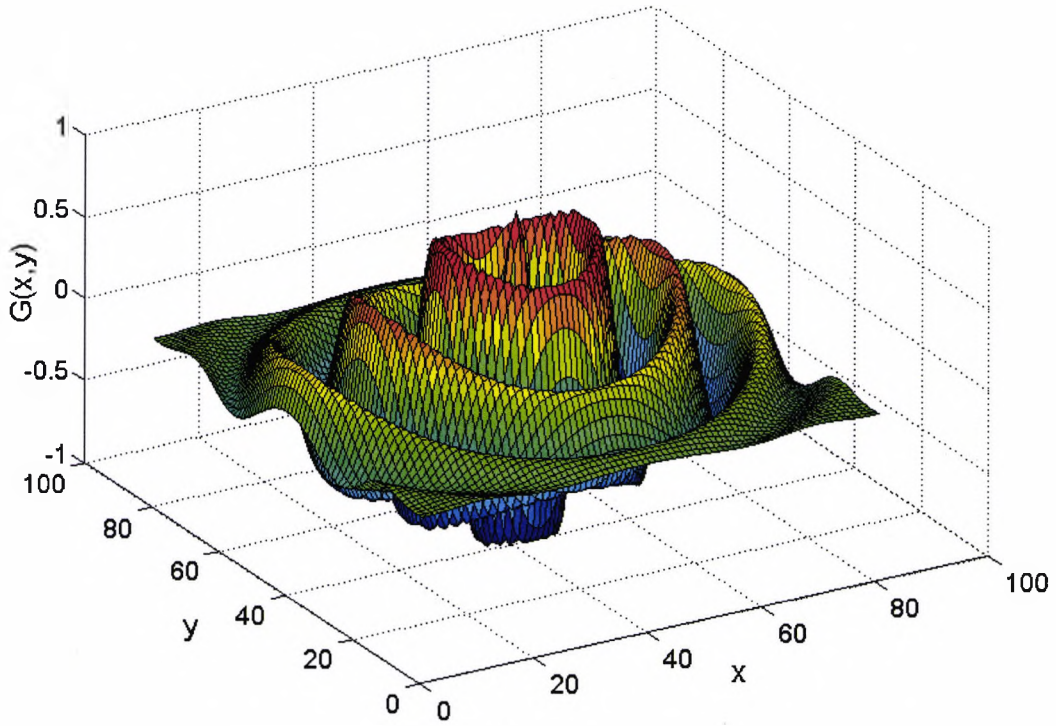

Figure 5.3. Circular symmetric filter with $\delta_x = 15$, $\delta_y = 25$ and f=0.8

Similar to the method proposed in (Ma, Wang et al. 2002), the unwrapped iris image is convoluted with the circular symmetric filter and the obtained image is divided into 10 by 10 pixel rectangles. Subsequently, for each 10 by 10 window, the mean and mean absolute deviation of the obtained values is computed. As the unwrapped image size is 360 by 100, there are in total 36*10*2=720 real valued components for one channel. This process is run for red, green and intensity channels, resulting in a raw feature of size 2160. The issue of alignment is addressed by rotating the unwrapped probe image 3 pixels to the left and 3 pixels to the right and extracting the features every time.

Genetic Algorithms were employed to search the 4 parameters of the circular symmetric filters (Chia-Te, Sheng-Wen et al. 2006) from equation 5.1. The fitness function employed was the mean rank 1 identification accuracy over three repetitions with randomly chosen probe and gallery images from the first 40 classes from UBIRISv1, session 1 dataset. 4 random images are used for training and 1 for testing from each class. The rank 1 identification rate is computed by using a set of base classifiers. As shown in the next subsection, the linear classifiers yield the best accuracy among the set of the base classifiers

that were employed in the present study (Delft 2012).

If the mean identification rate is above 95%, the parameters are considered satisfactory and are saved. The used implementation of the genetic algorithm was the one from Matlab Optimization Toolbox (Mathworks 2012). The initial population has 40 members. The members of the next population are created by one of the following means:

1) Elite members, for which the fitness function has the best value in the generation. These members are automatically added to the next generation.
2) Crossover members, which are created by combining the values of the parents.
3) Mutation members, are generated by creating random changes to a single parent.

The mutation function of the genetic algorithm adds a random vector from a Gaussian distribution to the parent. The crossover function of the employed genetic algorithm creates the child as a random weighted average of the parents. Out of the 40 members, an elite count of 10% was used, and a crossover fraction of 0.8 is used. These are the default values of the genetic algorithms implementation from Matlab Optimization Toolbox. Therefore, from the 40 members of a population at one iteration, 4 are elite members, 29 are obtained by mutation and the remaining 7 are obtained by crossover.

The rationale behind this approach is to obtain a population of useful sets of features for every unwrapped iris image in order to train the base classifiers on the obtained feature set and to combine them to enhance the system's accuracy. However, as the features are obtained by applying the same filter but with different parameters, the feature vector components obtained with different parameters will be highly correlated. Moreover, the parameters of one filter will be the same for all three channels, so the features will contain redundant data. A significant improvement cannot be obtained by fusing the base linear classifiers unless the correlation between the features obtained with different parameters of the filters is decreased. Principal Component Analysis (PCA) was applied to reduce the correlation between the features and in the same time the feature dimensionality. After that, a number of generic classifiers were trained and used in the fitness function of the genetic algorithm to determine which classifier performs better. The final feature size, obtained by applying PCA was reduced from 2160 components to only 360 components, as it will be shown in the following subsection.

5.3.3 Multiple Classifier System Design

By training the individual classifiers on features extracted using different sets of parameters of the circular symmetric filters, a MCS is aimed to be build, where the component classifiers make diverse (de Souto, Soares et al. 2008) decisions when an input feature is processed. In this way, if some of the samples are misclassified by some classifiers, it is likely that they are correctly classified by a larger set of classifiers from the ensemble, thus increasing the accuracy of the MCS.

The proposed MCS architecture enhances the robustness of the iris recognition system by fusing information from 2 colour spaces and using only the most discriminative real valued features from the 2 colour spaces (Radu, Sirlantzis et al. 2013). The obtained feature size of 360 components is smaller than that obtained in (Ma, Wang et al. 2002), which contains 384 real values. Due to the feature type used, the proposed biometric system will work on near infrared images as well, not only on colour iris images.

5.3.3.1 Design steps

The first step in the design of the proposed MCS was to determine which base classifier works best and what is the optimum PCA dimension of the features extracted from the three colour channels. The parameters of the circular symmetric filters were searched using genetic algorithms for 6 base classifiers: linear classifier, Fisher classifier, Nearest Neighbour classifier, Parzen classifier, Tree classifier and SVM classifier (Delft 2012). The optimum rank 1 identification accuracy obtained by the genetic algorithm for each classifier on 40 classes from UBIRISv1, session 1 dataset, for different PCA dimensions may be observed in Table 5.1. The rank 1 identification accuracy is the average of 3 runs with 4 randomly selected images for training and one for testing.

PCA dimension / Classifier	60	90	180	360
Fisher	99.0 %	98.5 %	99.0 %	99.1 %
Linear	99.0 %	99.0 %	98.5 %	99.0 %
Knn	91.0 %	93.5 %	91.5 %	90.5 %
Parzen	7.0 %	7.0 %	3.0 %	2.5 %
Tree	64.5 %	64.0 %	64.5 %	79.5 %
SVM	97.5 %	96.0 %	97.5 %	98.0 %

Table 5.1. Performance of 6 base classifiers on 40 classes from UBIRISv1, Session 1 dataset

To find which base classifier is the most appropriate to be used, the 6 base classifiers were employed using the feature selection made by PCA. From the original 2160 dimensions, the PCA was applied to reduce the number of dimensions to 360, then 180, 90 and finally 60. From Table 5.1 it may be observed that Linear and Fisher classifiers perform best for a range of different number of dimensions after PCA was applied. The third place was obtained by the SVM, but this classifier requires a significantly larger time for training compared to Linear and Fisher classifiers.

The second step in designing the MCS is to determine whether linear or Fisher classifiers have to be chosen to increase the MCS's accuracy. A desirable property of a MCS is to include component classifiers which do not make the same errors on a given set of test samples. After the genetic algorithm runs for a given classifier, it finds multiple sets of parameters for which the fitness function has a minimum value. By training the same type of base classifier separately on features extracted using different parameters of the filters, it was observed that the errors are different from one classifier to another.

2 Fisher classifiers and 2 linear classifiers were trained on features extracted from the same iris images using different parameters to detect which of the two classifiers makes more diverse errors. Then, the trained classifiers were tested on the same 40 images, belonging to the first classes from UBIRISv1 session 1. For each of the 40 images, a binary

vector is formed which takes the value of 0 if the corresponding image was correctly classified and 1 if the corresponding image was not correctly classified. Subsequently, to observe if the errors are different for the same type of classifier, an exclusive or operation was performed between the two binary vectors corresponding to the Fisher classifiers and then for the vectors corresponding to the Linear classifiers. By summing the components of the obtained binary vectors we are able to see which of the two types of classifiers makes different errors. A large value of the sum means that the classifier is making different decisions for feature extracted using different parameters. This process was repeated 25 times for 1 randomly chosen test and 4 train samples and the final values of the sums corresponding to the 2 classifiers are the average of the 25 runs.

It was found that the average sum of the binary vectors obtained after the exclusive or operation was 0.6 for the Fisher classifier and 1.7 for the linear classifier. The average sums' values indicate that Fisher classifiers trained on features extracted using different parameters of the circular symmetric filter misclassify the same images, while Linear classifiers make different errors. Therefore, the linear classifier will be chosen as a base classifier of the MCS.

To optimize the feature dimension obtained by using PCA, genetic algorithms were run for various PCA dimensions using the linear classifier. In Figure 5.4 the rank 1 identification accuracies are plotted for the optimum solution found by the GA when the dimensionality of the features is decreased. As it is shown in Figure 5.4, the identification accuracy of the linear classifier is decreasing when the number of dimensions drops below 50. However, the number of solutions found by the genetic algorithm that are above the 95% identification threshold was higher for a PCA dimension of 60. Thus, the optimum PCA dimension for the proposed iris recognition system is 60.

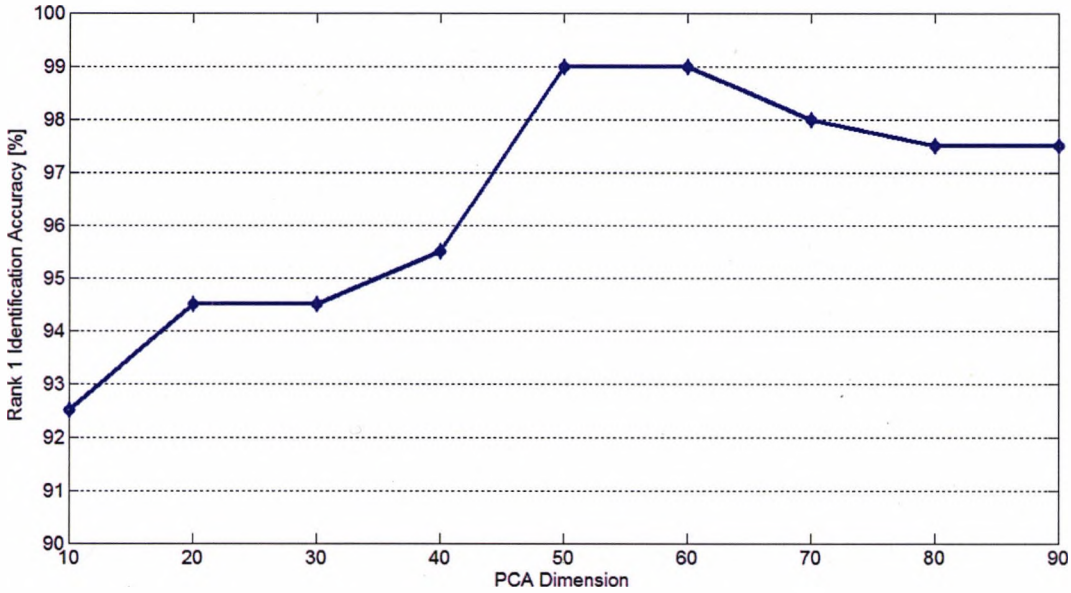

Figure 5.4. PCA Dimension vs Identification accuracy for linear classifier

The third step in the design of the proposed MCS is to find the optimum number of the base classifiers and the appropriate fusion method for the posteriors of the component classifiers. In a MCS, the module that combines the outputs of different base classifiers is usually called *combiner*.

Initially two linear classifiers were trained on features extracted using different sets of parameters of the circular symmetric filter. 6 non-trainable class-conscious fusion methods for the posterior probabilities of the base classifiers were tested: average, product, majority voting, minimum, maximum and sum. This process was repeated 25 times with randomly chosen train and test images and the average of the 25 runs was obtained for all the fusion methods. Subsequently, the number of base classifiers was incremented by 1 and the sequence of operations mentioned above was executed. As the identification accuracy of one Linear classifier is approximately 99%, there is no much room for improvement, therefore the experiments were ran on all the classes of UBIRISv1 session 1 dataset, keeping 4 random images for training and one for testing for each iteration.

It was observed that the best performing fusion method was the average and by adding more than 6 base classifiers, the accuracy of the MCS will not increase, as shown in the experimental results section. The usage of 6 base classifiers to build the MCS implies

that the final feature size will have 360 real valued components.

The architecture of the designed MCS is illustrated in Figure 5.6 for the verification scenario. As it may be observed from Figure 5.6, the structure of the MCS is augmented with 2 distance matchers, a HD matcher and a Pearson Distance (PD) matcher. PD is a similarity measure of two sets of values, having the form given by equation 5.2:

$$PD = 1 - 2\frac{Z(X) \cdot Z(Y)}{N} \tag{5.2}$$

It may be observed that the numerator of the fraction in equation 5.2 is the dot product between the standard errors of the 2 vectors X and Y and N is the size of the vectors X and Y.

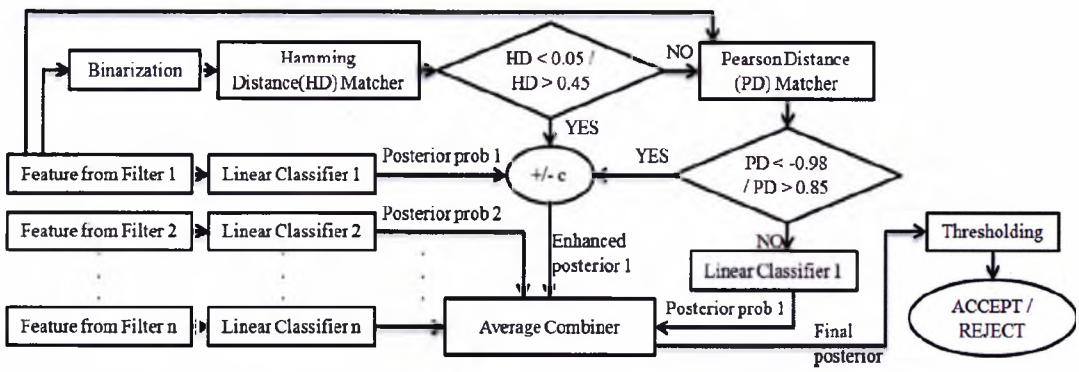

Figure 5.5. MCS architecture for verification scenario

The logic of the MCS augmented with the distance matchers is the following: one of the n input features (in Figure 5.5 feature 1) obtained with different filters is binarized by comparing the 60 real values with their median value. If a feature component is greater than the median value, then the corresponding binary component will be a logical one, otherwise a logical 0. Then, a HD is computed between the probe and gallery features. If the HD is considerably low (less than 0.05 in our implementation) or considerably high (greater than 0.45 in our implementation), then the posterior probabilities of the linear classifier

corresponding to that particular feature is increased or decreased by a constant c. If the HD is between the low and high certainty thresholds, a PD is computed between the 60 components gallery feature and its corresponding probe feature.

Again, if the PD of probe and gallery features is below a threshold (-0.98 in our implementation) or above a threshold (0.85), then the posterior of the linear classifier corresponding to that particular feature is increased or decreased by a constant c. The value of constant c is chosen such that it will modify significantly the posterior probability of the corresponding LDC. If the distance matchers indicate that the test and training features belong to the same class, the posterior probability will be increased to 1. If the distance matchers indicate that the features belong to different classes, the posterior will be decreased to 0.01 (if it is not already smaller than this value).

The two distance matchers are used to provide complementary information to the Linear classifiers in order for the MCS to take a correct decision. The accept /reject decision is taken by thresholding the final averaged posterior outputted by the average combiner. The two distance matchers are serially connected and they enhance the parallel architecture of the 6 linear classifiers.

It is interesting to observe how the MCS performs in the verification scenario when different features out of the 6 are chosen to be processed by the distance matchers. Also, it is desirable to see if the addition of the distance matchers improves or not the verification accuracy of the iris recognition system. These analyses will be made in the experimental results section. In the identification scenario, the outputs of the linear classifiers are averaged and the class label corresponds to the class with the largest average posterior probability.

5.3.3.2 Discussion

The most significant advantage of using MCS for identification scenario of any biometric system is that once the base classifiers have been trained, there is no need to query the database when identifying a user. Therefore, a MCS approach for identification scenarios of an iris recognition system is beneficial due to the following three reasons:

1) The issue of database security on an operational device disappears.

2) On large scale databases (millions of users), the time needed to identify a subject

is significantly reduced compared to a system which uses classical binary features and HDs. This is a valid observation, since the time of accessing the templates on the storage devices is eliminated.

3) The iris recognition system becomes suitable for embedded and mobile applications, a desirable attribute of any biometric system (Radu, Sirlantzis et al. 2012).

4) The range of scenarios where the colour iris recognition may be deployed is increased, with an enhanced potential for ubiquitous biometric identification (Sirlantzis, Howells et al. 2010).

The disadvantage of using a MCS approach in an iris recognition system is that the base classifiers have to be retrained every time one user is enrolled in the database. In a classical iris recognition system, where only distances are computed between the probe and gallery images, enrolling a new user is not an issue. However, a distance based matching does not yield an acceptable accuracy for noisy colour iris images, as shown in (Radu, Sirlantzis et al. 2011). Thus, a trade-off between a matching-based (near infrared) iris recognition system and a MCS-based (colour) iris recognition system has to be made according to the application for which the biometric system is designed.

A MCS approach is more appropriate for biometric authentication in industry or institutional environments, where there are a few hundred users and there is no need to enrol users in the database every day. Also, the financial resources of such organizations are often limited, but a high performing colour iris recognition system is an affordable biometric authentication system. A near infrared iris recognition system with a distance-based matching, where no retraining is necessary after every enrolment, is suitable for border control environments, where there is no tolerance for false matches.

5.4 Experiments

The efficiency of the proposed iris recognition system is benchmarked on UBIRISv1 database. The images were collected from 241 individuals in 2 sessions. The users are enrolled by acquiring 5 images of their right eye. A description of the database may be

found in subsection 2.3.1.

5.4.1. Experimental setup

Both verification and identification scenarios were explored in the experiments. For all the experiments 4 out of 5 images from each class were used as gallery, and one as probe. The probe image from each class was chosen randomly. All the experiments were carried out separately for session 1 and session 2 of the UBIRISv1 database. In the identification scenario, this process is repeated 100 times and the final rank 1 identification accuracy is the mean of the 100 runs.

In the verification scenario four random gallery images are kept in the database for all classes. Then an unseen probe image, randomly chosen, claims to have a certain identity and the obtained posterior probability corresponding to the claimed class label is compared with a threshold. The FAR and FRR were computed for 90 values of the threshold, within interval [0.1; 1] and for each step the current threshold was obtained by adding to the previous threshold 0.01. This process is repeated 100 times and the FAR and FRR for every value of the threshold is the average of the 100 runs. The EER is obtained for the threshold where FAR and FRR have approximately equal values.

The experiments were conducted using 100 pixels around the pupil and the obtained accuracies are compared to the results obtained in using only 50 pixels around the pupil. As mentioned in the previous chapters, 100 pixels around the pupil correspond to approximately 100% of the available texture information for the UBIRISv1 database and 50 pixels around the pupil correspond to approximately 50% of the available information.

5.4.2 Identification results

The base classifiers are trained on features extracted using different parameters of the circular symmetric filters, as explained in section 5.3. Initially the experiments were conducted for identification scenario for different numbers of base classifiers, to find the optimum number of linear classifiers needed in the design of the MCS. One base classifier was trained on 4 random iris images from all classes of UBIRISv1 Session1 dataset and

tested on the remaining image from each class. The process was repeated 25 times and then the number of the base classifiers was incremented. In the box plots from Figure 5.6 it may observed how the rank 1 identification accuracy increases with the number of base classifiers. By analysing Figure 5.6, it was concluded that the optimum number of base classifiers is 6. Also, it may be observed from the same figure how the stability of the biometric system increases as more classifiers are added to the ensemble. The boxplots from Figure 5.6 were generated using 100 pixels around the pupil.

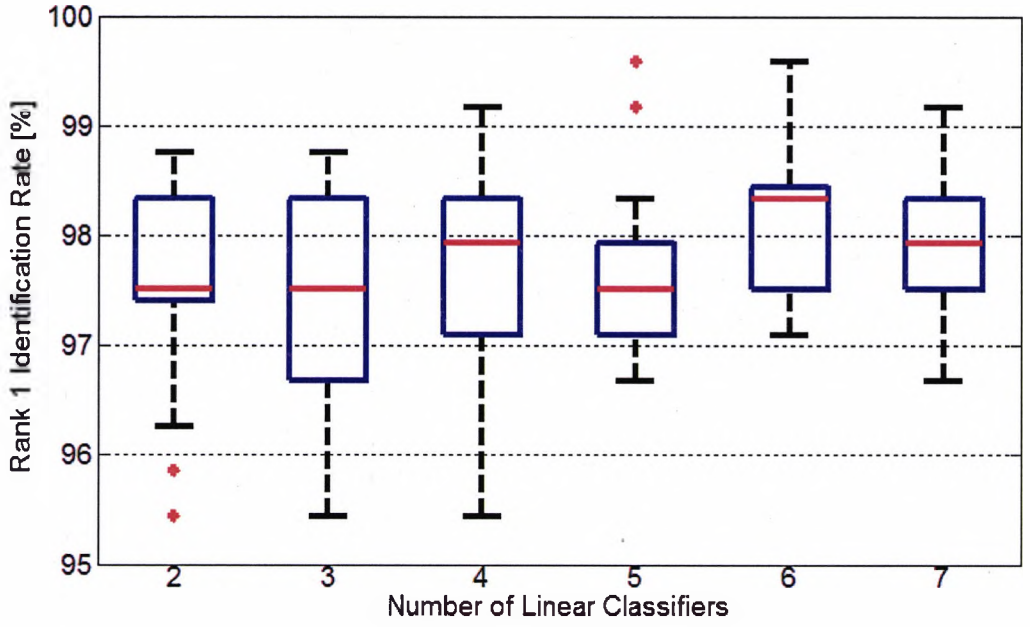

Figure 5.6. Rank 1 identification accuracy for different number of base classifiers

Initially all the images from the two sessions are used in identification scenario. In session 1, 10 are strongly or totally occluded, therefore, no useful iris information can be extracted from them. From Session 2, 13 images out of 662 are strongly occluded. The occluded images were manually detected. To assess more objectively the system's performance, a reject option was added to the MCS, so that when an occluded image is chosen as probe, the system ignores it without counting a transaction. However, the occluded images are used in the training stage of the MCS.

In Table 5.2, a comparison between the mean rank 1 identification accuracies obtained using 100% and 50% of the available iris texture is made, when all the iris images from the database are used and when the occluded images are rejected.

Iris texture usage / Method	Session 1		Session 2	
	50%	100%	50%	100%
Radu et al (Radu, Sirlantzis et al. 2011)	99.25 %	-	91.96 %	-
Proposed using red channel	98.10 %	97.15 %	87.26 %	92.67 %
Proposed using fusion	97.63 %	98.20 %	90.03 %	95.43 %
Proposed using fusion and rejection of occluded images	98.38 %	99.27 %	91.18 %	95.79 %

Table 5.2. Rank 1 identification accuracy of the proposed biometric system for all images of UBIRISv1 database

From Table 5.2 it may be observed that when 50 pixels were used around the pupil, the red channel showed a slightly higher rank 1 identification accuracy than the fusion of red, green and intensity channels, but only on the iris images from session 1, which are good quality. This may be due to the fact that the red channel has the closest wavelength to the near infrared spectrum, thus the noises such as reflections are not affecting significantly the red channel. In the second session, where the images contain more noise factors, the fusion between the three channels performed better than the red channel.

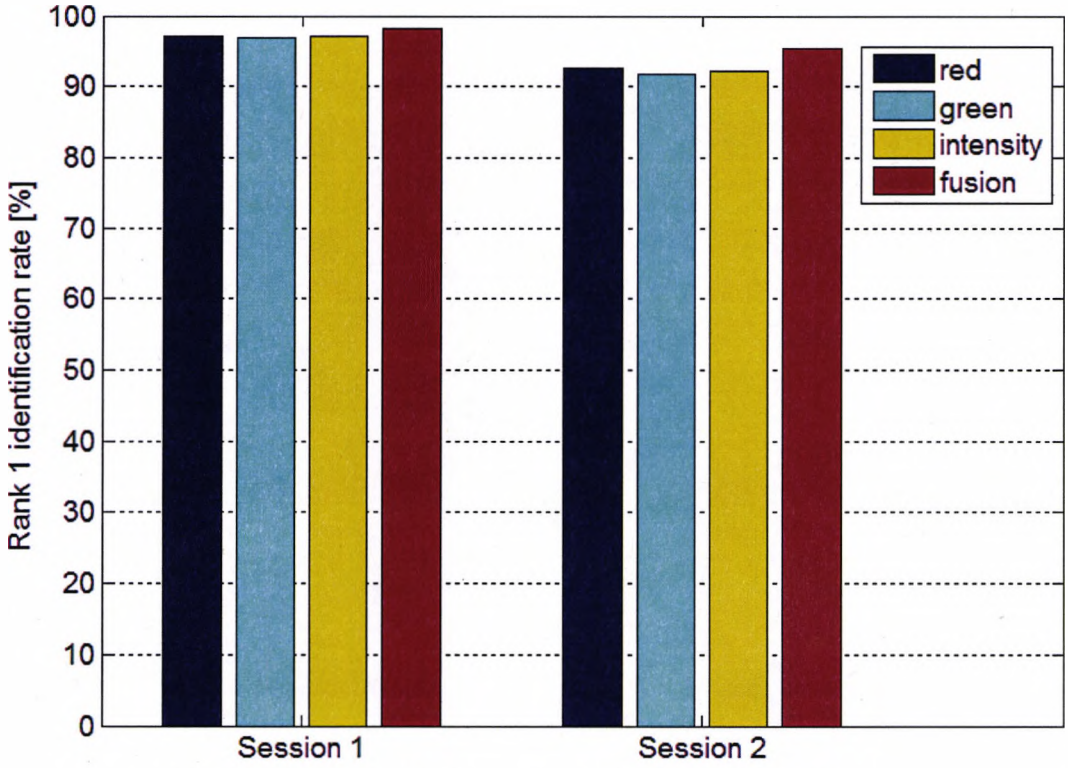

Figure 5.8. Rank 1 identification rate for all images of UBIRISv1 database

In Figure 5.8 the rank 1 identification accuracies produced by the proposed iris recognition approach are plotted for all the 3 channels. It may be observed that the three channels perform similarly, but the information fusion approach is efficient when the iris image quality drops.

5.4.2 Verification results

In the verification scenario, initially it was tested whether the distance matchers improve the system's EER or not (see Figure 5.5). One of the 6 input features at a time was considered as an input to the distance matchers. The verification experiments were ran on all the images of session 1 and session 2. This process was repeated 10 times, with a random probe image for every run. The final EER was the mean of the 10 runs for every case. Then, the verification experiment was conducted for the case when the distance

matchers are not included in the MCS architecture. Table 5.3 summarizes the EER obtained for the above mentioned cases, when 100 pixels around the pupil are used.

Feature used as input for the distance matchers	Equal Error Rate [%]	
	Session 1	Session 2
Feature 1	3.86	5.36
Feature 2	4.18	4.78
Feature 3	3.70	5.40
Feature 4	3.69	4.65
Feature 5	3.81	4.98
Feature 6	3.78	4.55
None	3.75	4.69

Table 5.3. EER for different features used as input for the distance matchers

The data from Table 5.3 shows that there is no significant difference between the EER obtained using the distance matchers and the EER obtained when only the base classifiers are employed. Nevertheless, the system will be able to *operate in the verification scenario without the database*, once the base classifiers have been trained. The Receiver Operational Characteristic (ROC) curves for all the images from session 1 and session 2 are shown in Figure 5.8 and Figure 5.9 respectively, for the cases when 50 pixels and 100 pixels around the pupil are used.

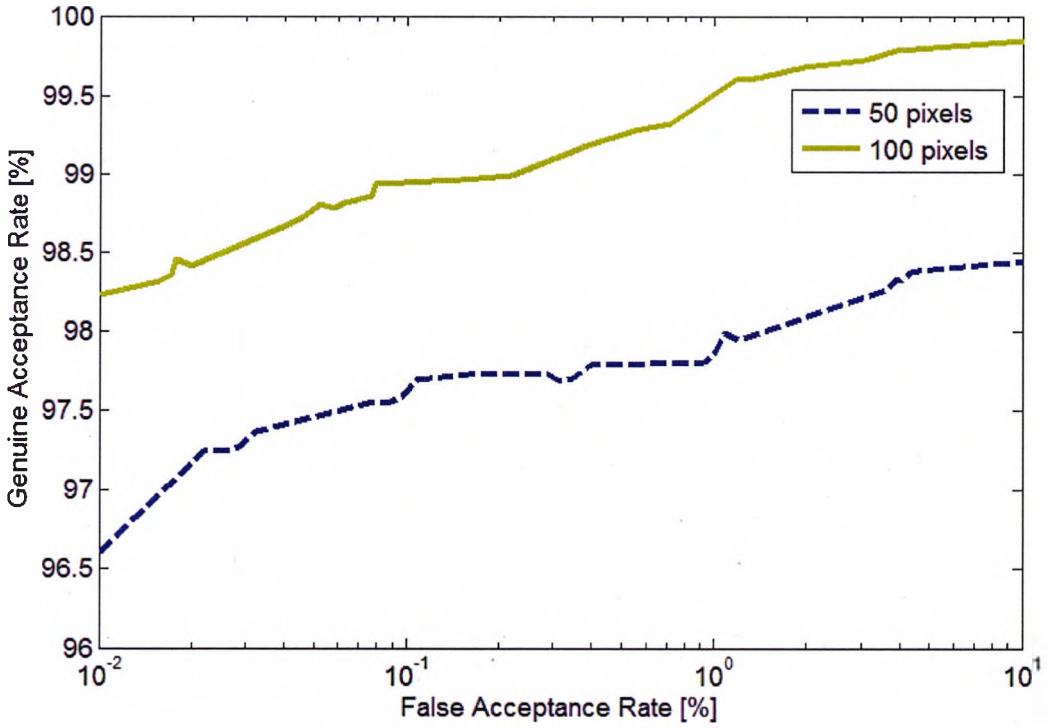

Figure 5.8. ROC curves for all images from UBIRISv1 session 1

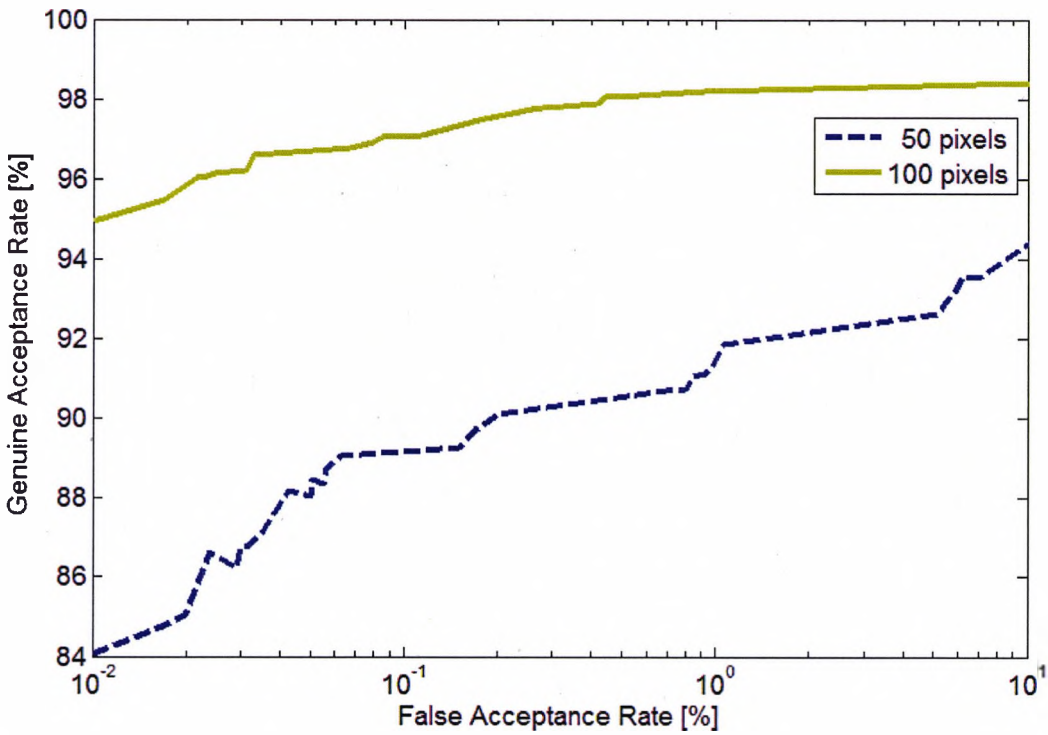

Figure 5.9. ROC curves for all images from UBIRISv1 session 2

From figures 5.8 and 5.9 it may be observed that the improvement brought by the usage of 100% iris texture is significantly larger on the low quality images from session 2. In order to compare the performance of the proposed iris recognition system with results published in the literature on the 2 sessions of UBIRISv1, the work from (Tajbakhsh, Araabi et al. 2009) was chosen, where the results are reported using 5 algorithms. In (Tajbakhsh, Araabi et al. 2009) approximately 7% out of the total number of images in the dataset were not used in the experiments. Details about the noisy iris images that represent the 7% are not reported.

For comparison purposes, 7% of the most noisy iris images from session 1 and 7% from session 2 were manually selected and a reject option was added for these images to the MCS, but the images were used in training. The comparison between the EER obtained using the proposed method and those reported in (Tajbakhsh, Araabi et al. 2009) is presented in Table 5.4.

Method	Session 1 EER [%]	Session 2 EER [%]
Poursaberi and Araabi (Poursaberi and Araabi	2.1	5.0
Ma et al (Ma, Tan et al. 2004)	1.9	5.0
Rakshit et al (Monro, Rakshit et al. 2007)	1.2	3.8
Ahmadi et al (Ahmadi, Pousaberi et al. 2007)	1.9	8.0
Tajbakhsh et al (Tajbakhsh, Araabi et al.	0.4	3.0
Proposed, using 50% of the iris	1.2	6.7
Proposed, using 100% of the iris	0.22	1.81

Table 5.4. Comparison of verification error rates without 7% of the iris images from UBIRISv1 database

When all images are used, the EER of the proposed iris recognition system is 0.41 % for session 1 images and 1.98% for session 2 images. The threshold corresponding to the EER is approximately 0.94. The results presented in this subsection may be further enhanced by employing image enhancement techniques, as showed in (Radu, Sirlantzis et al. 2012).

5.5 Chapter conclusions

One of the most desirable characteristics of an iris recognition system operating in a reduced constraints environment is to be able to cope with colour iris images. The accuracies reported in the literature for colour iris recognition systems are not yet comparable to those reported for near infrared iris recognition systems. In this chapter an iris recognition system is proposed which works on colour iris images by adapting a feature type proposed for near infrared images in the literature to work successfully with colour iris images.

Unlike the majority of the iris recognition systems available in the literature, which are employing a distance-based matching, the proposed method uses MCS in both verification and identification scenarios. A bank of 6 circular symmetric filters with different parameters was used to extract the features from red, green and intensity channels. The fusion of the three channels is made at feature level by using PCA. Subsequently, a MCS is employed in the matching phase to combine the features extracted using different parameters of the filters. The main advantage of using a MCS approach for iris recognition is that the system is able to operate without the need of querying the database, once the MCS is trained.

The extensive set of experiments that were conducted on UBIRISv1 dataset show that the proposed approach outperforms other colour iris recognition methodologies published in the literature. With a feature size of only 360 real-valued components, the proposed system is suitable to be deployed on embedded or mobile devices. Also, the proposed iris recognition system operates in both identification and verification scenario without the database available, eliminating any concern of securing the enrolled images database.

The proposed colour iris recognition system does not rely on image enhancement techniques to increase its accuracy, fact which makes it highly computationally efficient. Nevertheless, the employed MCS approach increases the robustness of the iris recognition system to various noises present in the images acquired in unconstrained environments.

The main contribution of the proposed iris recognition system is that of showing that the MCS techniques are a promising approach towards iris recognition with reduced constraints. The accuracies reported in this study may be enhanced by using one or more of

the following 4 approaches:

1) enriching the architecture of the MCS with base classifiers trained on other feature types than the one used in this study;
2) applying image enhancement techniques;
3) using the eye colour and periocular information as additional information;
4) using a multi-instance approach, i.e. both irises of a person.

This chapter concludes the information fusion approaches explored in the present work. which are aimed for developing colour iris recognition systems with reduced constraints. The next chapter will present the overall conclusions drawn from this study.

Chapter 6
Final remarks

This chapter will present a summary of all issues addressed in this thesis as well as all the contributions given. An analysis of the potential impact of the proposed approaches in the field of iris recognition will be discussed and possible future research directions will be highlighted.

6.1 Introduction

This thesis has presented novel foundations on how to design iris recognition systems with reduced constraints by employing various information fusion techniques. The iris recognition approaches explored along this study take into account what additional sources of information are available to the reduced constraints biometric system designer, as well as the requirements of the system itself. The contributions of this thesis can be divided in three main areas corresponding to three different degrees of complexity of the information fusion techniques employed. We have referred to these as multi-algorithmic approach, texture and colour fusion approach and multi-classifier approach.

The work conducted has focussed on developing iris recognition techniques suitable to be used on colour iris images. Unlike the classical near infrared iris recognition systems, where the images are of good quality, in the visible spectrum the dissimilarity based algorithms may be less efficient than in the near infrared spectrum. In this thesis, the issues of colour iris recognition were identified and possible solutions were proposed in the field of iris recognition with reduced constraints. The proposed designs for colour iris recognition systems are aimed to increase the practicability of the state of the art iris biometric technology.

Generally, the three information fusion approaches that were explored along this study were aimed to cover the major alternatives to the classical distance based iris recognition algorithms that were proposed in the literature for near infrared iris images. Solutions were found for the challenging task of iris recognition under less constrained environments, with potential application in ubiquitous iris recognition. Moreover, the proposed iris recognition approaches were designed to be computationally efficient as they rely on information fusion to increase the biometric system's accuracy, not on image quality enhancement. Thus, the developed iris recognition systems are suitable to be implemented on embedded and mobile devices.

More specifically, each chapter from this thesis has made an important contribution from the point of view of the information fusion approach that was applied to the iris recognition system design. Issues dealt in each of the five chapters can be listed as follows:

Chapter 1: Introduction

This chapter presents a generic introduction to the field of iris recognition and a discussion of some particular problems in the design of iris recognition systems with reduced constraints. The research objectives are highlighted.

Chapter 2: Literature review

This chapter presents the state of the art in iris recognition techniques applied on colour iris images. The review is organized systematically, according to the level of complexity of the information fusion techniques employed in the colour iris recognition systems. The benefits and drawbacks of the fusion mechanisms employed in the surveyed iris recognition works are presented.

Chapter 3: Basic fusion of iris recognition algorithms with adaptations for visible spectrum

This chapter presents the first information fusion approach proposed for iris recognition with reduced constraints. Specifically, a multi-algorithmic system was built from 3 component algorithms that operate independently on colour iris images. The fusion of the three algorithms is done at the score level.

Chapter 4: Fusing texture and colour for less constrained iris recognition systems

This chapter explores the fusion between the information extracted from the iris texture and eye colour. A technique for optimising the texture data is proposed. The biometric system matching module is designed by employing a Fuzzy Logic score level fusion.

Chapter 5: Enhanced information fusion for colour iris recognition

This chapter proposes a multi-classifier approach for colour iris recognition. Features are extracted from different colour spaces and a feature selection technique keeps only the most discriminant subset of features. The main contribution of this chapter consists of designing an iris recognition system which is capable of operating without the database,

once the MCS is trained.

The main contributions made by this thesis in the field of iris recognition with reduced constraints will be discussed in more detail in Section 6.2. Section 6.3 will present a list of possible future research which can further enhance the work and results reported in this study. Finally, Section 6.4 will present some concluding remarks about this work.

6.2 Impact of the contributions in field of iris recognition with reduced constraints

From the most general perspective, but also from more specialized perspectives, this thesis addresses some very important issues in the field of iris recognition. The conclusions which can be drawn from the contributions made in this study can be listed as follows:

- Iris recognition systems operating on visible spectrum images have not yet reached a mature stage and a possible method to enhance their performances is to use various information sources and fusion methodologies (Chapter 2).
- Although there is an extensive literature on MCS, adopting such a classification mechanism in colour iris recognition systems is a relatively little used option (Chapter 2).
- The visible spectrum iris recognition approaches which rely on a distance based matching module, do not yield comparable accuracies to those reported for near infrared spectrum (Chapter 2 and Chapter 3).
- The classical near infrared iris recognition approach, which uses phase based feature extraction and Hamming distance for matching is only effective if the acquired iris images are of high quality. However, it is still highly efficient when applied on good quality visible spectrum images (Chapter 3 and Chapter 4).
- A methodology of finding the channels that reveal the most discriminative information available in the iris texture from multiple colour spaces leads to a more robust colour iris recognition system design. Such a method is presented in Chapter 3.

- A multi-algorithmic approach for iris recognition, which uses a simple score level fusion, does not improve significantly the accuracies of the biometric system over the performances obtained by the best component algorithm (Chapter 3).
- Due to the radial orientation of the iris texture, the most discriminant features extracted using 2D Gabor filters are obtained for a value of the orientation of the filter of 90° (Chapter 3 and Chapter 4).
- When designing an optimized 2D Gabor filter bank for iris feature extraction, adding filters with different orientations to the bank enhances more the accuracy of the iris recognition system than adding filters with different sizes and frequencies (Chapter 4).
- Knowledge about the eye colour of an individual can be integrated into the architecture of an iris recognition system with reduced constraints with minimal computational effort to reduce its false match rate (Chapter 4).
- For visible spectrum iris recognition systems, the fusion of classical phase based features generated by an optimized 2D Gabor filter bank and features extracted from the eye colour yield a comparable ROC curve to the state of the art near infrared iris recognition systems, when a similar number of good quality iris images are used (Chapter 4).
- Multiple classifier techniques exhibit high accuracies when employed in iris recognition systems operating on visible spectrum images. Their main advantage is the database free operation, once the classifier ensemble has been trained (Chapter 5).
- The real-valued iris features extracted using a bank of circular symmetric filters with optimized parameters represent an excellent choice as input features for the base classifiers of an MCS architecture of a visible spectrum iris recognition system (Chapter 5).
- The high accuracies obtained by the colour iris recognition system which employs MCS indicate that this type of approach is one of the paths to be explored in order to achieve a robust biometric system that is capable of reduced

constraints operation (Chapter 5).

- The obtained results from Chapter 4 and Chapter 5 point to the potential benefits of augmenting the MCS architecture with information extracted from the eye colour.
- Employing MCS architectures in iris recognition systems has the disadvantage of needing a retrain procedure when new users are enrolled, but for small to medium size databases this issue is alleviated by the continuously increasing computational power (Chapter 5).

The above mentioned findings have very exciting implications. The results obtained in this study point to an interesting strand of investigation, which has an enhanced potential in developing practical, more robust, flexible and cost effective iris recognition systems in the near future.

In the same time, the solutions proposed in the present thesis have certain limitations. First, it is assumed that the all the iris images are correctly segmented and this makes the developed iris recognition systems semi-automatic approaches. Then, the unconstrained environment is considered as a whole since the performance assessment has not been made on images which contain only one particular type of imperfection.

6.3 Future work

The research presented in this thesis has aimed to increase the performance of iris recognition systems with reduced constraints by focusing on the design of the biometric system in general, not only on specific stages of it. In addition to the very interesting contributions presented along this thesis, naturally, some new ideas have emerged from the conducted work.

Sections 6.3.1, 6.3.2 and 6.3.3 will propose some suggestions for future work in relation to multi-algorithmic approach, texture and periocular data fusion approach and MCS approach respectively.

6.3.1 Future research in multi-algorithmic approach

In this thesis, the multi-algorithmic approach employed 3 iris recognition systems. A more detailed investigation should be made using more iris recognition component algorithms which perform similar to the classical 2D Gabor filter based approach.

It is also interesting to find if there are some types of features which perform better than the other feature types on a subset of colour iris images. Such a study would enable us to establish a relationship between the characteristic of the iris image and the feature type which should receive the highest weight in the multi-algorithmic approach. In this context, the characteristic of the iris image does not have to be an image quality measure, it could be the eye colour or pupil to iris ratio.

The score fusion technique employed in the multi-algorithmic iris recognition system is simple and straightforward. Therefore a more complex score fusion technique is needed to maximize the accuracy of the biometric system.

6.3.2 Future research in texture and periocular data fusion approach

The soft biometrics are useful in specific scenarios when the user is less cooperative with the data acquisition protocol. In this thesis, only the eye colour was used in addition to the information extracted from the iris texture.

Additional investigations should be made using other soft biometrics apart from the eye colour. Effects of the information extracted from the skin texture, skin colour, eyelid shape, eyelid distribution, left or right side or eyeball veins distributions could be fused with the texture information to boost the colour iris recognition system's accuracy.

Another direction of future work is represented by the analysis of the above mentioned soft biometrics in relation to their contribution to the iris recognition accuracy improvement. An intelligent methodology of selecting the most useful soft biometric information for colour iris recognition is a highly desirable one.

6.3.3 Future research in MCS fusion approach

This thesis presented an initial investigation on how MCS approaches may be employed in colour iris recognition. A more detailed investigation using more complex

MCS structures has to be conducted.

Significant achievements may be reached in iris recognition with reduced constraints by augmenting the structure of the MCS with base classifiers trained on different real valued feature types. By having more feature types, the diversity of the MCS is increased. Furthermore, the MCS structure could be enhanced by adding image quality measures which will influence the weight of the classifiers trained on different feature types in the final decision.

A highly important future research path is represented by the development of colour iris recognition systems that employ dynamic MCS architectures which do not need a training procedure when new users are enrolled.

6.4 Chapter conclusions

This thesis has presented significant contributions to the field of iris recognition with reduced constraints by exploring various options of building such a biometric system. New approaches for improving the accuracy of an iris recognition system which operates on visible spectrum images were introduced.

An iris segmentation methodology which can cope with both near infrared and visible spectrum iris images is introduced. A methodology of selecting the channels of a colour space, where the iris texture information is more discriminant is also proposed.

The use of multiple iris recognition algorithms that work in parallel and are fused at the score level has been shown to be not significantly better than the best performing component algorithm.

Combining texture and colour for iris recognition systems with reduced constraints is one of the major contributions of this thesis. For the texture feature extraction, a methodology of optimizing the parameters of a 2D Gabor filter bank is proposed. Significant modifications were proposed for a colour feature extraction methodology to adapt it for the task of iris recognition. The fusion between the texture and colour data was done at the score level using Fuzzy Logic fusion. It was shown that for good quality colour iris images, the accuracy of the proposed iris recognition system is comparable to the accuracy of near infrared iris recognition systems.

Another significant contribution of this thesis is represented by a reduced constraints iris recognition system design that has an increased practicability due to the fact the MCS structures are employed for classification. The proposed MCS approach increases the robustness of the biometric system when noisy iris images are presented to the system.

These contributions appear to be well suited to the existing problem of iris recognition under visible spectrum, and provide a strong support for future research directions. The results of the study indicate that there are two main directions to be followed when designing iris recognition systems with reduced constraints: 1) fusion of texture and periocular data; 2) MCS approach.

In summary, the research reported in this thesis has improved the state of the art of iris recognition systems with reduced constraints. The work conducted has contributed some new ideas to how colour iris recognition systems could be enhanced and developed in an enhanced way in the near future. The proposed iris recognition algorithms are accurate, robust, flexible and computationally efficient. Their suitability of being implemented on mobile or embedded devices is increased. The ability of implementing a working iris recognition system on generic devices, such as laptops, tablets or mobile phones will have a significant impact on sustainable and inclusive social development. This thesis makes a step toward ubiquitous and mobile iris recognition.

References

Ahamed, A. and M. I. H. Bhuiyan (2012). "Low complexity iris recognition using curvelet transform". *Proceedings of International Conference on Informatics, Electronics & Vision (ICIEV),* Dhaka, Bangladesh, 2012, pp. 548 - 553.

Ahmadi, H., A. Pousaberi, A. Azizzadeh and M. Kamarei (2007). "An Efficient Iris Coding Based on Gauss-Laguerre Wavelets". *Advances in Biometrics.* S.-W. Lee and S. Li, Springer Berlin / Heidelberg. 4642: 917-926.

Babu, N. T. N. and V. Vaidehi (2011). "Fuzzy based IRIS recognition system (FIRS) for person identification". *Proceedings of International Conference on Recent Trends in Information Technology (ICRTIT),*Chennai, India, 2011, pp. 1005 - 1011.

Bharadwaj, S., H. S. Bhatt, M. Vatsa and R. Singh (2010). "Periocular biometrics: When iris recognition fails". *Proceedings of the Fourth IEEE International Conference on Biometrics: Theory Applications and Systems (BTAS),* Washington, U.S.A., 2010, pp. 1 - 6.

Bodade, R. M., S. N. Talbar and S. K. Ojha (2008). "Iris Recognition Using Rotational Complex Wavelet Filters: A novel approach". *Proceedings of International Conference on Innovations in Information Technology,* Al Ain, United Arab Emirates, 2008, pp. 658 - 662.

Boles, W. W. and B. Boashash (1998). "A human identification technique using images of the iris and wavelet transform." *IEEE Transactions on Signal Processing* 46(4): 1185-1188.

Bouridane, A. (2009). "Recent Advances in Iris Recognition: A Multiscale Approach". *Imaging for Forensics and Security,* Springer US: 49-77.

Bowyer, K., K. Hollingsworth and P. Flynn (2012). "A Survey of Iris Biometrics Research: 2008-2010". *Handbook of Iris Recognition.* M. Burge and K. W. Bowyer, Springer.

Bowyer, K. W., K. Hollingsworth and P. J. Flynn (2008). "Image understanding for iris biometrics: A survey." *Computer Vision and Image Understanding* 110(2): 281-307.

Boyce, C., A. Ross, M. Monaco, L. Hornak and L. Xin (2006). "Multispectral Iris Analysis: A Preliminary Study51". *Proceedings of Computer Vision and Pattern Recognition Workshop,* New York, U.S.A., 2006, pp. 51 - 56.

C. Tisse, L. Martin, L. Torres and M. Robert (2002). "Person identification technique using human iris recognition." *Proceedings of Conference on Vision Interface,* Calgary, Italy, 2002, pp. 294 - 299.

Caitang, S., F. Melgani, F. De Natale, Z. Chunguang, Z. Libiao and L. Xiaohua (2008). "Incremental Learning Based Color Iris Recognition". *Proceedings of the Seventh Mexican International Conference on Artificial Intelligence,* Mexico City, Mexico, 2008, pp. 319 - 324.

Camus, T. A. and R. Wildes (2002). "Reliable and fast eye finding in close-up images". *16th International Conference on Pattern Recognition,* Quebec, Canada, 2002, pp. 389 - 394.

Castañon, L., S. de Oca and R. Morales-Menéndez (2006). "Optimal Sampling for Feature Extraction in Iris Recognition Systems". *MICAI 2006: Advances in Artificial Intelligence*. A. Gelbukh and C. Reyes-Garcia, Springer Berlin / Heidelberg. 4293: 810-819.

Chen, W.-S., R.-H. Huang and L. Hsieh (2009). "Iris Recognition Using 3D Co-occurrence Matrix". *Advances in Biometrics*. M. Tistarelli and M. Nixon, Springer Berlin / Heidelberg. 5558: 1122-1131.

Chia-Te, C., S. Sheng-Wen and C. Duan-Yu (2006). "Design of Gabor Filter Banks for Iris Recognition". *International Conference on Intelligent Information Hiding and Multimedia Signal Processing,* Pasadena, California, U.S.A., 2006, pp. 403 - 406.

Chia-Te, C., S. Sheng-Wen, C. Wen-Shiung, V. W. Cheng and C. Duan-Yu (2010). "Non-Orthogonal View Iris Recognition System." *IEEE Transactions on Circuits and Systems for Video Technology,* 20(3): 417-430.

Ciobanu, A., M. Costin and T. Barbu (2013). "Image Categorization Based on Computationally Economic LAB Colour Features". *Soft Computing Applications*. V. E. Balas, J. Fodor, A. R. Várkonyi-Kóczy, J. Dombi and L. C. Jain, Springer Berlin Heidelberg. 195: 585-593.

Cortes, C. and V. Vapnik (1995). "Support-vector networks." *Machine Learning,* 20(3): 273-297.

Daily Mail (2012), "£9 million iris recognition scheme introduced to slash queues at airports is scrapped", retrieved 01.11.2012 from http://www.dailymail.co.uk/travel/article-2102489/Iris-recognition-scheme-airports-scrapped-years.html"

Dantcheva, A., N. Erdogmus and J.-L. Dugelay (2011). "On the reliability of eye color as a soft biometric trait". *IEEE Workshop on Applications of Computer Vision (WACV),* Kona, Hi, U.S.A, 2011, pp. 227 - 231.

Daubechies, I. (1992). "Ten Lectures on Wavelets".

Daugman, J. (2004). "How iris recognition works." *IEEE Transactions on Circuits and Systems for Video Technology,* 14(1): 21-30.

Daugman, J. (2007). "New Methods in Iris Recognition." *IEEE Transactions on Systems, Man, and Cybernetics, Part B: Cybernetics,* 37(5): 1167-1175.

Daugman, J. G. (1980). "Two-Dimensional Spectral-Analysis of Cortical Receptive-field Profiles." *Vision Research* 20(10): 847-856.

Daugman, J. G. (1988). "Complete discrete 2-D Gabor transforms by neural networks for image analysis and compression." *IEEE Transactions on Acoustics, Speech and Signal Processing,* 36(7): 1169-1179.

Daugman, J. G. (1993). "High confidence visual recognition of persons by a test of statistical independence." *IEEE Transactions on Pattern Analysis and Machine*

Intelligence, 15(11): 1148-1161.

De Marsico, M., M. Nappi and D. Riccio (2012) "Noisy Iris Recognition Integrated Scheme." *Pattern Recognition Letters*, 33(8): 1006 - 1011.

de Souto, M. C. P., R. G. F. Soares, A. Santana and A. M. P. Canuto (2008). "Empirical Comparison of Dynamic Classifier Selection Methods based on Diversity and Accuracy for Building Ensembles". *2008 IEEE International Joint Conference on Neural Networks, Vols 1-8*. New York, Ieee: 1480-1487.

Delft, U., of, Technology. (2012). "PRTools - A Matlab toolbox for pattern recognition." Retrieved 12.12.2012, 2012, from http://prtools.org/.

Demirel, H. and G. Anbarjafari (2008). "Iris Recognition System Using Combined Colour Statistics". *Proceedings of the IEEE International Symposium on Signal Processing and Information Technology*, Sarajevo, Bosnia & Herzegovina, 2008: 1 - 4.

Dietterich, T. (2000). "Ensemble Methods in Machine Learning". *Multiple Classifier Systems*, Springer Berlin / Heidelberg. 1857: 1-15.

Dietterich, T. G. (1997). "Machine-learning research - Four current directions." *Ai Magazine* 18(4): 97-136.

Dobeš, M. and L. Machala (2004). "UPOL Iris Image Database".

Duda, R. O., P. E. Hart and D. G. Stork (2001). "Pattern Classification, 2nd Edition". New York, Wiley.

Farouk, R. M. (2011). "Iris recognition based on elastic graph matching and Gabor wavelets." *Computer Vision and Image Understanding* 115(8): 1239-1244.

Fenghua, W. and H. Jiuqiang (2009). "Information fusion in personal biometric authentication based on the iris pattern." *Measurement Science and Technology* 20: 1-8.

Ferreira, A., A. Lourenço, B. Pinto and J. Tendeiro (2010). "Tuning Iris Recognition for Noisy Images". *Biomedical Engineering Systems and Technologies*. A. Fred, J. Filipe and H. Gamboa, Springer Berlin Heidelberg. 52: 211-224.

Fu, J., H. J. Caulfield, S. M. Yoo and V. Atluri (2005). "Use of Artificial Color filtering to improve iris recognition and searching." *Pattern Recognition Letters* 26(14): 2244-2251.

Garza Castañón, L., S. de Oca and R. Morales-Menéndez (2006). "An Application of ARX Stochastic Models to Iris Recognition". *Professional Practice in Artificial Intelligence*. J. Debenham, Springer Boston. 218: 343-352.

Ghouti, L. and F. S. Al-Qunaieer (2009). "Color Iris Recognition Using Quaternion Phase Correlation". *Proceedings of Bio-inspired Learning and Intelligent Systems for Security*, Edimburgh, U.K., 2009, pp. 20-25.

Gonzalez, R. and R. Woods (2008). "Digital Image Processing 3rd Edition", Prentice Hall.

Grother, P., E. Tabassi, G. W. Quinn and W. Salamon (2009). "IREX I Report - Performance of Iris Recognition Algorithms on Standard Images".

Hariprasath, S. and V. Mohan (2008). "Biometric personal identification based on iris

recognition using complex wavelet transforms". *International Conference on Computing, Communication and Networking,* St. Thomas, U.S.A., 2008, *pp. 1-5.*

Hastie, T., Tibshirani, Robert, Friedman, Jerome (2009). "The Elements of Statistical Learning, Data Mining, Inference, and Prediction, Second Edition". New York, Springer.

Hollingsworth, K. P., S. S. Darnell, P. E. Miller, D. L. Woodard, K. W. Bowyer and P. J. Flynn (2012). "Human and Machine Performance on Periocular Biometrics Under Near-Infrared Light and Visible Light." *Information Forensics and Security, IEEE Transactions on* 7(2): 588-601.

Hosseini, M. S., B. N. Araabi and H. Soltanian-Zadeh (2010). "Pigment Melanin: Pattern for Iris Recognition." *Instrumentation and Measurement, IEEE Transactions on* 59(4): 792-804.

HTC. (2012). "HTC Desire." Retrieved 29.11.2012, 2012, from http://www.htc.com/uk/help/htc-desire/.

Huang, Y. S. and C. Y. Suen (1995). "Method of Combining Multiple Experts for the Recognition of Unconstrained Handwritten Numerals." *IEEE Transactions on Pattern Analysis and Machine Intelligence* 17(1): 90-94.

Hui, L., x, S. Jin, L. Lintao and Y. Tao (2010). "An improved algorithm for iris feature extraction". *Proceedings of the IEEE International Conference on Intelligent Computing and Intelligent Systems (ICIS),*Xiamen, China, 2010, pp. 167 - 171.

Inst. of Automation, C. A. o. S. (2004). "CASIA Iris Image Database." from http://www.sinobiometrics.com.

Inst. of Automation, C. A. o. S. (2006). "CASIA-IrisV3." Retrieved 10.05.2010, 2010, from http://www.cbsr.ia.ac.cn/IrisDatabase.

Jain, A. K., R. P. W. Duin and J. C. Mao (2000). "Statistical pattern recognition: A review." *IEEE Transactions on Pattern Analysis and Machine Intelligence* 22(1): 4-37.

Jain, A. K., P. Flynn and A. A. Ross (2007). "Handbook of Biometrics". New York, Springer.

Jing, H., Y. Xinge and T. Yuan Yan (2008). "Iris recognition based on non-separable wavelet". *Systems, Man and Cybernetics, 2008. SMC 2008. IEEE International Conference on.*

Jing, H., Y. Xinge and T. Yuan Yan (2008). "Iris Recognition Based on the Barycenter Distance Vector of New Non-Separable Wavelet". *Proceedings of the Chinese Conference on Pattern Recognition,* Beijing, China, *2008, pp. 1 - 6.*

Jinyu, Z., F. Nicolo and N. A. Schmid (2010). "Cross spectral iris matching based on predictive image mapping". *Proceedings of the Fourth IEEE International Conference on Biometrics: Theory Applications and Systems (BTAS),* Washington, U.S.A., 2010, pp. 1-5.

Joshi, A., A. Gangwar, R. Sharma and Z. Saquib (2012). "Periocular Feature Extraction Based on LBP and DLDA". *Advances in Computer Science, Engineering & Applications.* D. C. Wyld, J. Zizka and D. Nagamalai, Springer Berlin / Heidelberg.

166: 1023-1033.

K. N. Pushpalatha, Aravind Kumar Gautham, D.R.Shashikumar and K. B. ShivaKumar (2012). "Iris Recognition System with Frequency Domain Features optimized with PCA and SVM Classifiers." *International Journal of Computer Science Issues* 9(5): 172-180.

Kittler, J., M. Hatef, R. P. W. Duin and J. Matas (1998). "On combining classifiers." *IEEE Transactions on Pattern Analysis and Machine Intelligence,* 20(3): 226-239.

Krichen, E., M. Chenafa, S. Garcia-Salicetti and B. Dorizzi (2007). "Color-Based Iris Verification". *Advances in Biometrics*. S.-W. Lee and S. Li, Springer Berlin / Heidelberg. 4642: 997-1005.

Kumar, A. and C. Tak-Shing (2012). "Iris recognition using quaternionic sparse orientation code (QSOC)". *Proceedings of the IEEE Computer Society Conference on Computer Vision and Pattern Recognition Workshops (CVPRW),* Providence, U.S.A., 2012, pp. 59 - 64.

Kuncheva, L. I. (2003). ""Fuzzy" versus "Nonfuzzy" in combining classifiers designed by boosting." *IEEE Transactions on Fuzzy Systems* 11(6): 729-741.

Kuncheva, L. I. (2004). "Combining Pattern Classifiers: Methods and Algorithms", John Wiley & Sons.

Kuncheva, L. I., J. C. Bezdek and R. P. W. Duin (2001). "Decision templates for multiple classifier fusion: an experimental comparison." *Pattern Recognition,* 34(2): 299-314.

Kyrki, V., J.-K. Kamarainen and H. Kälviäinen (2004). "Simple Gabor feature space for invariant object recognition." *Pattern Recognition Letters,* 25(3): 311-318.

Lab, S. (2009). "NICE: II Noisy Iris Challenge Evaluation - Part II." Retrieved 23.11.2011, 2011, from http://nice2.di.ubi.pt/index.html.

Lam, L. (2000). "Classifier combinations: Implementations and theoretical issues". *Multiple Classifier Systems*. J. Kittler and F. Roli. Berlin, Springer-Verlag Berlin. 1857: 77-86.

Lam, L. and C. Y. Suen (1997). "Application of majority voting to pattern recognition: An analysis of its behavior and performance." *IEEE Transactions on Systems Man and Cybernetics Part a-Systems and Humans* 27(5): 553-568.

Lee, J.-C., P. Huang, C.-P. Chang and T.-M. Tu (2007). "A Novel Approach for Iris Recognition Using Local Edge Patterns". *Advances in Visual Computing*. G. Bebis, R. Boyle, B. Parvinet al, Springer Berlin / Heidelberg. 4842: 479-488.

Li, P., X. Liu and N. Zhao (2012). "Weighted co-occurrence phase histogram for iris recognition." *Pattern Recognition Letters* 33(8): 1000-1005.

Li, P. and H. Ma (2012). "Iris recognition in non-ideal imaging conditions." *Pattern Recognition Letters* 33(8): 1012-1018.

Li, S. Z. and J. W. Lu (1999). "Face recognition using the nearest feature line method." *IEEE Transactions on Neural Networks* 10(2): 439-443.

Lili, H., C. Wen-Shiung and L. Tzung-Hao (2010). "Personal Authentication Using Human Iris Recognition Based on Embedded Zerotree Wavelet Coding". *Proceedings of the Fifth International Multi-Conference on Computing in the Global Information Technology (ICCGI),* Valencia, Spain, 2010, pp. 99 - 103.

Liu, X. and P. Li (2012). "An Iris Recognition Approach with SIFT Descriptors". *Advanced Intelligent Computing Theories and Applications. With Aspects of Artificial Intelligence.* D.-S. Huang, Y. Gan, P. Gupta and M. Gromiha, Springer Berlin / Heidelberg. 6839**:** 427-434.

Lu, C. and Z. Lu (2005). "Efficient iris recognition by computing discriminable textons". *Proceedings of the International Conference on Neural Networks and Brain,* Beijing, China, 2005, pp. 1164 - 1167.

Ma, L., T. Tan, Y. H. Wang and D. X. Zhang (2003). "Personal identification based on iris texture analysis." *IEEE Transactions on Pattern Analysis and Machine Intelligence* 25(12): 1519-1533.

Ma, L., T. N. Tan, Y. H. Wang and D. X. Zhang (2004). "Efficient iris recognition by characterizing key local variations." *IEEE Transactions on Image Processing* 13(6): 739-750.

Ma, L., Y. Wang and T. Tan (2002). "Iris recognition based on multichannel Gabor filtering". *Proceedings of the 5th Asian Conference on Computer Vision,* 2002, pp. 279 - 283.

Ma, L., Y. H. Wang and T. N. Tan (2002). "Iris recognition using circular symmetric filters". *16th International Conference on Pattern Recognition, Vol II, Proceedings.* R. Kasturi, D. Laurendeau and C. Suen. Los Alamitos, IEEE Computer Soc**:** 414-417.

Makthal, S. and A. Ross (2005). "Synthesis of Iris Images Using Markov Random Fields". *Proceedings of the 13th European Signal Processing Conference (EUSIPCO).* Antalya, Turkey, 2002.

Mamdani, E. H. and S. Assilian (1975). "An experiment in linguistic synthesis with a fuzzy logic controller." *International Journal of Man-Machine Studies* 7(1): 1-13.

Masek, L. (2003). "Recognition of Human Iris Patterns for Biometric Identification". *Master of Science*, The University of Western Australia.

Mathworks. (2012). "Global Optimization Toolbox." Retrieved 12.1.2013, from http://www.mathworks.co.uk/products/global-optimization/description4.html.

McConnon, G., F. Deravi, S. Hoque, K. Sirlantzis and G. Howells (2011), "An Investigation of Quality Aspects of Noisy Colour Images for Iris Recognition", *International Journal of Signal Processing, Image Processing and Pattern Recognition* 4 (3): 165-178.

Melgosa, M., M. J. Rivas, L. Gómez and E. Hita (2000). "Towards a colorimetric characterization of the human iris." *Ophthalmic and Physiological Optics* 20(3): 252-260.

Miyazawa, K., K. Ito, T. Aoki, K. Kobayashi and H. Nakajima (2005). "An efficient iris recognition algorithm using phase-based image matching". *Proceedings of the IEEE*

International Conference on Image Processing, 2005, pp. 49 - 52.

Mobbeel. (2009). "Mobbeel-You are the key." Retrieved 25/02/2011, 2011, from http://www.mobbeel.com/.

Monro, D. M., S. Rakshit and Z. Dexin (2007). "DCT-Based Iris Recognition." *Pattern Analysis and Machine Intelligence, IEEE Transactions on* 29(4): 586-595.

Mukherjee, S. and B. Chanda (2011). "A Robust Human Iris Verification Using a Novel Combination of Features". *Proceedings of the Third National Conference on Computer Vision, Pattern Recognition, Image Processing and Graphics (NCVPRIPG)*, Hubli, India, 2011, pp. 162 - 166.

Ngo, H. T., R. W. Ives, J. R. Matey, J. Dormo, M. Rhoads and D. Choi (2009). "Design and implementation of a multispectral iris capture system". *Signals, Systems and Computers, 2009 Conference Record of the Forty-Third Asilomar Conference on*.

Oprea, P. (2012). "Fast Iris Recognition System for Mobile Devices". *Master of Science*, University of Kent.

Padole, C. N. and H. Proenca (2012). "Periocular recognition: Analysis of performance degradation factors". *Proceedings of the 5th IAPR International Conference on Biometrics (ICB)*, New Delhi, India, 2012, pp. 439 - 445.

Park, J. and M. Kang (2005). "Iris Recognition Against Counterfeit Attack Using Gradient Based Fusion of Multi-spectral Images". *Advances in Biometric Person Authentication*. S. Li, Z. Sun, T. Tanet al, Springer Berlin / Heidelberg. 3781: 150-156.

Park, U., R. R. Jillela, A. Ross and A. K. Jain (2011). "Periocular Biometrics in the Visible Spectrum." *IEEE Transactions on Information Forensics and Security*, 6(1): 96-106.

Partridge, D. and N. Griffith (2002). "Multiple classifier systems: Software engineered, automatically modular leading to a taxonomic overview." *Pattern Analysis and Applications* 5(2): 180-188.

Peng, Y., L. Jun, Y. Xueyi, Z. Zhenquan and L. Bin (2006). "Iris Recognition Algorithm Using Modified Log-Gabor Filters". *Proceedings of the 18th International Conference on Pattern Recognition*, Hong Kong, 2006, pp. 461 - 464.

Phillips, P. J., K. W. Bowyer, P. J. Flynn, X. Liu and W. T. Scruggs (2008). "The Iris Challenge Evaluation 2005". *Proceedings of the 2nd IEEE International Conference on Biometrics: Theory, Applications and Systems*, Arlington, U.S.A., 2008, pp. 1 - 8.

Popescu-Bodorin, N., V. E. Balas and I. M. Motoc (2011). "8-valent fuzzy logic for iris recognition and biometry". *Proceedings of the 5th International Symposium on Computational Intelligence and Intelligent Informatics (ISCIII)*, 2011, pp. 149 - 154.

Poursaberi, A. and B. N. Araabi (2007). "Iris recognition for partially occluded images: Methodology and sensitivity analysis." *Eurasip Journal on Advances in Signal Processing*, 2007 (1).

Proença, H. and L. Alexandre (2005). "UBIRIS: A Noisy Iris Image Database". *Image Analysis and Processing – ICIAP 2005*. F. Roli and S. Vitulano, Springer Berlin / Heidelberg. 3617: 970-977.

Proença, H. and L. Alexandre (2007). "Iris Recognition: An Entropy-Based Coding Strategy Robust to Noisy Imaging Environments". *Advances in Visual Computing*. G. Bebis, R. Boyle, B. Parvinet al, Springer Berlin / Heidelberg. 4841: 621-632.

Proenca, H. and L. A. Alexandre. (2004). "UBIRIS iris image database." from http://iris.di.ubi.pl.

Proenca, H. and L. A. Alexandre (2006). "Iris segmentation methodology for non-cooperative recognition." *Vision, Image and Signal Processing, IEEE Proceedings* - 153(2): 199-205.

Proenca, H. and L. A. Alexandre (2007). "Iris Recognition: A Method to Increase the Robustness to Noisy Imaging Environments through the Selection of the Higher Discriminating Features". *Proceedings of the International Conference on Computational Intelligence and Multimedia Applications,* 2007, pp. 301 - 307.

Proenca, H. and L. A. Alexandre (2007). "Toward noncooperative iris recognition: A classification approach using multiple signatures." *IEEE Transactions on Pattern Analysis and Machine Intelligence* 29(4): 607-612.

Proenca, H. and L. A. Alexandre (2012). "Toward Covert Iris Biometric Recognition: Experimental Results From the NICE Contests." *Information Forensics and Security, IEEE Transactions on* 7(2): 798-808.

Proenca, H., S. Filipe, R. Santos, J. Oliveira and L. A. Alexandre (2010). "The UBIRIS.v2: A Database of Visible Wavelength Iris Images Captured On-the-Move and At-a-Distance." *Pattern Analysis and Machine Intelligence, IEEE Transactions on* 32(8): 1529-1535.

Proença, H. and G. Santos (2012). "Fusing color and shape descriptors in the recognition of degraded iris images acquired at visible wavelengths." *Computer Vision and Image Understanding* 116(2): 167-178.

Qin, Z. (2011). "A new approach for noisy iris database indexing based on color information". *Proceedings of the 6th International Conference on Computer Science & Education (ICCSE),* Singapore, 2011, pp. 28 - 31.

Qiu, X., Z. Sun and T. Tan (2005). "Global Texture Analysis of Iris Images for Ethnic Classification". *Advances in Biometrics*. D. Zhang and A. Jain, Springer Berlin / Heidelberg. 3832: 411-418.

Radman, A., K. Jumari and N. Zainal (2011). "Iris Segmentation: A Review and Research Issues". *Software Engineering and Computer Systems*. J. Mohamad Zain, W. M. b. Wan Mohd and E. El-Qawasmeh, Springer Berlin Heidelberg. 179: 698-708.

Radu, P., K. Sirlantzis, G. Howells, F. Deravi and S. Hoque (2012). "A Review of Information Fusion Techniques Employed in Iris Recognition Systems." *International journal of Advanced Intelligence Paradigms* 4(4): 211-240.

Radu, P., K. Sirlantzis, G. Howells, S. Hoque and F. Deravi (2011). "Information Fusion for Unconstrained Iris Recognition." *International Journal of Hybrid Information*

Technology 4(4): 1-12.

Radu, P., K. Sirlantzis, G. Howells, S. Hoque and F. Deravi (2011). "A Versatile Iris Segmentation Algorithm". "BIOSIG 2011". C. B. Arslan Bromme. Darmstadt, Germany, Kollen Druck+Vwrlag. P-191: 137-151.

Radu, P., K. Sirlantzis, G. Howells, S. Hoque and F. Deravi (2012). "Image Enhancement vs Feature Fusion in Colour Iris Recognition". *Third International Conference on Emerging Security Technologies (EST)*, Lisbon, Portugal, 2012, pp. 53 - 57.

Radu, P., K. Sirlantzis, G. Howells, S. Hoque and F. Deravi (2012). "A Visible Light Iris Recognition Sytem Using Colour Information". *Proceedings of the 9th International Conference on Signal Processing Pattern Recognition and Applications (SPPRA 2012)*, Crete , Greece, 2012, pp. 106 - 113.

Radu, P., K. Sirlantzis, G. Howells, S. Hoque and F. Deravi (2013). "A Colour Iris Recognition System Employing Multiple Classifier Techniques." *Electronic Letters on Computer Vision and Image Analysis* 12(2): 54-65.

Rogova, G. (1994). "Combining the Results of Several Neural-Network Classifiers." *Neural Networks* 7(5): 777-781.

Ross, A. and A. Jain (2003). "Information fusion in biometrics." *Pattern Recognition Letters*, 24(13): 2115-2125.

Ross, A., R. Pasula and L. Hornak (2009). "Exploring Multispectral Iris Recognition beyond 900nm". *Proceedings of the IEEE 3rd International Conference on Biometrics: Theory, Applications and Systems*, New York, IEEE.

Ross, A. A., K. Nandakumar and A. K. Jain (2006). "Handbook of Multibiometrics". New York, Springer.

Roy, K. and P. Bhattacharya (2009). "Level Set Approaches and Adaptive Asymmetrical SVMs Applied for Nonideal Iris Recognition". *Image Analysis and Recognition*. M. Kamel and A. Campilho, Springer Berlin / Heidelberg. 5627: 418-428.

Roy, K., P. Bhattacharya and C. Y. Suen (2011). "Towards nonideal iris recognition based on level set method, genetic algorithms and adaptive asymmetrical SVMs." *Engineering Applications of Artificial Intelligence* 24(3): 458-475.

Sanchez-Avila, C., R. Sanchez-Reillo and D. de Martin-Roche (2002). "Iris-based biometric recognition using dyadic wavelet transform." *Aerospace and Electronic Systems Magazine, IEEE* 17(10): 3-6.

Santos, G. and E. Hoyle (2012). "A fusion approach to unconstrained iris recognition." *Pattern Recognition Letters* 33(8): 984-990.

Shapiro, J. M. (1993). "Embedded image coding using zerotrees of wavelet coefficients." *IEEE Transactions on Signal Processing*, 41(12): 3445-3462.

Shin, K. Y., G. P. Nam, D. S. Jeong, D. H. Cho, B. J. Kang, K. R. Park and J. Kim (2012). "New iris recognition method for noisy iris images." *Pattern Recognition Letters* 33(8): 991-999.

Sirlantzis, K., G. Howells, F. Deravi, S. Hoque, P. Radu, G. McConnon, X. Savatier, J. Y. Ertaud, N. Ragot, Y. Dupuis and A. Iraqui (2010). "Nomad Biometric

Authentication: Towards Mobile and Ubiquitous Person Identification". *Proceedings of the International Conference on Emerging Security Technologies (EST),* Canterbury, U.K., 2010, pp. 1 - 6.

Sudha, N., N. B. Puhan, H. Xia and X. Jiang (2009). "Iris recognition on edge maps." *Computer Vision, IET* 3(1): 1-7.

Sun, C. T., F. Melgani, C. G. Zhou, D. Francesco, L. B. Zhang and X. D. Liu (2008). "Semi-Supervised Learning Based Color Iris Recognition". Los Alamitos, IEEE Computer Soc.

Sundaram, R. M. and B. C. Dhara (2011). "Neural network based Iris recognition system using Haralick features". *Proceedings of the 3rd International Conference on Electronics Computer Technology (ICECT),* Kanyakumari, India, 2011, pp. 19 - 23.

Szewczyk, R. (2007). "New Features Extraction Method for People Recognition on the Basis of the Iris Pattern". *Proceedings of the 14th International Conference on Mixed Design of Integrated Circuits and Systems,* Ciechocinek, 2007,pp. 645 - 650.

Szewczyk, R., K. Grabowski, M. Napieralska, W. Sankowski, M. Zubert and A. Napieralski (2012). "A reliable iris recognition algorithm based on reverse biorthogonal wavelet transform." *Pattern Recognition Letters* 33(8): 1019-1026.

Tabassi, E., P. Grother and W. Salamon (2011). "IREX II - IQCE (Iris Quality Calibration and Evaluation) Report", from http://www.nist.gov.

Tajbakhsh, N., B. Araabi and H. Soltanian-zadeh (2009). "Noisy Iris Verification: A Modified Version of Local Intensity Variation Method". *Advances in Biometrics.* M. Tistarelli and M. Nixon, Springer Berlin / Heidelberg. 5558: 1150-1159.

Tajbakhsh, N., K. Misaghian and N. Bandari (2009). "A Region-Based Iris Feature Extraction Method Based on 2D-Wavelet Transform". *Biometric ID Management and Multimodal Communication.* J. Fierrez, J. Ortega-Garcia, A. Esposito, A. Drygajlo and M. Faundez-Zanuy, Springer Berlin / Heidelberg. 5707: 301-307.

Tan, T., Z. He and Z. Sun (2010). "Efficient and robust segmentation of noisy iris images for non-cooperative iris recognition." *Image and Vision Computing* 28(2): 223-230.

Tan, T., X. Zhang, Z. Sun and H. Zhang (2012). "Noisy iris image matching by using multiple cues." *Pattern Recognition Letters* 33(8): 970-977.

Technology, N. I. o. S. a. (2006). "Iris Challenge Evaluation." from http://iris.nist.gov/ICE/.

Technology, N. I. o. S. a. (2012). "National Institute of Standards and Technology." Retrieved 06.02.2013, from http://www.nist.gov.

Unsang, P., A. Ross and A. K. Jain (2009). "Periocular biometrics in the visible spectrum: A feasibility study". *Proceedings of the IEEE 3rd International Conference on Biometrics: Theory, Applications, and Systems,* Washington, U.S.A., 2009, pp. 153 - 158.

Vasile Palade, R. R. (2006). "Multi-Classifier Systems - A Review and Roadmap for Developers." *International Journal of Hybrid Intelligent Systems* 3(2).

Vatsa, M., R. Singh and A. Noore (2006). "Reducing the False Rejection Rate of Iris Recognition Using Textural and Topological Features." *International Journal of*

Signal Processing 2(2): 66-72.

Vatsa, M., R. Singh and A. Noore (2008). "Improving iris recognition performance using segmentation, quality enhancement, match score fusion, and indexing." *IEEE Transactions on Systems Man and Cybernetics Part B-Cybernetics* 38(4): 1021-1035.

Vatsa, M., R. Singh, A. Ross and A. Noore (2010). "Quality-Based Fusion for Multichannel Iris Recognition". *Proceedings of the 20th International Conference on Pattern Recognition (ICPR),* Istambul, Turkey, 2010, pp. 1314 - 1317.

Wang, F., J. Han and X. Yao (2007). "Iris recognition based on multialgorithmic fusion." *WSEAS Trans. Info. Sci. and App.* 4(12): 1415-1421.

Wang, Q., X. Zhang, M. Li, X. Dong, Q. Zhou and Y. Yin (2012). "Adaboost and multi-orientation 2D Gabor-based noisy iris recognition." *Pattern Recognition Letters* 33(8): 978-983.

Wang, Y. and J.-q. Han (2006). "Minimax probability machine for iris recognition". *Proceedings of the Third international conference on Advnaces in Neural Networks - Volume Part II*, Chengdu, China, Springer-Verlag.

Wen-Shiung, C., C. Chi-An, S. Sheng-Wen and C. Shun-Hsun (2009). "Iris recognition using 2D-LDA + 2D-PCA". *Proceedings of the IEEE International Conference on Acoustics, Speech and Signal Processing,* Washington, U.S.A. 2009, pp. 869 - 872.

Wernecke, K. D. (1992). "A Coupling Procedure for the Discrimination of Mixed Data." *Biometrics* 48(2): 497-506.

Wildes, R. P. (1997). "Iris recognition: An emerging biometric technology." *Proceedings of the IEEE* 85(9): 1348-1363.

Wildes, R. P., J. C. Asmuth, G. L. Green, S. C. Hsu, R. J. Kolczynski, J. R. Matey and S. E. McBride (1996). "A machine-vision system for iris recognition." *Machine Vision and Applications* 9(1): 1-8.

Xu, L., A. Krzyzak and C. Y. Suen (1992). "Methods of Combining Multiple Classifiers and Their Applications to Handwriting Recognition." *IEEE Transactions on Systems Man and Cybernetics* 22(3): 418-435.

Yazhuo, G., D. Zhang, S. Pengfei and Y. Jingqi (2012). "High-Speed Multispectral Iris Capture System Design." *IEEE Transactions on Instrumentation and Measurement,* 61(7): 1966-1978.

Yu, L., D. Zhang and K. Q. Wang (2007). "The relative distance of key point based iris recognition." *Pattern Recognition* 40(2): 423-430.

Zadeh, L. (1965). "Fuzzy Sets." *Information and Control* 8(3): 338-353.

Zhenan, S. and T. Tieniu (2009). "Ordinal Measures for Iris Recognition." *IEEE Transactions on Pattern Analysis and Machine Intelligence,* 31(12): 2211-2226.

Zhu, S.-C., C.-e. Guo, Y. Wu and Y. Wang (2005). "What Are Textons?" *International Journal of Computer Vision* 62(1-2).